Combination Strategies for the Treatment of KRAS Mutant Colorectal and Pancreatic Cancer

by

Joel D. Maust

A dissertation submitted in partial fulfillment
of the requirements for the degree of
Doctor of Philosophy
(Pharmacology)
in the University of Michigan
2018

Doctoral Committee:

Associate Professor Christine E. Canman, Co-Chair
Research Professor Judith S. Sebolt-Leopold, Co-Chair
Professor Thomas Carey
Professor Howard Crawford
Professor Nouri Neamati

Joel D. Maust

joeldm@umich.edu

ORCID iD: 0000-0001-8690-5545

Dedication

Brian Maust and Marcia Good,

whose example set the bar.

Acknowledgements

Mention of my mentor, Dr. Judith Sebolt-Leopold, is needed first and foremost to acknowledge significant instruction, pain and headaches. Initially criticized for being overly flowery and embellished, she has helped instruct me in everything from everyday niceties and conventions to long term career goals. Without her expert writing instruction, this dissertation would've been twice as long and less than half as effective. Dr. Sebolt-Leopold has been a critical piece of the puzzle during my time here, instructing me in the drug discovery process, talks, poster presentations, manuscripts, research and even office décor. While it'll be a burden lifted for her after I finish, she'll suffer from the lack of an on-call endnote librarian and technical support.

I am further pleased to acknowledge the roles that my committee, composed of Drs. Christine Canman, Thomas Carey, Howard Crawford and Nouri Neamati, played in helping me get to this point. Without expert advice during committee meetings, it is not likely I would have been able to produce the research presented here. There were roadblocks on the journey which they helped me navigate and gave me prudent advice.

It is important to also acknowledge my collaborators, one of which, Dr. Diane Simeone and laboratory members, provided the bulk of the pancreatic models that formed the basis for Chapter 2. Dr. Howard Crawford provided ongoing support with these models following Dr. Simeone's departure from University of Michigan. Dr. Armand Bankhead was also instrumental in providing a sound statistical backbone to Chapter 2 and always

provided expert advice and curated presentations. Morgan Phillips, an undergraduate ASPET summer student, generated a lot of the synergy assays performed in Chapter 2, saving me considerable toil.

Acknowledging my lab members almost goes without saying. Special thanks to Libby Ziemke for being especially kind and understanding while introducing me to the lab, as well as teaching me the majority of what I now know how to do in the lab, especially animal work. She became a kind of big sister to me, always loose with leftovers and deserved admonishments. Dr. Joseph Dosch also was pivotal in teaching me how to navigate graduate school and experimental techniques prior to his departure. Rachel Mumby was a late addition to the lab in my time and was always pleasant and supportive. Dr. Andrew Kocab was an honorary member of the Leopold Lab and was always free with needed advice and encouragement, with our office a pit stop of his daily procrastination.

Dr. Christopher Whitehead was always on-call for advice, merriment and barbecued rib-eyes. In addition to his extensive stories and instruction regarding the world of medicinal and computational chemistry, he introduced me to Satchel BBQ, which I'll always be grateful of. While the NCRC may have confused the smell of Satchel's for a fire breaking out, their worry was a secondary concern to delicious brisket with great friends, which included Christy McGregor. Christy was my cheeky office co-occupant for several years, who taught me all the molecular biology I know and was an invaluable friend during difficult times, and who I must acknowledge for all the coffee, food and advice she's selflessly provided.

Table of Contents

List of Figures

List of Tables

Chapter 1

Chapter 3

Abstract

A large percentage of human cancers show mutations in RAS, a critical activator of the mitogen activated protein kinase (MAPK) signaling cascade that has been well documented for its role in driving tumorigenesis. While there have been numerous attempts to inhibit RAS signaling, efforts have largely been unsuccessful. The major reason leading to the lack of success is the small size of the RAS protein, which prevents the discovery of adequate binding sites for small molecules. While directly inhibiting RAS has not been achieved except in isolated cases, there has been much better success at inhibiting downstream effectors of RAS. Inhibition of downstream effectors have focused on MAPK pathway kinases RAF, MEK and ERK. Additionally, inhibition of PI3K as well as the human growth factor receptors (HERs) have been moderately successful. However, resistance and adaptive signaling in response to therapy is prevalent. A new trend of combination therapies is emerging within the field, allowing effective inhibition of multiple proteins in ways that reduce the ability of tumor cells to escape inhibition.

The goal of this dissertation is to delineate downstream effectors that are effective in blocking RAS signaling when combined with another kinase inhibitor and evaluate efficacy of these combination strategies. Focus was placed on developing novel strategies for the treatment of patients diagnosed with KRAS-activated pancreatic or colorectal cancer, an isoform of the RAS oncogene. These cancers show high mutation rates in KRAS: up to 90% in pancreatic cancer and 30-50% in colorectal cancer. The high mutation

rate and lack of effective therapies for patients diagnosed KRAS-mutant disease is a critical unmet need.

These two chapters approach the problem in different ways. In Chapter 2, which explores co-inhibition of MEK and CDK4/6, a screen was employed to find the most responsive cancer cell line models of a panel. This study identified two pancreatic cancer models, L3.6pl and UM59, that exhibited the highest response to treatment. In these models, it was found that COX-2 expression was higher than in those that did not respond as well. These findings identify a potential biomarker that could have implications for current and future clinical trials evaluating this treatment strategy.

Chapter 3 evaluates the activity of a rationally designed molecule that inhibits PI3K and EGFR. These are two prominent proteins central to growth signaling in the cell that participate with RAS for malignant growth. The activity of MTX-211 was screened for activity on the NCI-60 panel, a curated collection of cancer cell line models from different tissues. From this screen, it emerged that MTX-211 was most effective in colorectal cancer models and in models with a PIK3CA mutation. Further evaluation of MTX-211 identified MEK, a downstream signaling effector of RAS, as an ideal combination partner. Inhibition of cancer cells with a MEK inhibitor activates EGFR and PI3K signaling, which MTX-211 can block. This is a novel combination strategy that is effective in targeting adaptive signaling that emerges from single agent MEK inhibition and causes apoptosis in treated

cells. It was further found that MTX-211 was effective as a single agent and in combination with a MEK inhibitor in several animal studies of tumor-bearing mice.

Chapter 1: Introduction

RAS BIOLOGY

A large percentage of human cancers show mutations in the protein RAS, a critical activator of the mitogen activated protein kinase (MAPK) signaling cascade that has been well documented for its role in driving tumorigenesis. Mutations in RAS regulators such as SPRED1 and neurofibromin also contribute to cancer. Germline mutations that lead to overactive RAS/MAPK signaling contribute to "RASopathies," developmental conditions which exist in over 400,000 people in the United States (Simanshu et al., 2017). RAS proteins function as molecular switches that cycle between inactive GDP-bound and active GTP-bound states. The exchange of GDP for GTP and vice versa is promoted by guanine

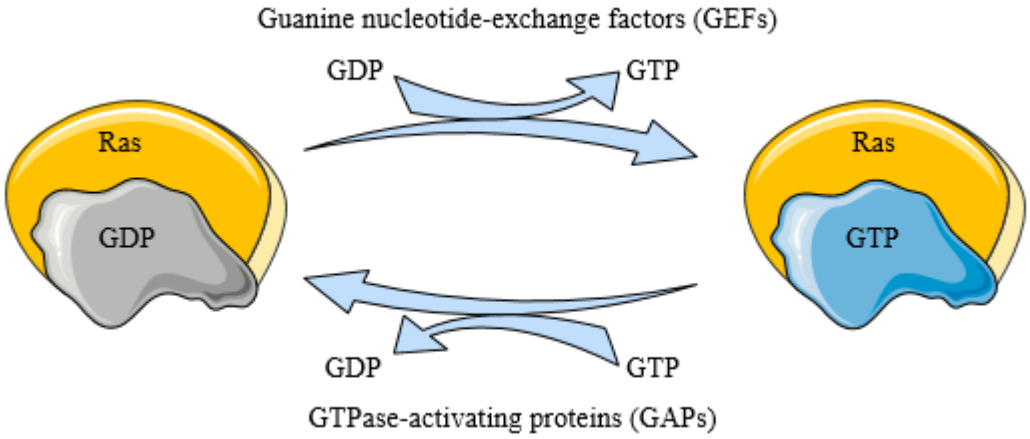

Figure 1.1: RAS-GDP → RAS-GTP cycle.
RAS proteins cycle between an inactive GDP-bound and an active GTP-bound state. These transitions are facilitated by the binding of GEFs (NF1/SOS1/many others) and GAPs. The presence of RAS-GTP activates many signaling pathways implicated in cancer, and oncogenic mutations in RAS cripple the GTPase activity and the ability to transition into the GDP-bound state.

nucleotide exchange-factors (GEFs) and GTPase-activating proteins (GAPs), respectively, shown in Figure 1.1 (Cherfils and Zeghouf, 2013). GEFs and GAPs are large multi-domain structures with varied interactions with other proteins, lipids and regulatory molecules that influence the activation of RAS (Bos et al., 2007). These varied signaling inputs to both GEFs/GAPs and RAS contribute to a complex network of growth signaling. Translocation to the plasma membrane governs RAS activation and modulation by GEFs and GAPs, as well as interaction of RAS with effectors. The RAF kinase is activated by translocation to the membrane, wherein its N-terminal RAS-binding domain (RBD) binds to RAS-GTP. This interaction leads to conformational changes that lead to phosphorylation of RAF and stimulate the serine/threonine kinase activity that sequentially phosphorylates and activates MEK and in turn MAPK, or ERK (extracellular signal regulated kinase, shown in Figure 1.2) (Wan et al., 2004). Activation of other RAS effectors also occurs by recruitment to the plasma membrane, such as certain phosphoinositol 3-kinase (PI3K) isoforms requiring myristoylation (Simanshu et al., 2017). Furthermore, activation and localization of RAS and effectors can be modulated by local lipid composition of the plasma membrane,

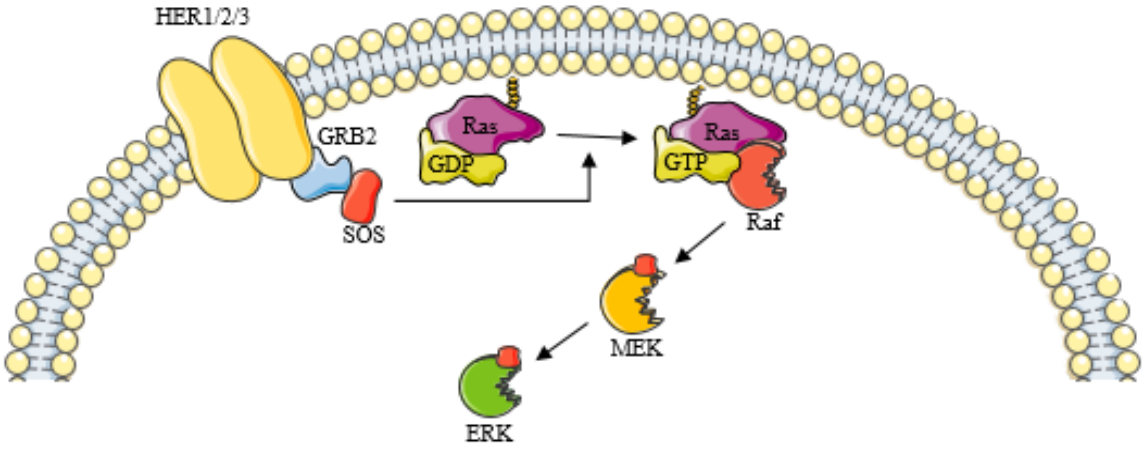

Figure 1.2: The canonical MAPK signaling pathway. The MAPK signaling pathway, in its simplest form, is initiated by growth factors/ligand binding the extracellular domain of HER1/2/3, inducing dimerization and the sequence of events leading to sequential activation of RAS-RAF-MEK-ERK.

drawing attention to the role of the plasma membrane in RAS biology and signaling (Zhou and Hancock, 2015; Zhou et al., 2017).

RAS is ubiquitously expressed in all tissue in three isoforms: NRAS, HRAS and KRAS. While all three isoforms are concurrently expressed in human tissue, tissue specific disparities in isoform expression exist (Fiorucci and Hall, 1988; Furth et al., 1987). Approximately 30% of all human cancer has a mutation in RAS, with KRAS being the most frequently mutated RAS isoform at 22%, followed by NRAS (8%) and HRAS (2%) (Prior et al., 2012). In colorectal cancer, 30 – 50% of cases have a mutation in KRAS (Vaughn et al., 2011) while for pancreatic cancer the mutation rate has been extensively reported to be >90% (Biankin et al., 2012; Witkiewicz et al., 2015b). Notably, KRAS is the most frequently mutated oncogene of either cancer subtype (Thomas et al., 2007).

KRAS was originally identified in the Kirsten sarcoma virus DNA and was one of the first oncogenes discovered through studies involving the ability of viral DNA and DNA fragments to transform cells (Tsuchida et al., 1982; Tsuchida and Uesugi, 1981). Since then, the role of RAS in cancer biology has been comprehensively studied. However, despite the field's best efforts, RAS has remained undruggable since it was discovered.

Inhibiting RAS Signaling

As summarized below some of the key approaches to target deregulated RAS signaling have included direct small molecule inhibition of RAS, blocking RAS membrane association and targeting downstream effectors targeting of synthetic lethal interactions (Cox et al., 2014; Lu et al., 2016; Papke and Der, 2017).

Inhibiting membrane association of RAS

Early efforts to target RAS signaling focused on inhibiting membrane association of the small GTPase, which is a critical step for signaling. The addition of a farnesyl isoprenoid lipid modification at RAS C-terminal CAAX motifs is one posttranslational modification controlling membrane association that was an early target for drug discovery (Cox et al., 2015). Research into this area led to the development of farnesyltransferase inhibitors (FTIs). However, FTIs categorically failed to inhibit RAS signaling, not because of a lack of target potency, but because cells responded with alternative prenylation by geranylgeranyltransferases (FTI induced alternative prenylation) (Rowell et al., 1997; Whyte et al., 1997). Two clinical candidates, lonafarnib and tipifarnib, advanced to phase III clinical trials but showed no efficacy in lung, pancreatic and colorectal cancer (Papke and Der, 2017).

Direct inhibition of RAS

There have been some efforts delving into direct inhibition of RAS by interfering with GDP/GTP binding. Some of these attempts have only met with limited success, largely because of the difficulty in antagonizing the picomolar affinity of RAS for GTP in a cellular context with millimolar concentrations of GTP (Cox et al., 2014). Other efforts have failed in part due to the small size of the GTPase, which limits the amount of available binding pockets other than the nucleotide binding site. Additional attempts have focused on disruption with either the interaction domain that binds RAF (Shima et al., 2013) or a SOS interaction domain that stimulates the exchange of GDP for GTP (Maurer et al., 2012; Papke and Der, 2017). Protein-protein interactions have been found to be largely intractable as druggable targets though, given the small size of RAS.

One development is rigosertib (Onconova Therapeutics), a small molecule RAS mimetic (Athuluri-Divakar et al., 2016). One thing in common between many RAS effectors is the presence of a RAS binding domain (RBD), which binds to the switch region of RAS and leads to the activation event. Rigosertib has been shown to bind to the RBDs of RAF, Ras-GDS and PI3Ks, which competes with RAS for binding to effectors. This disruption in protein-protein interactions therefore leads to an inability of RAS to activate effector pathways. Rigosertib is currently being evaluated in a Phase 3 cohort of higher-risk myelodysplastic syndromes (MDS) who have progressed on prior hypomethylating agent (HMA) therapy (Onconova, 2018).

Another attempt to target KRAS is specific for the G12C mutation. Compounds have been designed that covalently bind specifically to this mutant form of KRAS, which is predominant in lung cancer, although these inhibitors have met with obstacles in preclinical studies (Janes et al., 2018; Ostrem et al., 2013). Also, this approach unfortunately caters only to the G12C mutant form due to the formation of a covalent bond. The G12C mutation is also one of the RAS mutations with the lowest frequency, limiting the therapeutic impact of this approach. Other attempts to directly inhibit other mutations in RAS are ongoing, with efforts by the NCI Ras initiative leading the field.

Synthetic lethal approaches to RAS^{mt} cancer

Another approach to target RAS signaling relies on the concept of synthetic lethality. A synthetic lethal interaction, in this context, would be a gene that is required for survival of RAS^{mt} cancer that is not required for a normal RAS wild type cell. In other words, a cell that does not normally rely on a gene may become dependent on this gene/pathway for survival in a RAS^{mt} context, and when removed or inhibited, the cell will die. A weakness

of this approach is the use of RNAi-based screens with RAS^{mt}/RAS^{wt} paired isogenic lines to determine which genes are synthetic lethal. In order to produce matched isogenic lines, stable deletion of RAS is required, which in itself is a potent cellular stimulus that would give rise to adaptive signaling in the cells that survive (Papke and Der, 2017). This concept has generated a lot of interest but has failed to deliver on high expectations, partly due to the inability to replicate results. Part of this may also be context-specific, wherein synthetic lethality is exclusive to a particular context, metabolic state or site-specific cancer.

One target identified as being synthetic lethal in $KRAS^{mt}$ NSCLC is CDK4, a protein critical for progression of the cell cycle from G1 to S phase (Mao et al., 2014; Puyol et al., 2010). In these studies, either genetic ablation of CDK4 (Puyol et al., 2010) or targeted delivery of CDK4 siRNA (Mao et al., 2014) to $KRAS^{mt}$ tumors led to senescence and prevented tumor progression. Recently, pharmacologic inhibition of CDK4 and CDK6 has been made possible with the discovery of small molecule inhibitors palbociclib (Pfizer, 2015), ribociclib (Eli Lilly, 2017) and abemaciclib (Novartis, 2017). In Chapter 2, a therapeutic approach to co-targeting of CDK4/6 and MEK is covered, partly based on these findings. The convergence of synthetic lethality research that identifies potential targets in the field and the ability to target effector signaling with emerging agents is a promising application of preclinical research in this area.

Targeting RAS^{mt} signaling through effector pathways

Targeting downstream signaling or effector pathways has been one of the most successful attempts at attenuating RAS^{mt} signaling. RAS signaling is multifaceted and significant attention has been afforded to inhibiting the two main downstream effector pathways of RAS: the RAF-MEK-ERK signaling pathway as well as the PI3K-AKT signaling axis

(Castellano and Downward, 2011; Ryan et al., 2015; Wong et al., 2010). Most of these effectors have been the target of kinase inhibitor development, with numerous inhibitors ranging from preclinical candidates to FDA approved small molecules having been developed. The field generally recognizes that RAF-MEK-ERK downstream pathway is critical for progression of RAS^{mt} tumors (Ryan et al., 2015). Part of the reason for the limited success of these kinase inhibitors in cancer is the presence of ERK-mediated regulatory feedback loops that normally limit pathway output. In a wild type RAS context, increased ERK activity leads to phosphorylation-based feedback inhibition of multiple kinases to dampen flux of the pathway (Lake et al., 2016). In response to inhibition of upstream kinases, ERK activity is diminished, which can lead to paradoxical activation of the pathway due to the loss of feedback inhibition by ERK.

MAPK signaling has been shown to lead to phosphorylation of epidermal growth factor receptor (EGFR) at Threonine 669 (T669) (Li et al., 2008b). While the physiological consequences of this phosphorylation site are somewhat disputed (Brewer et al., 2009; Heisermann et al., 1990; Kovacs et al., 2015; Welsh et al., 1991), it is a putative regulatory site of EGFR. Studies have shown that MEK inhibition can lead to the loss of this inhibitory threonine phosphorylation, thereby hyperactivating HER3/ERBB3, which increases flux through the PI3K/AKT pathway in $KRAS^{wt}$ cells and the MAPK pathway in $KRAS^{mt}$ cells (Turke et al., 2012b). This introduces a viable therapeutic approach to this resistance, wherein targeting the RTKs responsible for resistance can result in synergistic activity (Chapter 3).

In addition to regulatory feedback at T669 of EGFR, intrinsic resistance to MEK inhibitors has been attributed to transcriptional activation of receptor tyrosine kinases (RTKs) HER2

and HER3. This leads to a subsequent increase in heterodimeric complexes such as EGFR/HER3 and HER2/HER3 which can lead to increased MEK-ERK and PI3K-AKT signaling (Ebi et al., 2011; Kitai et al., 2016; Sun et al., 2014). Moreover, several other RTKs have shown induction in response to MEK inhibition: PDGFR, VEGFR2, CSFR1, DDR1/2 and AXL, highlighting the complexity of feedback networks impacted by pharmacologic manipulation of ERK activation levels (Duncan et al., 2012). In addition to feedback inhibition of EGFR, ERK also phosphorylates and plays similar roles in inhibiting MEK and RAF (Lake et al., 2016; Ueki et al., 1994; Wartmann et al., 1997). ERK also has inhibitory effects on SOS1 (disrupting interaction with GRB2), DUSP6 stability (ERK1/2 phosphatase) and the scaffold protein SPRY (disrupts SOS1 interaction with GRB2 as well, Figure 1.3) (Corcoran et al., 2012; Red Brewer et al., 2009; Turke et al., 2012b; Zhang et al., 2010).

The dynamic regulatory feedback mechanisms in place in the MAPK pathway is exacerbated by the numerous effector pathways of RAS, of which the canonical RAF-mediated MAPK signaling is only one. Another important pathway that carries RAS oncogenic signaling is the phosphatidylinositol 3-kinase (PI3K) pathway and receptor tyrosine kinases (RTKs) involved in activation of RAS.

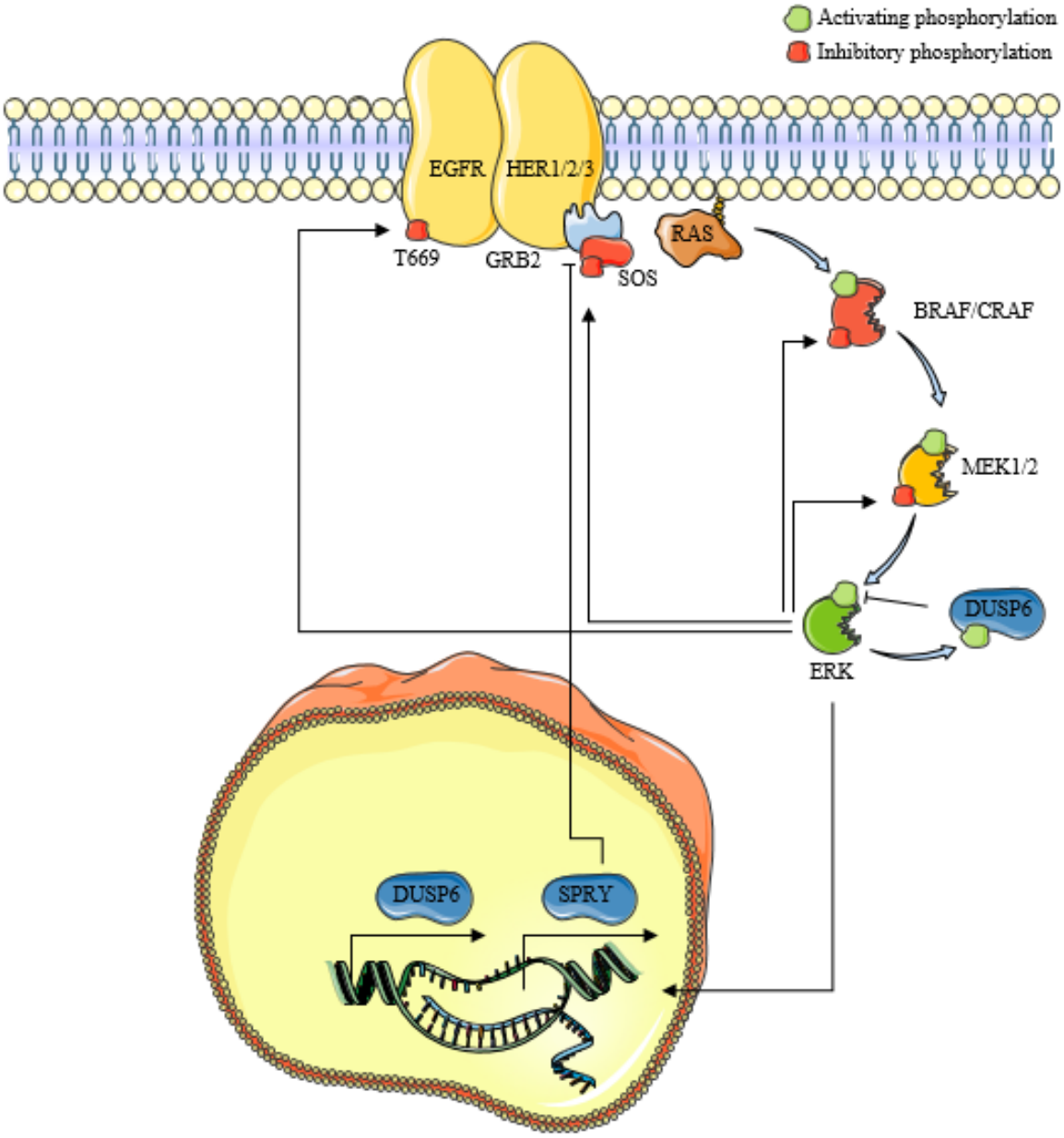

Figure 1.3: Regulation of ERK activation and ERK feedback inhibition mechanisms. ERK activation sets into motion several regulation events designed to inhibit basal tone of the pathway. ERK phosphorylates and inhibits EGFR in the juxtamembrane region at threonine 669. It also phosphorylates RAF and MEK, which limits activation of these kinases. In addition to phosphorylation-based regulation events, ERK activation leads to transcription of SPRY which disrupts the GRB2/SOS1 interaction, limiting RAS activation. It also leads to upregulation of DUSP6 expression, an ERK phosphatase, which is additionally activated by direct phosphorylation by ERK. Inhibition of ERK via any node in this pathway will reduce this feedback activation, leading to relief of feedback activation an and increase in basal tone.

RTKs involved in RAS activation

Broadly speaking, the human epidermal growth factor receptor (HER) family activates many different growth pathways that are Ras-dependent as well as independent. There is significant overlap in some of these pathways as covered with the Ras-PI3K crosstalk. The HER family is composed of four members: HER1 (EGFR), HER2, HER3 and HER4. Of these, HER4 has not been shown to significantly contribute to oncogenesis, and of the remaining, HER3 does not have catalytic activity but contributes to the autophosphorylation of the other members when dimerized.

The general structure of this family is comprised of an extracellular domain, a transmembrane domain and an intracellular domain containing the C-terminal tail and the catalytic domain (Sergina and Moasser, 2007). Dimerization, either through hetero- or homodimerization, is required for activation of the receptors through transphosphorylation of the C-terminus. The dimerization events are controlled by extracellular ligands that induce conformational changes in the receptors leading to dimerization. When no ligand is bound, the extracellular dimerization domain is involved in an intra-molecular interaction that keeps it inactivated. Ligand binding induces a conformational change that exposes this dimerization interface for inter-receptor interactions. Upon binding of the extracellular domains, the intracellular domain of these proteins simultaneously engage in transphosphorylation events, leading to activation and recruitment of downstream effectors that recognize these tyrosine phosphorylations (also known as docking sites for SH2 and PTB domains, Figure 1.4) (Burgess et al., 2003). In this regard, HER2 is unique, as the extracellular domain exists in a conformation similar to the ligand-bound states of other HER extracellular domains. Therefore, no ligand exists for the activation of HER2 and

activation of this member is likely governed by factors differing from the other family members (Garrett et al., 2003).

A hierarchical network of inter-receptor interactions determines the potency of the homo- and heterodimer pairs, with heterodimers being more potent than homodimers. Of these, the HER2-HER3 interaction is the most active (Tzahar et al., 1996). Selectivity for downstream interaction pathways is controlled by many factors including the amount of interaction motifs for factors such as Grb2, PI3K, STAT5, as well as phosphorylation kinetics of various tyrosine residues that are correlated with interaction partner preferences (Schulze et al., 2005). In other words, this selectivity is controlled by consensus binding sequences that are phosphorylation dependent as well as independent (Jones et al., 2006). The interactomes of each HER family member reveal patterns of partner selection that are dynamic, not static, as studies examining the genome set of SH2 and PTB domains and their interactions with HER family peptide fragments find differences in binding locations in comparison to known interaction sequences. The recruitment sites on HER2 were found to be the most promiscuous to diverse domains and higher concentrations of EGFR and HER2 led to increased promiscuity of these interactions with the SH2 and PTB domains. The authors hypothesized that this contributes to the high oncogenic activity of these oncogenes, especially considering the frequency of gene amplification occurring within the gene loci encoding the HER family members (Garrett et al., 2003; Jones et al., 2006; Slamon et al., 1987). Furthermore, HER3 is characterized by many p85 binding sites, consistent with reports implicating HER3 in activation of the PI3K-MTOR signaling axis both basally and in resistance to tyrosine kinase inhibitor therapy (Sergina et al., 2007).

Each HER family member additionally has a Grb2 docking site, consistent with the ability to activate the Ras-ERK pathway (Sergina and Moasser, 2007).

RAF

RAF is a dual serine/threonine kinase and the family is comprised of three isoforms: ARAF, BRAF and CRAF. Of these, BRAF has the highest basal activity, activates MEK more potently than the others, and is the most frequently activated isoform in human cancer (Fiskus and Mitsiades, 2016). RAF activation occurs when Ras-GTP binds to the RBD of RAF (N-terminal region). Conformational changes and recruitment to the plasma membrane caused by this interaction induces RAF phosphorylation, which facilitates the kinase activity of RAF (Figure 1.4) (Wan et al., 2004). The majority of mutations in BRAF occur in the activation segment, flanking regions, and the negatively charged regulatory region (glycine-rich P loop of the N lobe). The negative charge of phosphorylation disrupts the hydrophobic interaction between the activation segment (T599 and S602) and the P loop, thereby activating the enzyme. The most common mutation in BRAF is the valine to glutamate (V600E) amino acid substitution, which occurs in the activation segment, disrupting the hydrophobic interaction keeping the enzyme in an inactive conformation. This mutation therefore explains the potent oncogenic activity of $BRAF^{V600E}$ (Fiskus and Mitsiades, 2016; Wan et al., 2004). Vemurafenib was the first FDA approved BRAF inhibitor for the treatment of BRAF mutant melanoma (Bollag et al., 2012). Since then, two additional BRAF inhibitors have been approved for treatment of this disease in combination with a MEK inhibitor, namely dabrafenib (co-administered with trametinib) and encorafenib (co-administered with binimetinib) (FDA, 2018). These are listed in Table 1.1. Vemurafenib and dabrafenib are approved for the treatment of BRAF-mutant

malignant melanoma based on progression-free and overall survival, and rapid tumor regression is observed in 70-80% of patients receiving therapy (Ryan et al., 2015). However, resistance to these inhibitors occurs rapidly in melanoma, colorectal, lung and thyroid cancers. Mechanisms of resistance to these inhibitors includes RTK activation, NRAS mutation, NF1 inactivation (a GTPase-activating protein [GAP] of RAS) (Kidger et al., 2018; Nissan et al., 2013; Simanshu et al., 2017) and increased RAF activity (truncation or increased expression) (Lidsky et al., 2014; Nazarian et al., 2010). These all lead to increased MAPK flux and activation of ERK. Considering that 80% suppression of phosphorylation of ERK is required to observe clinical activity, these resistance mechanisms limit the utility of these inhibitors as therapies in patients (Bollag et al., 2010).

Furthermore, despite the activity of vemurafenib and dabrafenib in patients diagnosed with BRAF-mutant disease, in RAS-mutant patients, cancer growth stimulation occurs when treated with these agents, increasing ERK activity (Callahan et al., 2012; Oberholzer et al., 2012). In the RAS-mutant context, the drug-inactivated form of BRAF forms a heterodimer with CRAF, which causes RAS-induced CRAF activation and flux through the pathway. This has been termed paradoxical ERK activation with BRAF inhibitors, and third-generation BRAF inhibitors were designed with this shortfall in mind and are termed "paradox breakers" (Ryan et al., 2015). More information on the nuances of RAF inhibitors are covered by Karoulia et al (Karoulia et al., 2016). PLX8394 (Plexxikon) was one of the first inhibitors of this third generation, with binding affinity for BRAF and CRAF as well as activity in RAS-mutant and vemurafenib resistant cells (Basile et al., 2014). More inhibitors that target the paradoxical activation are in development, such as LY3009120, a panRAF and dimer inhibitor by Eli Lilly (Vakana et al., 2017). This inhibitor has also

shown promising preclinical activity in $KRAS^{mt}$/$BRAF^{mt}$ colorectal cancer patient derived xenograft (PDX) models.

RAF inhibitor	Target	Company	Clinical Phase
Vemurafenib (PLX4032)	$BRAF^{V600E}$, $BRAF^{WT}$, CRAF	Plexxikon/Genentech	FDA approved
Dabrafenib (GSK2118436)	$BRAF^{V600E}$, $BRAF^{WT}$, CRAF	Novartis/GlaxoSmithKline	FDA approved
Encorafenib (LGX818)	$BRAF^{V600E}$	Array BioPharma	FDA approved
Sorafenib	$BRAF^{V600E}$, $BRAF^{WT}$, CRAF, RET, c-KIT, Flt-3, VEGFR1, VEGFR2, FGFR1, p38	Bayer	FDA approved
LY3009120	panRAF	Eli Lilly and Company	Pre-
PLX4720	$BRAF^{V600E}$, $BRAF^{WT}$, CRAF	Plexxikon	Pre-
SB-590885	$BRAF^{V600E}$, $BRAF^{WT}$, CRAF	GlaxoSmithKline	Pre-
GDC-0879	$BRAF^{V600E}$, $BRAF^{WT}$, CRAF	Genentech	Pre-
Regorafenib	$BRAF^{V600E}$, $BRAF^{WT}$, CRAF, RET, c-KIT, TIE2, VEGFR1, VEGFR2, VEGFR3. FGFR1, PDGFR-β	Bayer	III
XL281	$BRAF^{V600E}$, $BRAF^{WT}$, CRAF	Exelixis	I/II
RAF265	$BRAF^{V600E}$, $BRAF^{WT}$, CRAF, c-KIT, VEGFR2, PDGFR-β	Novartis	II
ARQ736	$BRAF^{V600E}$, $BRAF^{WT}$, CRAF	ArQule	I

Table 1.1: RAF clinical inhibitors. Adapted from (Rahman et al., 2014; Ryan et al., 2015).

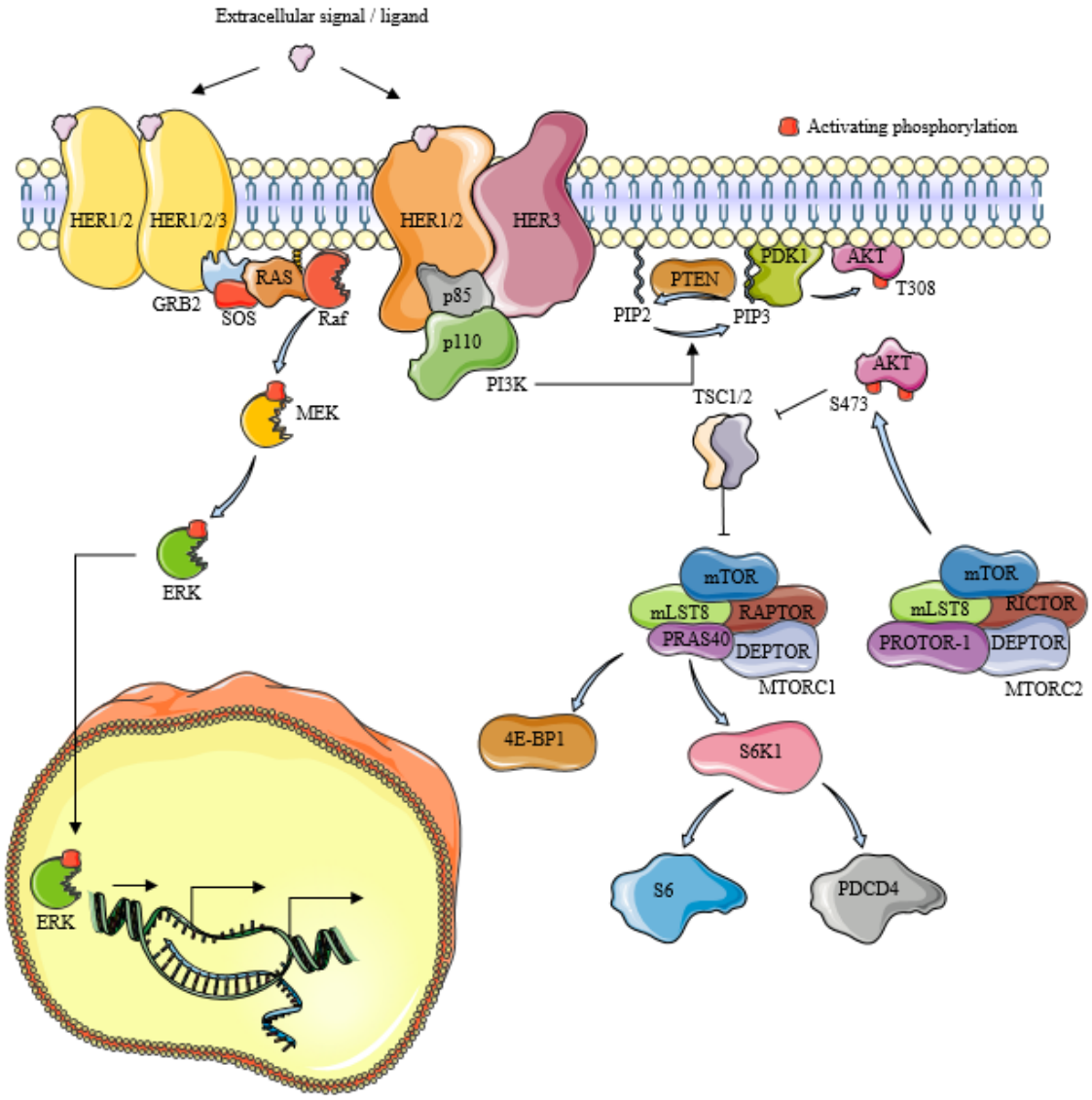

Figure 1.4: A snapshot of MAPK and PI3K-AKT signaling axes. Included in this figure is the MAPK signaling pathway shown on the left, with the addition of PI3K (p85-p110) activation and the sequence of events leading to AKT and MTOR activation. Briefly, PI3K phosphorylates and converts PIP2 → PIP3 (a process which PTEN, a tumor suppressor, reverses), which recruits PDK1 to the plasma membrane, leading to phosphorylation of AKT on T308. AKT activation leads to mammalian target of rapamycin (MTOR) activation which phosphorylates AKT on S473 to increase its activity. MTOR is involved in facilitating cap-dependent translation and additionally leads to activation of S6 and programmed cell death 4 (PDCD4), a tumor suppressor in facilitating cap-dependent translation and additionally leads to activation of S6 and programmed cell death 4 (PDCD4), a tumor suppressor.

MEK

MEK directly phosphorylates ERK and is the closest upstream kinase to RAS, which initially was part of the rationale for the development of MEK inhibitors for therapeutic intervention. MEK1 and MEK2 are highly homologous kinases and are comprised of a kinase domain, ERK-docking region, a negative regulatory region, a nuclear export sequence and a proline-rich insert (Zhao and Adjei, 2014). What makes these kinases favorable to therapeutic intervention is the presence of a unique pocket structure adjacent but separate to the ATP-binding site, which was discovered by crystallography of MEK bound to highly selective agents (Ohren et al., 2004). Inhibition within this pocket locks unphosphorylated MEK into a catalytically inactive state. The presence of this unique pocket leads therapeutic interventions to be highly specific for MEK, bypassing the pitfall of ATP-competitive inhibitors that are less selective.

The first MEK inhibitor to enter clinical trials was CI-1040, which is the first reported orally active agent in this target class (Sebolt-Leopold et al., 1999). It is a potent inhibitor of MEK1/2 (17 nM IC_{50} against MEK1). Similar to the MEK inhibitors discovered prior to it, PD98059 and U0126, CI-1040 inhibits MEK1/2 in a non-ATP/non-ERK1/2 competitive way (Allen et al., 2003; Frémin and Meloche, 2010). While the clinical trials with CI-1040 failed to advance, this prototype MEK inhibitor helped set the field for future MEK inhibitors.

Further, while development of MEK inhibitors began in the early 1990s, the first MEK inhibitor to gain FDA approval was trametinib in 2013 for the treatment of $BRAF^{mt}$ melanoma (cobimetinib was second in 2015). Despite their potent *in vitro* activity against KRAS mutant tumor cells (Wee et al., 2009), *in vivo* activity of MEK inhibitors as single

agents has been disappointing due to the development of resistance (Little et al., 2011; Poulikakos and Solit, 2011; Turke et al., 2012b; Wee et al., 2009). Table 1.2 shows some of the current MEK inhibitors in the field.

MEK inhibitor	Target	Company	Clinical Phase
MEK162/binimetinib	MEK1/2	Array BioPharma	FDA approved
Cobimetinib	MEK1/2	Exelixis/Genentech	FDA approved
Trametinib	MEK1/2	Novartis	FDA approved
PD-0325901	MEK1/2	Pfizer	Phase II
CI-1040	MEK1/2	Pfizer	Terminated
Selumetinib	MEK1/2	AstraZeneca	Phase III
AZD8330	MEK1/2	AstraZeneca	Phase I
TAK-733	MEK1/2	Millenium Pharmaceutical/Takeda	Phase I
GDC-0623	MEK1/2	Genentech	Phase I
Refametinib	MEK1/2	Ardea Biosciences/Bayer	Phase II
Pimasertib	MEK1/2	Merck and co.	Phase II
RO4987655	MEK1	Hoffman-La Roche	Phase I
RO5126766	RAF/MEK1/2	Hoffman-La Roche	Phase I
WX-554	MEK1/2	Wilex, AG. Germany	Terminated
HL-085	MEK1	Binjiang Pharma	Phase I

Table 1.2: MEK clinical candidates. Adapted in part from (Cheng and Tian, 2017; Ryan et al., 2015; Zhao and Adjei, 2014).

Through analysis of 17 unique MEK mutants from the CBioPortal genomic database of human cancer, Gao et al (Gao et al., 2018) classify these MEK mutations into Class 1/2/3, which drive ERK signaling and are sensitive to feedback inhibition in different ways (described in detail in Figure 1.5). The implications of these new mutations carve a new niche for ATP-competitive MEK inhibitors, as allosteric inhibitors are ineffective at

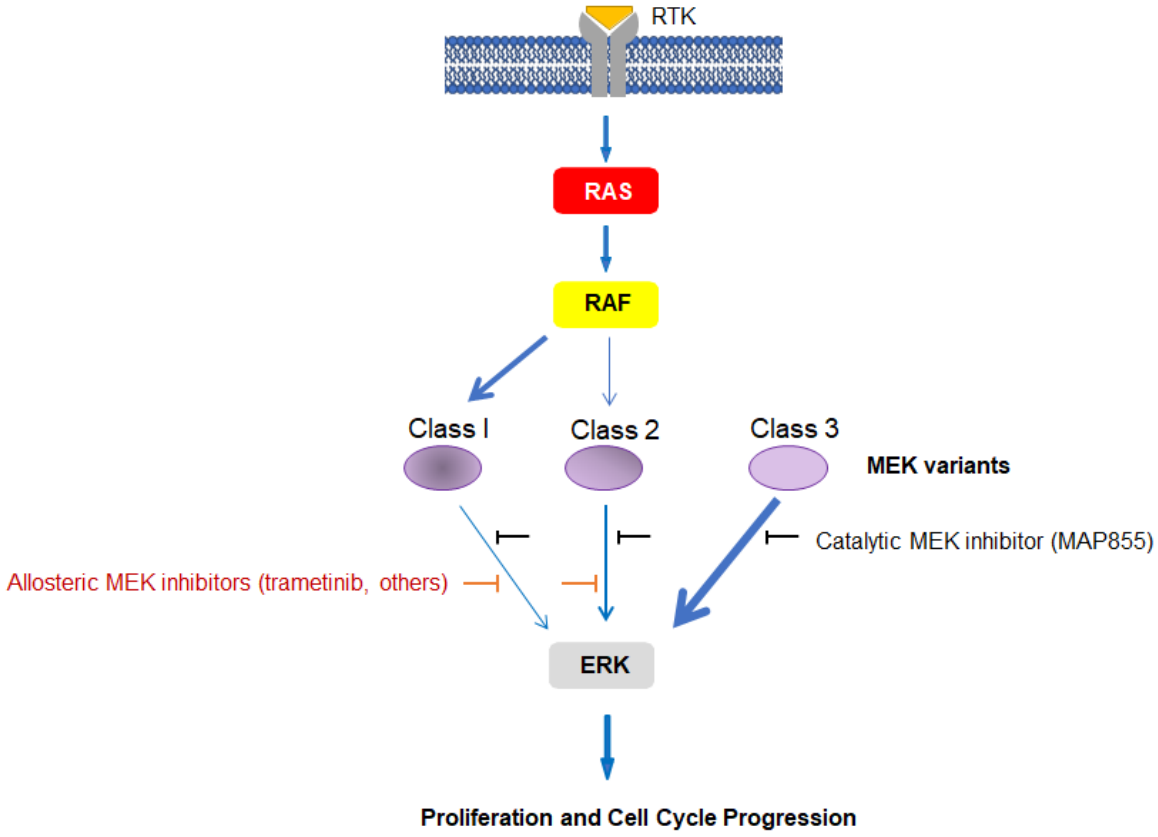

Figure 1.5: Mapping the path to ERK activation in the context of MEK mutations. Sequential RAS-RAF-MEK-ERK activation defines the wild type context. Class I MEK mutants behave in a similar manner to wild type MEK which is completely reliant on RAF for activation. Class I MEK mutants are sensitive to ERK mediated feedback inhibition, with a decrease in upstream signaling leading to a reduction in MEK activation. Class 2 MEK mutants retain activity in the absence of RAF but are stimulated in the presence of RAF. For this reason, class 2 mutants have been termed "RAF-regulated," or dependent on RAF for only a portion of their activity. ERK feedback inhibition therefore only partially reduces the activity of Class 2 mutants. Class 3, or "RAF-independent," MEK mutants have a deletion in the 98-104 amino acid region that eliminates binding and reliance on RAF for activation. Gao et al posit that this region is a potent negative regulator of MEK activity, and its absence drives Class 3 mutants to constitutive activity and the ability to auto-phosphorylate in *cis*. Since this class does not rely on RAF for activation, it is also immune to feedback inhibition, thereby driving higher basal levels of ERK activation than the other two classes. Furthermore, allosteric MEK inhibitors show significantly reduced potency against Class 3 mutants compared to Class 1 and 2 mutants, while an ATP-competitive MEK inhibitor (MAP855) showed similar potencies against all MEK mutants. It is thought that the permanent active conformation of Class 3 mutants negatively affects the ability of allosteric inhibitors to bind, since they preferentially bind the inactive conformation.

targeting the Class III MEK mutations, which are characterized by insensitivity to RAF feedback inhibition and can drive ERK activation autonomously. The authors describe an ATP-competitive inhibitor from Novartis that inhibits all three classes of MEK mutations (MAP855). It remains to be seen whether ATP-competitive MEK inhibitors can replace the highly selective allosteric MEK inhibitors or whether they are reserved for cases in which resistance is developed.

ERK

ERK1/2 are two dual serine/threonine kinases with 85% identical sequences and function. They are activated by dual phosphorylation on threonine and tyrosine residues in the activation loop by MEK1/2, which stimulates nuclear translocation. They have a broad range of target substrates, such as phospholipases, cytoskeleton proteins and transcription factors. They are activated by serum, growth factors, phorbol esters as well as G protein coupled receptor (GPCR) ligands, cytokines, microtubule disorganization and osmotic stress (Figure 1.4) (Roux and Blenis, 2004).

The utility of RAF and MEK inhibitors has been limited by emergence of resistance and compensatory activation of the pathway. While the reactivation of ERK signaling in response to RAF and MEK inhibitors is the basis for their combination in new clinical trials, novel pathway inhibitors are still needed.

Recent studies have focused on development and comparative evaluation of ERK inhibitors. One of the first ERK inhibitors that advanced to the clinic, SCH772984, is a highly selective, ATP-competitive inhibitor of ERK1/2 (4 and 1 nM $IC_{50,}$ respectively). SCH772984 inhibits both ERK kinase activity as well as MEK-mediated phosphorylation

of ERK, as the compound was designed to bind to unphosphorylated, or inactive, ERK2 (Morris et al., 2013). Interestingly, <50% of RAS^{mt} cell lines responded to therapy with SCH882984 and <20% of $BRAF^{wt}$ and RAS^{wt} responded. In $BRAF^{mt}$ cell lines in which resistance emerged to vemurafenib or trametinib due to RAS or MEK1 mutations, SCH722984 had demonstrable activity. These data prompted the first ERK inhibitor clinical trials for patients that initially responded to trametinib or vemurafenib but developed resistance.

ERK inhibitor	Target	Company	Clinical Phase
SCH772984	ERK1/2	Merck	Pre-clinical
FR180204 (reversible-ATP competitive)/ FR148083 (covalent)	ERK1/2	Astellas pharmaceuticals	Pre-clinical
GDC-0994	ERK1/2	Genentech/Array BioPharma	Phase I
CC-90003	ERK1/2	Celgene	Phase I
AZ13767370	ERK1/2	AstraZeneca	Pre-clinical
KO-947	ERK1/2	Kura Oncology	Phase I
LY3214996	ERK1/2	Eli Lilly	Phase I
CC-90003	ERK1/2	Celgene	Phase I
Ravoxertinib (GDC-0994, RG-7842)	ERK1/2	Genentech	Phase I
MK-8353, SCH900353	ERK1/2	Merck Sharp & Dohme	Phase I
BVD-523, Ulixertinib	ERK1/2	BioMed Valley Discoveries	Phase I/II

Table 1.3: ERK clinical inhibitors. Adapted from (Kidger et al., 2018; Ryan et al., 2015)

Furthermore, the combination of ERK and RAF inhibition is warranted for the same reason as RAF and MEK, due to reactivation of ERK signaling (Nissan et al., 2013). In fact, SCH772984 and other ERK inhibitors that work in a similar manner might function better

than MEK inhibitors due to the ability to block phosphorylation of ERK as well as inhibit the catalytic activity. Some of the current ERK inhibitors being evaluated in the clinic are listed in Table 1.3.

PI3K

The PI3Ks are heterodimeric lipid kinases that have catalytic and regulatory/adaptor subunits encoded by several genes and alternative splicing. The PI3Ks play several roles in the cell, from cellular growth, transformation and adhesion to survival and motility, which makes it an important player in cancer (Castellano and Downward, 2011). Additionally, the role of PI3K in the inhibition of apoptosis and promotion of tumorigenesis has been reported, cementing its role in cancer (She et al., 2005; Will et al., 2014). The PI3K family can be divided into three main classes of enzymes (class I, II and III), based on substrate specificity, regulation and structure. The catalytic subunits for class I PI3Ks, the most well characterized class, are p110α, p110β, p110γ and p110δ. These are the products of the PIK3CA, PIK3CB, PIK3CG and PIK3CD genes, respectively (Castellano and Downward, 2011; Vivanco and Sawyers, 2002). p110 subunits are often divided into class IA groups which bind the p85 subunit (α, β and δ), and class IB, which do not.

Activation of PI3K can occur through three independent pathways that are initiated by ligand binding to RTKs, which causes dimerization, auto phosphorylation and activation (Pawson and Nash, 2003; Schlessinger, 2002). The first occurs upon the SH2 domain of p85 binding to phospho-YXXM motifs in the RTKs, which triggers p110 catalytic activation (Figure 1.4) (Domchek et al., 1992). Activation can also occur through the adaptor protein GRB2, which can bind phospho-YXN motifs in the RTK (Pawson, 2004).

GRB2 can bind to the scaffolding protein GAB, which activates p85. The third pathway to initiate PI3K signaling occurs through activation of RAS, which occurs through GRB2 binding SOS which leads to activation of RAS. RAS can then directly activate the p110 subunit of PI3K independently of p85 (Castellano and Downward, 2011). PI3K has been a target of numerous drug discovery efforts, listed in Table 1.4.

PI3K inhibitor	Target	Company	Clinical Phase
Buparlisib (BKM120)	Pan-PI3K	Novartis	III
Pictilisib (GDC-0941)	Pan-PI3K	Genentech	II
Sonolisib (PX-866)	Pan-PI3K	Oncothyreon	II
Pilaralisib	Pan-PI3K	Sanofi Oncology/Exelixis	II
Copanlisib	Pan-PI3K	Bayer	FDA approved
Dactolisib (BEZ235)	PI3K/MTOR	Novartis	Discontinued
Omipalisib (GSK2126458)	PI3K/MTOR	GlaxoSmithKline	I
Gedatolisib	PI3K/MTOR	Wyeth/Pfizer	III
Apitolisib (GDC-0980)	PI3K/MTOR	Genentech	I
Bimiralisib (PQR309)	PI3K/MTOR	PIQUR Therapeutics	I/II
Alpelisib	p110α	Novartis	III
Taselisib	p110β-sparing	Roche (Genentech)	III
GSK2636771	p110β	GlaxoSmithKline	I/II
AZD8186	p110β	AstraZeneca	I
SAR260301	p110β	Sanofi	I
Nivolumab (IPI-549)	p110γ	Infinity Pharmaceuticals	I

Table 1.4: PI3K clinical candidates. Adapted from (Janku, 2017), with additional information from the NCI and ASCO websites.

Prevalence of Aberrant KRAS Signaling in GI Cancers

Colorectal Cancer

Colorectal cancer (CRC) is the second leading cause of cancer related deaths worldwide (Jemal et al., 2011). According to the 2017 American Cancer Society statistics, early stage disease (Stage I – III) 5-year survival rates exceed 70% on average, while patients with distant (metastatic) disease have 5-year survival rates of ~13-14% (Siegel et al., 2017). It is recognized that metastatic colorectal cancer (mCRC) has a dismal prognosis and lacks effective therapies. Presently, mCRC patients are treated with a combination of fluoropyrimidine (5-fluorouracil or 5-FU) or capecitabine with either oxaliplatin (FOLFOX) or irinotecan (FOLFIRI) (Prenen et al., 2010). However, two monoclonal antibodies targeting epidermal growth factor receptor (EGFR) have been approved for treatment of mCRC: panitumumab and cetuximab. Cetuximab competitively inhibits ligand binding and has shown clinical activity as a single agent and in combination with irinotecan for the treatment of mCRC (Cunningham et al., 2004; Jonker et al., 2007; Saltz et al., 2004; Sobrero et al., 2008). Despite the high incidence rate of KRAS mutations in colorectal cancer, a consensus on the prognostic effect of KRAS mutations does not exist based on numerous studies of all stages of CRC. However, it has been shown that patients harboring a KRAS or BRAF mutation are not responsive to EGFR-based therapies (Lievre et al., 2006). KRAS mutations have therefore become a biomarker that preclude patients from EGFR based therapies, creating a critical unmet need for this metastatic CRC patient population. 40-50% of patients diagnosed with CRC have a mutation in KRAS, which makes these patients viable candidates for therapies targeting RAS signaling (covered in Chapter 3).

Pancreatic Cancer

Pancreatic cancer is currently the third leading cause of cancer-related deaths in the United States and has the lowest 5-year relative survival rate of any cancer (Rahib et al., 2014; Siegel et al., 2016). Projections predict it will surpass breast and colorectal cancer by 2030 to become the second leading cause of cancer-related deaths (Rahib et al., 2014). General advancements in screening, prevention and treatment of cancer has positively impacted cancer incidence and mortality rate for most cancers, while pancreatic cancer has lagged in this area. This disease is recalcitrant to chemotherapeutic approaches as first-line therapy and recently approved therapies afford only modest improvements in survival. Few targeted therapies exist for the treatment of pancreatic cancer and because of poor outcome with standard therapies, patients are often encouraged to participate in clinical trials. Consequently, the 5-year survival rate since the 1970's has only improved from 3% to 8%, and patients diagnosed with metastatic pancreatic cancer have a life expectancy of 2.8-5.7 months (Carrato et al., 2015; Siegel et al., 2016). There exists a critical unmet need for development of novel treatments for patients diagnosed with this disease.

The most commonly mutated genes in pancreatic cancer are KRAS, which occurs in over 90% of tumors, and CDKN2A (>90% of cases), the gene encoding for endogenous CDK4/6 inhibitor p16ink4a (Jaffee et al., 2002; Liggett and Sidransky, 1998; Maitra and Hruban, 2008). p16 is a potent suppressor of oncogenic transformation and a key mediator of Ras induced senescence, a tumor suppressor phenomenon that occurs upon oncogenic transformation of fibroblasts with the Ras oncogene that causes them to senesce (Serrano et al., 1997). CDK4/6 is a kinase critical for progression of the cell cycle and is widely considered to be the gatekeeper of the restriction point in the G1 to S transition phase (Blagosklonny and Pardee, 2002). A therapeutic approach dual-targeting MEK and CDK4/6 is covered in Chapter 2.

Dissertation Objectives

The goal of this dissertation is to delineate novel strategies for the treatment of patients diagnosed with RAS activated pancreatic or colorectal cancer. Novel strategies explored here include dual-targeting of MEK and CDK4/6 as well as the rational design and evaluation of a novel dual-inhibitor of EGFR and PI3K (MTX-211). The following individual chapters describe two very different approaches to develop improved therapies for the treatment of pancreatic and colorectal cancer, one involving the use of pre-existing agents and the other involving the design of new agents.

Chapter 2: Co-targeting MEK and CDK4/6 in pancreatic cancer and discovery of predictive biomarkers of activity.

Chapter 3: Design and evaluation of the novel, first-in-class small molecule dual EGFR/PI3K inhibitor MTX-211 for its potential utility in combination with MEK inhibition in colorectal cancer.

Appendix A

Information presented and reviewed in Chapter 1 was published in Cancer Discovery.

Maust, J.D., Whitehead C.E., Sebolt-Leopold, J.S. (2018) Oncogenic Mutants of *MEK1*: A Trilogy Unfolds. Cancer Discovery. doi:10.1158/2159-8290.CD-18-0192

Chapter 2: Co-Targeting MEK and CDK4/6 to Treat KRAS Mutant Cancer

Summary

The ineffectiveness of chemotherapy in patients with pancreatic cancer highlights a critical unmet need in pancreatic cancer therapy. Two commonly mutated genes in pancreatic cancer, KRAS and CDKN2A, have an incidence exceeding 90%, supporting investigation of dual targeting of MEK and CDK4/6 as a potential therapeutic strategy for this patient population. An *in vitro* proliferation synergy screen was conducted to evaluate response of a panel of high passage and patient-derived pancreatic cancer models to the combination of trametinib and palbociclib to inhibit MEK and CDK4/6, respectively. Two adenosquamous carcinoma models, L3.6pl and UM59, stood out for their high synergy response. *In vivo* studies confirmed that this combination treatment approach was highly effective in subcutaneously implanted L3.6pl and UM59 tumor-bearing animals. Both models were refractory to single agent treatment. Reverse phase protein array analysis of L3.6pl tumors excised from treated animals revealed strong down regulation of cyclooxygenase-2 (COX-2) expression in response to combination treatment. Expression of COX-2 under a CMV-driven promoter and shRNA knockdown of COX-2 both led to resistance to combination treatment. Our findings suggest that COX-2 may be involved in the improved therapeutic outcome seen in some pancreatic tumors that fail to respond to MEK or CDK4/6 inhibitors alone but respond favorably to their combination.

Introduction

Pancreatic cancer is the third leading cause of cancer-related deaths in the US and has the lowest 5-year relative survival rate of any cancer (Rahib et al., 2014; Siegel et al., 2016). This disease is recalcitrant to chemotherapeutic approaches and recently approved therapies afford only modest improvements in survival. Consequently, the 5-year survival rate since the 1970's has only improved from 3% to 8% (Siegel et al., 2016). There exists a critical unmet need for development of novel treatments for patients diagnosed with this disease.

The most commonly mutated genes in pancreatic cancer are KRAS, which occurs in over 90% of tumors, and CDKN2A (inactivated in >90% of cases), the gene encoding the endogenous CDK4/6 inhibitor $p16^{INK4a}$ (Cox et al., 2014; Jaffee et al., 2002; Liggett and Sidransky, 1998; Maitra and Hruban, 2008). KRAS is a small GTPase that activates the mitogen activated protein kinase (MAPK) signaling pathway, whereas p16 is a potent suppressor of oncogenic transformation and a key mediator of RAS induced senescence (Serrano et al., 1997). While MEK inhibitors have exhibited potent *in vitro* activity in KRAS mutant tumor cells (Wee et al., 2009), the *in vivo* activity of these agents has been disappointing due to the development of resistance (Little et al., 2011; Poulikakos and Solit, 2011; Turke et al., 2012b; Wee et al., 2009).

An attractive target for MEK inhibitor-based combinations is CDK4/6, a kinase crucial for the transition from G1 to S phase (Blagosklonny and Pardee, 2002). In support of co-targeting MEK and CDK4/6, a synthetic lethal interaction between KRAS and CDK4 was found in non-small cell lung cancer (Puyol et al.). Furthermore, CDK4 was identified as a key driver of an alternative phenotype induced by MEK inhibition, but not genetic

extinction of NRAS in mouse models of melanoma (Kwong et al., 2012). Our laboratory as well as Kopetz and colleagues subsequently demonstrated *in vivo* efficacy of this combination approach in KRAS mutant patient-derived xenograft (PDX) models of colorectal cancer (Lee et al., 2016; Ziemke et al., 2015). Pancreatic cancers should also derive therapeutic benefit from this combination strategy based on their genomic features. Specifically, activating KRAS mutations have been shown to initiate formation of premalignant lesions in mouse models of pancreatic cancer, while loss of p16 has been shown to enable their malignant progression (Bardeesy et al., 2006). Ectopic p16 expression can induce senescence and apoptosis when reintroduced into pancreatic cancer cell lines with CDKN2A deletions (Calbo et al., 2001). Since CDK4 and CDK6 are the sole targets of p16, a unique opportunity is present to leverage recently approved CDK4/6 inhibitors to recapitulate this phenotype in pancreatic cancer.

The effectiveness of dual targeting of MEK and CDK4/6 to treat pancreatic cancer has been reported for high passage models (Franco et al., 2016; Franco et al., 2014). The present report extends these findings to include patient derived xenograft (PDX) models of pancreatic cancer and concurrent phosphoproteomic profiling to identify potential prognostic biomarkers of response. We report here that two adenosquamous pancreatic models are highly responsive to dual targeting of these kinases both *in vitro* and *in vivo*. We further find that genetic manipulation of cyclooxygenase-2 (COX-2) expression, which is highly expressed in both of these models, blunts therapeutic effectiveness of combination treatment. Our results therefore provide the impetus to further explore the prognostic role of COX-2 to aid in the identification of a subpopulation of pancreatic cancer patients who

might derive the greatest therapeutic benefit from combination therapy directed against MEK and CDK4/6.

Materials and Methods

Chemicals

Trametinib and binimetinib (MEK162) were purchased from LC Laboratories. Ribociclib (LEE011) was purchased from Chemietek. Palbociclib isethionate was purchased from Selleckchem. Drug stocks were dissolved in DMSO at 10 mM and stored at -20 °C.

Cell proliferation assays

For growth inhibition and synergy analyses, cells were seeded in white-walled/clear bottom tissue culture treated 96-well plates at 5,000-10,000 cells/well and allowed to adhere for 24 hours followed by addition of growth media containing serial dilutions of trametinib, palbociclib, or both drugs in combination. Cells were incubated for 5 days in the continuous presence of drug or DMSO and viability was measured using CellTiter-Glo (Promega). Viability was calculated as a percentage of DMSO treated cells. Concentration response curves were modeled using a nonlinear regression curve fit with a sigmoidal concentration response using GraphPad Prism 6. Synergy plot calculations were performed using Combenefit software (Cancer Research UK Cambridge Institute) and scores were generated using Chalice Bioinformatics Software (Horizon Discovery Group), both using the Loewe model of synergy.

Cell lines

All cell lines were cultured at 37°C in 5% CO2 in 10% FBS and 1% penicillin/streptomycin (Thermo Fisher Scientific). L3.6pl, pL45, MiaPaCa-2, Panc-1 and HS766T cell lines were

grown in DMEM. HPAFII was grown in EMEM. ASPC1, Bxpc-3 and Panc10.05 were cultured in RPMI media. The PDX models UM8, UM15, UM16, UM19, UM32, UM53, UM59, UM81, UM90, UM91 and UM123 originated from patients undergoing surgical resection at University of Michigan and were established to grow in animals and in culture. All PDX lines were grown in RPMI media. All lines were negative for mycoplasma contamination when tested with MycoAlert Mycoplasma Detection Kit (Lonza). All high passage cell lines were authenticated by short tandem repeat (STR) profiling at the University of Michigan Sequencing Core.

Cell cycle analysis

Cells were seeded into 6 well plates at ~150,000 cells/well and treated the next day at the indicated concentrations, with a maximum DMSO concentration of 0.1%. Cells were harvested with 0.05% trypsin, washed twice with PBS and fixed with 70% ethanol at 4°C for at least 24 hr. Cells were washed twice with PBS and incubated for 30 minutes in a solution of 50 μg/ml propidium iodide (Life Technologies, P3566), 0.1% Triton X- 100 (Sigma-Aldrich, T9284), 50 μg/ml RNase A (Qiagen, 1007885) and PBS. Data were collected on a Cyan ADP Analyzer (Beckman Coulter), with collection of at least 10,000 events. The analysis was performed using flow cytometry analysis software ModFit LT V4.0.5 (Verity Software House).

Animal studies

Cells (1×10^6) were injected subcutaneously into the region of the right axilla of 6- to 7-week-old female NCR nude mice (NCRNU-F sp/sp CrTac:NCr-*Foxn1*^{nu}, Taconic) in a 50:50 mixture of DMEM/F12 and Matrigel. Tumors were allowed to grow until 150-300 mm^3, at which time mice were randomized into different treatment groups (4-5 animals per

group). Trametinib and palbociclib were administered as a fine suspension in 0.5% hydroxypropyl methylcellulose (HPMC) with 0.2% Tween-80 or saline, respectively, based on individual animal body weight (0.2 ml/20 g), once daily via oral gavage. Tumor volumes were measured using calipers and calculated using the formula: tumor volume = (length*width^2)/2. Efficacy was calculated as the ratio of change in mean tumor burdens at time t ($_{\Delta}T/_{\Delta}C$) where $_{\Delta}T$ and $_{\Delta}C$ is calculated as mean tumor burden at time t minus the mean tumor burden on the first day of treatment. Percent regression is calculated as [–($_{\Delta}T/T_0$)*100], where T_0 is initial body weight of treated animals. Tumor growth delay was calculated based on the time required for the mean to reach ~750 mm^3. Where applicable, statistical significance between groups was calculated on the last day of treatment via one-way ANOVA analysis with multiple comparisons between all treatment arms.

Western blotting and reverse-phase protein array (RPPA) analysis

Cells were harvested by scraping in the presence of radioimmunoprecipitation (RIPA) buffer plus phosphatase and protease inhibitors (Roche). Samples were denatured and normalized to 1 μg/μl in LDS sample buffer (ThermoFisher) and 62.5 mM DTT (ThermoFisher). For immunoblotting, multiple independent immunoblots were used to present data from single experiments. Loading controls were probed on the same blot, with a representative image shown for experiments with multiple antibodies. Ten micrograms of protein were run on precast 4-12% polyacrylamide gels (ThermoFisher). The following antibodies were used: pRb S780, pRb S807/11, Cdc6, total Rb, pERK, cyclin D1, COX-2, EGFR Y1068, FOXM1 (Cell Signaling), Pdcd4 (Rockland), Beta-actin and GAPDH (Abcam). For RPPA analysis, tumors were homogenized and protein was extracted utilizing NP-40 lysis buffer plus phosphatase and protease inhibitors. Samples were

denatured and normalized to 1 μg/μl in SDS sample buffer/β-mercaptoethanol (ThermoFisher) and shipped to the MD Anderson RPPA Core Facility, where samples were profiled and processed. Per the protein loading protocol, all antibodies were median centered per antibody, then median centered per sample, and log2 normalized. Trametinib, palbociclib and combination treated samples were compared to control samples using a two-sample t-test for each treatment/control comparison. T-test p-values were adjusted for multiple testing using the FDR method and resulting qValues < 0.1 were considered to represent significant changes. Significant antibodies and treatment sample replicates are clustered using agglomerative hierarchical clustering with a Euclidean distance metric.

Immunohistochemistry

Tissues were fixed in 10% NBF, embedded in paraffin and sectioned according to standard procedures. The Ki67 antibody was obtained from Cell Signaling Technology. Representative images were obtained with a Nikon E-800 microscope, Olympus DP71 digital camera, and DP Controller software. To quantify the ratio of Ki67 positive nuclei to total nuclei, 5-8 snapshots of different sections of the tumor were used to determine the average Ki67 nuclear ratio using online software tool ImmunoRatio (Tuominen et al., 2010). Statistical significance was calculated between groups using one-way ANOVA (GraphPad Prism).

COX-2 plasmid construction and shRNA transduction

Full length human COX-2 cDNA was excised as a BamHI/XhoI fragment from the huCOX-2 pcDNA5/FRT/TO construct, generously provided by Dr. William Smith (University of Michigan, Ann Arbor, MI), and ligated into pcDNA3.1. Transfections of L3.6pl cells were performed in six-well dishes using huCOX-2 pcDNA3.1 linearized with

Bgl II (2.5 µg plasmid/well) and Lipofectamine 2000 (ThermoFisher) according to manufacturer's instructions. Clones stably expressing full length human COX-2 were established after selection in medium containing 1 mg/mL G418 (ThermoFisher). Control (sc-108080) and COX-2 (sc-29279-V) shRNA lentiviral particles (Santa Cruz Biotechnology) were transduced into cells according to manufacturer's directions and clones were established after selection with 10 µg/ml puromycin.

Reverse-transcription quantitative PCR (RT-qPCR)

Total RNA was isolated from cell lines treated for 5 days using the RNeasy Mini Kit (Qiagen). First-strand cDNA was reverse-transcribed from total RNA using the SuperScript III First-Strand Synthesis System (Invitrogen) according to the manufacturer's instructions. Quantitative targeted amplification of cDNAs was performed using Taqman Gene Expression Assays primer/probe sets for COX-2 (Hs00153133_m1), Pdcd4 (Hs00377253_m1), GAPDH (Hs02786624_g1) and Fast Advanced Master Mix (Thermo Fisher) according to the manufacturer's instructions. GAPDH was used as an endogenous control. The amplification conditions for the ViiA 7 Real-Time PCR System (Applied Biosystems) consisted of an initial step of 2 min at 50°C and 10 min at 95°C followed by 40 cycles of 15 sec 95°C, 1 min 60°C. For treated cells, data were analyzed using the $\Delta\Delta C_t$ method and expressed as fold change over control. Data from the panel of cell lines were calculated as one C_t equals a 2-fold difference in expression and are represented as relative expression to the highest expressing cell line.

Results

Inhibitors of MEK and CDK4/6 synergistically inhibit pancreatic cancer cell line growth

Screening of high passage and PDX models of pancreatic cancer was carried out to identify models in which the combined action of trametinib and palbociclib showed the greatest degree of synergy. Cell lines showed a wide range of response to combination treatment, as depicted in Figure 2.1A where models are listed in the order of a consolidated synergy score. L3.6pl cells showed the highest degree of synergy followed by UM59 cells, with both models exhibiting at least a two-fold increase over the panel median (2.35) (Fig. 2.1B). Synergistic response was greatest in response to the combination of trametinib and palbociclib at concentrations of 10 nM and 1 μM, respectively, concentrations which led to a median reduction in viability of 59% across the panel (Supplementary Fig. 2.7/S1A). These optimal concentrations are consistent with our previous work in colorectal cancer models (Ziemke et al., 2015) as well as the studies of others carried out in lung cancer models (Tao et al., 2016). A similar degree of synergy was observed when L3.6pl cells were treated with the MEK inhibitor binimetinib (Cheng and Tian, 2017) and the CDK4/6 inhibitor ribociclib (Duso et al., 2018), confirming that synergy is not likely attributable to off target activities (Supplementary Fig. 2.7/S1B). Comparative analysis of concentration response curves for high (L3.6pl), intermediate (UM59) and low (Bxpc-3 and Panc10.05) synergy models is shown in Figure 2.1C to better understand the relationship between synergy and sensitivity. As shown here, the degree of synergy decreased as the concentration of trametinib was raised. No synergy was observed in Bxpc-3 and Panc10.05 cells at concentrations greater than approximately 20 nM, where the concentration response curves for trametinib single agent and the combination treatment plots intersect. In contrast,

the concentration response curves for L3.6pl cells never intersected, since viability could not be reduced beyond 50% despite use of high (1-10 μM) concentrations of trametinib. These cells are also refractory to palbociclib treatment alone (Supplementary Figure 2.8/S2A).

Co-targeting MEK and CDK4/6 leads to profound G1 arrest

MEK and CDK4/6 have both been shown to play a role in controlling cell cycle progression, either through induction of cyclins or phosphorylation of Retinoblastoma protein (Rb), a master regulator of G1-S progression. Cell cycle studies carried out in the L3.6pl and UM59 models confirmed that combination treatment with trametinib and palbociclib induces a strong time-dependent G1 arrest at concentrations previously shown to be synergistic (Fig. 2.2A). Immunoblotting analysis further revealed that expression levels of Cdc6, a protein critical for initiation of DNA synthesis and pre-replication complex assembly (Braden et al., 2008; Liu et al., 2000), and phosphorylated Rb, were selectively reduced in L3.6pl cells treated with the combination, consistent with G1 arrest (Fig. 2.2B). These data suggest that synergy between trametinib and palbociclib to inhibit cell growth is driven at least in part by enhancement of G1 arrest.

Uncoupling of Cyclin D1 and pRB expression in response to MEK inhibition is cell line dependent

Immunoblotting analyses confirmed that phosphorylated ERK levels were suppressed by trametinib treatment in all lines at concentrations consistent with a reduction in viability (Fig. 2.3A & 2.3B). MEK inhibition additionally led to a reduction of total and phosphorylated Rb levels in a concentration-dependent manner. This result is not surprising, as MAPK signaling has been shown to contribute to control of cyclin D1

expression in response to growth factor stimulation (Lavoie et al., 1996), thereby indirectly reducing CDK4/6 phosphorylation of Rb. Cyclin D1 levels were recalcitrant to MEK inhibition in cell lines previously found to be most responsive to combination treatment (L3.6pl, UM59), despite reduction in pRb expression. This reduction in pRb can be explained by increased p27 expression in response to trametinib treatment (Supplementary Fig. 2.8/S2B), which has been shown to bind and contribute to inhibition of the CDK4/cyclin D complex (Ray et al., 2009). In contrast, models showing a low degree of synergy (Panc10.05, Bxpc-3) exhibited significant reduction in levels of both cyclin D1 and pRb in response to trametinib single agent treatment. While UM59 may be as sensitive to trametinib as Panc10.05 and Bxpc-3 (Fig. 2.3A), trametinib clearly shows cell line-dependent effects on expression of these cell cycle proteins, likely contributing to comparative differences in synergistic potential with palbociclib. Collectively, these data suggest that tumors exhibiting MEK-dependent uncoupling of cyclin D1 and pRb expression *in vitro* may be most sensitive to dual targeting of MEK and CDK4/6.

Combination treatment with trametinib and palbociclib provides therapeutic benefit in vivo

Based on the high degree of *in vitro* synergy seen when MEK and CDK4/6 are both inhibited in L3.6pl cells, we evaluated the *in vivo* efficacy of the combination of trametinib and palbociclib in L3.6pl tumor-bearing animals. Daily treatment was initiated when tumors were advanced (~300 mm^3) for a total of 7 days. No signs of toxicity were noted at the doses administered. Neither single agent elicited a meaningful effect on $_{\Delta}T/_{\Delta}C$ or tumor growth delay after cessation of treatment (Fig. 2.4A). In contrast, a $_{\Delta}T/_{\Delta}C$ of 28% and a tumor growth delay of 10 days was observed in the combination arm. Tumors were harvested on the last day of treatment for immunohistochemical analysis of Ki67

expression (Fig. 2.4B-C), revealing a significant reduction in expression in tumors from the combination group compared to the control and single agent groups. The results from this study were subsequently confirmed with less advanced L3.6pl tumors at treatment initiation, showing a $_{\Delta}T/_{\Delta}C$ of 1% and a 15 day growth delay, versus 1 & 2 days for trametinib and palbociclib, respectively (Supplementary Fig. 2.9/S3).

COX-2 expression is downregulated and Pdcd4 is upregulated in response to co-targeting of MEK and CDK4/6

L3.6pl tumors evaluated for *in vivo* efficacy were further analyzed for selective proteomic changes as a consequence of combination treatment. Two proteins, COX-2 and programmed cell death 4 (Pdcd4), emerged from Reverse Phase Protein Array (RPPA) analyses showing inverse dysregulation in response to treatment with trametinib and palbociclib (Fig. 2.4D). COX-2 expression showed the highest magnitude of change in the combination arm among all the proteins measured in the RPPA platform. Palbociclib treatment caused a small decrease in COX-2, but this change was not significant. Others have noted the role of palbociclib in mediating a c-jun-dependent decrease in COX-2 expression, but the impact of this change outside of the epithelial-mesenchymal transition is unclear (Qin et al., 2015). An induction of Pdcd4 expression in response to the combination of trametinib and palbociclib was also observed, suggesting that dual targeting of MEK and CDK4/6 leads to initiation of cell death signaling. It appears that this effect is independent of apoptosis, as no significant changes were observed in PARP, caspase-3, 7 or 8 in the RPPA dataset (Fig. 2.4D). Subsequent immunoblotting studies were carried out to confirm that COX-2 is downregulated and Pdcd4 is upregulated in response to combination treatment with trametinib and palbociclib (Fig. 2.4E). Modulation of these biomarkers at the RNA level was addressed by carrying out RT-qPCR analysis of treated

L3.6pl and UM59 cells, showing a reduction of COX-2 and an increase in Pdcd4 in treated samples of both cell lines (Supplementary Fig. 2.10/S4A; UM59 protein expression changes shown in Fig. 2.10/S4B). Given that a decrease in COX-2 expression was the most significant change associated with activity in this study, we tested the COX-2 inhibitors celecoxib and NS-398 in the L3.6pl and UM59 models. Neither COX-2 inhibitor elicited significant anti-proliferative effects at concentrations lower than 50 μM. Concentrations in this range have been associated with COX-independent effects and have not been achieved in humans (Supplementary Fig. 2.10/S4C) (Davies et al., 2000; Hawk et al., 2002). The lack of efficacy is not surprising, as significant increases in COX-2 expression in response to these inhibitors has been shown (Ferguson et al., 1999).

Ectopic overexpression of COX-2 lowers sensitivity to dual inhibition of MEK and CDK4/6

Based on the reduction of COX-2 expression seen when cells were co-treated with trametinib and palbociclib, experiments were undertaken to explore a direct role for COX-2 in affecting sensitivity to dual inhibition of MEK and CDK4/6. FOXM1, a transcription factor whose stability is controlled by CDK4/6 phosphorylation (Anders et al., 2011) and whose activity and cellular localization is controlled by ERK (Ma et al., 2005b), could be involved in driving this reduction in COX-2. This is possible considering FOXM1 activity has been implicated in promoting transcription of COX-2 in conjunction with Sp1 (Xu and Shu, 2013a). The expression of FOXM1 is decreased selectively in L3.6pl cells exposed to combination treatment (Fig. 2.5A). Therefore, we hypothesized that combination treatment leads to synergy by decreasing expression of COX-2 through abrogation of FOXM1 activity. To test this hypothesis, a COX-2 plasmid under control of the cytomegalovirus (CMV) promoter was constructed for ectopic expression in L3.6pl cells. In this manner,

removal of endogenous control of COX-2 expression would render cells unresponsive to FOXM1. After transfection, clones were selected and lysates were generated to track COX-2 expression, whereupon clone L3.6pl-C5 was found to comparatively exhibit the highest amount of COX-2 (Fig. 2.5B). Synergy of the parent line to the combination of trametinib and palbociclib was subsequently compared to that of the L3.6pl-C5 line and found to be significantly higher (synergy score, 7.35 vs 1.69, respectively). This finding suggests that overexpression of COX-2 by removing it from endogenous control influences the degree of synergy observed between trametinib and palbociclib. Importantly, response of the L3.6pl-C5 line to single agent treatment remained unchanged in comparison to the parent line (Supplementary Fig. 2.11/S5A). However, the L3.6pl-C5 line showed a blunted shift in the concentration response curves when combining both agents at clinically relevant concentrations (1 to 10 nM trametinib and 100 nM to 1 μM palbociclib) (Supplementary Fig. 2.11/S5B). This provides evidence that, although changes in COX-2 expression may not significantly affect response to either single agent, therapeutic efficacy of the combination is reduced upon alternate transcriptional control of COX-2.

To confirm these findings *in vivo*, the parent and C5 lines were compared in tumor-bearing animals in a head to head study comparing efficacy from single agent vs combination therapy (Fig. 2.5C). On the last day of treatment, combination treated animals implanted with the parent line exhibited a $_{\Delta}T/_{\Delta}C$ value of 17%, confirming the *in vitro* synergy seen with this combination against the L3.6pl model. In contrast, animals implanted with COX-2 overexpressing C5 tumors, exhibited a $_{\Delta}T/_{\Delta}C$ value of 57%. Lysates generated from tumors harvested on the last day of treatment showed decreased FOXM1 expression in both studies, consistent with earlier *in vitro* studies. Furthermore, a greater ability of

combination treatment to decrease COX-2 expression was observed in the parent line in comparison to L3.6pl-C5 (Supplementary Fig. 2.11/S5C). These results suggest that endogenous COX-2 expression in a model with high COX-2 expression is critical for activity and removing this factor substantially reduces *in vivo* efficacy of combination therapy in the L3.6pl model.

Knockdown of COX-2 reduces synergy to MEK and CDK4/6

Studies were designed to test the hypothesis that reduction of COX-2 expression through transcriptional control affects response to combination treatment. To explore the impact of COX-2 knockdown, L3.6pl and UM59 cells were virally transduced with COX-2 and control shRNA vectors. Despite harvesting numerous clones (>30), COX-2 was not successfully knocked down in UM59 cells, presumably due to reliance on expression for survival. In L3.6pl cells, transduction resulted in a successful knockdown of COX-2 (Fig. 2.5D). When these cells were evaluated for their response to combination treatment, knockdown cells showed reduced synergy in comparison to control cells (Fig. 2.5E). This reduction in synergy is consistent with results obtained with cells previously transfected with CMV-controlled COX-2 (Fig. 2.5F), confirming the impact of COX-2 expression levels on therapeutic outcome in this model.

Low innate expression of COX-2 correlates with reduced benefit to combination treatment

In L3.6pl tumors, COX-2 appears to play a role in potentiating response to combination treatment. We explored the potential of COX-2 to serve as a prognostic marker of response to combination treatment across a broad panel of pancreatic cancer models. Lysates prepared from our pancreatic cell line panel were probed for expression of COX-2 (Fig.

2.6A). COX-2 appears as several bands, which likely represent different potential post-translational modifications, since this protein has multiple sites for potential N-linked glycosylation, phosphorylation, and myristoylation (Wennogle et al., 1995). The expression levels of COX-2 in these lines was confirmed via RT-qPCR of RNA harvested from the panel (Supplementary Fig. 2.12/S6A). L3.6pl and UM59 showed relatively high expression of COX-2 alongside Bxpc-3. Whereas L3.6pl and UM59 both exhibited a high degree of *in vitro* synergy to the combination of trametinib and palbociclib, a low synergy score was observed for the Bxpc-3 model. The lack of *in vitro* synergy seen here for Bxpc-3 cells is consistent with the observation that this model is exquisitely sensitive to MEK inhibition alone both *in vitro* and *in vivo* (Allen et al., 2003). Like L3.6pl, the UM59 model, which exhibited the second highest *in vitro* synergy score, showed improved therapeutic response when exposed to combination treatment, as evidenced by a 16-day tumor growth delay and $_{\Delta}T/_{\Delta}C$ of 5% compared to ineffective single agent therapies (Fig. 2.6B). Neither L3.6pl nor UM59 tumors were responsive to MEK inhibition alone. Panc-1 and Panc10.05 tumors, which exhibit low COX-2 expression (Supplementary Fig. 2.12/S6B) and low *in vitro* synergy scores, showed somewhat improved response in the combination arms, as reflected by a $_{\Delta}T/_{\Delta}C$ value of 14% and percent regression of 21%, respectively. Most notably, one tumor-bearing mouse for each of these models showed a complete regression when treated with the combination. However, the overall improvement in response of these models to combination treatment compared to either single agent, as measured by tumor growth delay or $_{\Delta}T/_{\Delta}C$, was reduced compared to the L3.6pl and UM59 models, which are characterized by high COX-2 expression. Therefore, consistent with our *in vitro* data,

tumors exhibiting low COX-2 expression do not appear to derive as much added benefit from the combination regimen.

Discussion

Novel therapeutic approaches for the treatment of pancreatic cancer are urgently needed due to the lack of significant improvements in patient survival over the past 40 years. Recent clinical approval of the CDK4/6 inhibitor palbociclib provides potential new opportunities for the treatment of cancers harboring CDKN2A (p16ink4a) aberrations, which includes the majority of pancreatic cancers. Due to the high incidence of KRAS mutations in pancreatic cancer and their co-occurrence with CDKN2A inactivation, a combination therapy approach targeting MEK and CDK4/6 was evaluated here. Cell line synergy screening was carried out in both high passage and PDX models, whereupon two lines, L3.6pl and UM59, exhibited at least a twofold greater response over the median. Both models, when implanted *in vivo*, proved to be refractory to single agent treatment, while deriving substantial therapeutic benefit from the combination approach.

Importantly, co-targeting MEK and CDK4/6 was further found to potentiate cell cycle arrest in both L3.6pl and UM59 cells over that with single agent CDK4/6 inhibition. The prominent G1 arrest observed in our studies was confirmed by synergistic reductions in total levels of Cdc6, a protein critical for initiation of DNA synthesis and implicated in response to CDK4/6 modulation and RB output (Braden et al., 2008). Furthermore, reduction was seen in the expression of FOXM1, a transcription factor involved in cell cycle progression. It is a target of both ERK (Ma et al., 2005b) and CDK4/6 (Anders et al., 2011), regulating cellular localization and stability, respectively.

Concurrent phosphoproteomic profiling of treated L3.6pl tumors revealed the interesting finding that COX-2 expression was downregulated in response to dual inhibition of MEK and CDK4/6. COX-2 is known for its role in mediating inflammation and promoting tumorigenesis in colorectal cancer and pancreatic cancer (Eberhart et al., 1994; Hill et al., 2012; Ogino et al., 2008; Yip-Schneider et al., 2000). While COX-2 expression can be affected by inhibition of MAPK signaling (Elder et al., 2002; Huang et al., 2013; Schmidt et al., 2003), it is unclear how inhibition of CDK4/6 synergizes with MEK to decrease expression of COX-2 in the absence of an effect by MEK inhibition. The significant reduction that we see in expression of COX-2 upon dual inhibition of MEK and CDK4/6 may ensue from reduced levels of FOXM1, as others have reported that COX-2 is in part controlled by FOXM1 activity (Ahmed et al., 2015; Xu and Shu, 2013a; Xu and Shu, 2013b). Another protein whose expression was significantly altered by combination treatment in L3.6pl tumors was programmed cell death 4 (Pdcd4), which showed significant upregulation. Studies have shown that this novel tumor suppressor negatively regulates gene expression by inhibiting Sp1/Sp3 binding at important motifs (Leupold et al., 2007) and may play a role in inactivating PI3K/AKT signaling and suppressing CCND1 and CDK4 expression in NCSLC (Zhen et al., 2016). This finding has potential implications for the current study in which FOXM1 is reduced by combination treatment, as other groups have shown FOXM1 cooperating with Sp1 to promote COX-2 expression (Xu and Shu, 2013a). Pdcd4 may be regulated itself by direct phosphorylation through AKT (Palamarchuk et al., 2005). It is intriguing that studies have identified Pdcd4 to be in part responsible for the anticancer effects of COX-2 inhibitor NS-398 (Zhang and DuBois, 2001) in colon carcinoma. Further studies are warranted to elucidate signaling dynamics

of these findings and further studies are ongoing to determine possible links. However, our studies unequivocally demonstrate that combining trametinib and palbociclib elicits a significant reduction of Ki67 staining in L3.6pl tumors, accompanied by a strong reduction in COX-2 and an increase in Pdcd4, both *in vivo* and *in vitro*.

COX-2 was expressed under CMV promoter control to test the hypothesis that transcriptional control of COX-2 was responsible for the reduction in expression seen. Ectopic expression of COX-2 increased resistance to combination therapy efficacy and blunted the reduction of COX-2 seen in response to combination treatment. However, a modest but significant reduction was still seen in L3.6pl-C5 cells. This could be explained by a low level of endogenous COX-2 that continues to be expressed in these cells. Post-translational degradation mechanisms may also be in place that are being induced by combination treatment. Reports indicate caveolin-1 co-localizes with COX-2 at the plasma membrane (Liou et al., 2001; Perrone et al., 2007) and participates in direct degradation of COX-2 (Chen et al., 2010). As a result, studies are warranted to investigate the role of caveolin-1 in the degradation of COX-2 in cells treated with combination therapy, as a modest increase in caveolin-1 expression was observed in the RPPA dataset in the combination arm. Furthermore, knockdown of COX-2 in L3.6pl cells blunted the synergistic response in comparison to control cells, confirming a role for COX-2 in mediating response to co-inhibition of MEK and CDK4/6. In summary, removing COX-2 gene expression from endogenous control, either through knockdown or expression of CMV-promoter driven COX-2, reduces synergistic response. This is expected, as modulation of COX-2 expression via control of FOXM1 is ostensibly what leads to synergy when co-inhibiting MEK and CDK4/6. It is important to keep in mind that several models

in our study are exceptionally sensitive to either trametinib or palbociclib alone when tested *in vitro*. Our data suggest that the usefulness of a synergy-based *in vitro* screen is biased towards models which show poor single agent activity. In particular, the L3.6pl model scored the highest in the *in vitro* combination screen and was subsequently shown to elicit no benefit from either single agent *in vivo*, while responding favorably to the combination. This is not to say that tumors exemplified by Panc-1 and Panc10.05, which produced low *in vitro* synergy scores, would not benefit from the combination *in vivo*. In fact, both of these models showed one complete regression in the combination arm. Their low synergy scores *in vitro* were partly due to their high *in vitro* sensitivity to trametinib alone. Nonetheless, trametinib monotherapy proved to be inactive in mice in all of the models tested here. This highlights the disconnect between the *in vitro* and *in vivo* settings where tumor heterogeneity, tumor microenvironment and adaptive signaling play a role.

Our goal was to identify models in which combination treatment disrupts signaling pathways that dictate their response. *In vitro* synergy screening facilitated the identification of two models, L3.6pl and UM59, that can derive substantial therapeutic benefit from dual targeting of MEK and CDK4/6. In those models, the interesting observation was made that COX-2 expression levels influence therapeutic outcome. Endogenous COX-2 expression appears to be critical for activity and its ablation substantially reduces *in vivo* efficacy of combination therapy. Interestingly, both models are adenosquamous carcinomas of the pancreas, a highly aggressive form of pancreatic cancer reported to show strong expression of COX-2 (Brody et al., 2009; Katz et al., 2011; Meitner et al., 1983; Okami et al., 1999; Wang et al., 2012). Further studies are warranted to better understand the prognostic significance of high expression of COX-2, a protein implicated in pancreatic cancer

development (Cascinu et al., 2007; Hill et al., 2012; Yip-Schneider et al., 2000). Our collective data suggest that such studies may help guide identification of a subpopulation of pancreatic cancer patients that could derive therapeutic benefit from co-targeting MEK and CDK4/6.

FIGURES

Figure 2.1

A

Cell Line	Synergy Score	KRAS	CDKN2A
L3.6pl	7.87 ± 0.71	G12D[4]	methylated[3]
UM59	4.69 ± 0.48	A146T	mut, p.D84G
UM8	4.13 ± 0.35	G12D	inactivated
UM90	3.55 ± 0.06	G12V	inactivated
UM91	3.48 ± 0.63	G12R	inactivated
UM32	3.29 ± 0.29	G12D	inactivated
pL45	3.05 ± 0.27	G12D[1]	methylated[1]
UM16	3.01 ± 0.37	wt	inactivated
UM15	2.32 ± 0.37	G12D	inactivated
HS766T	2.28 ± 0.58	Q61H[2]	Splice mut[3]
Mia Paca-2	2.27 ± 0.37	G12C[1]	HD[1]
UM19	2.26 ± 0.30	G12D	inactivated
UM53	2.22 ± 0.18	G12C	inactivated
UM123	2.09 ± 0.68	Q61H	inactivated
Panc-1	2.06 ± 0.10	G12D[3]	HD[3]
ASPC1	1.83 ± 0.03	G12D[1]	mut, p.L78fs-41[1]
HPAFII	1.54 ± 0.38	G12D[1]	HD[1]
Bxpc-3	1.43 ± 0.05	BRAF^{mt*,2}	HD[1]
UM81	1.26 ± 0.40	G12D	inactivated
Panc 10.05	0.71 ± 0.19	G12D[1]	inactivated

B

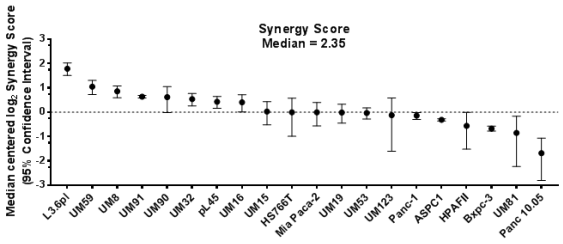

C

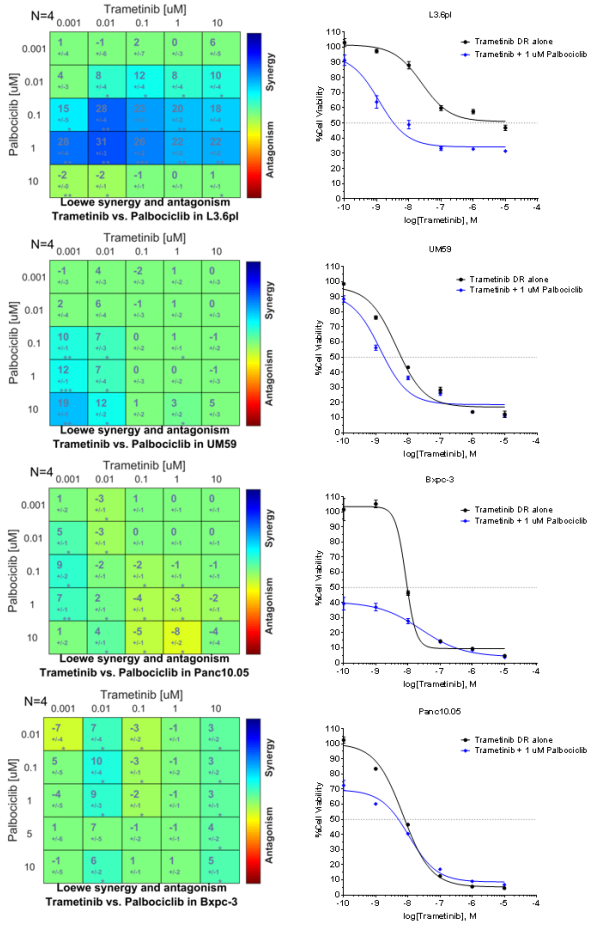

Figure 2.1: : Dual inhibition of MEK and CDK4/6 shows synergy in pancreatic cancer cell lines. (A) Evaluation of synergy in 20 pancreatic cancer cell lines identifies a range of response to combination treatment. Synergy scores represent a consolidated quantitative measure of proliferation in response to 25 unique combinations of trametinib and palbociclib concentrations after being treated for 5 days, as calculated by Chalice software. Scores represent the mean of 2-4 biological replicates +/- standard error of the mean (SEM). Genetic alterations for CDKN2A and KRAS are shown for each line. (B) Synergy scores were median centered and expressed as the $\log_2$ difference from the median with a 95% confidence interval. (C) Synergy plots generated by Combenefit showing the interaction between trametinib and palbociclib are shown for the highest and lowest responder models (n=4, technical replicates), alongside the primary data from the same experiment showing the shift in the trametinib concentration response curve upon addition of 1 μM palbociclib for each line (n = 4, +/- SEM). Data shown are representative and consistent with replicate experiments.

[1]ATCC database, [2]COSMIC (Forbes et al., 2010), [3]Genetics of Pancreatic Cancer (Kern), [4](Souchek et al., 2014)

*p.V487_P492>A, HD = homozygous deletion, methylated = promoter methylation, fs = frameshift mutation. p16 mutation D84G confers loss of function (Yarbrough et al., 1999). Inactivation of CDKN2A was determined via immunoblot (no detectable protein).

Figure 2.2

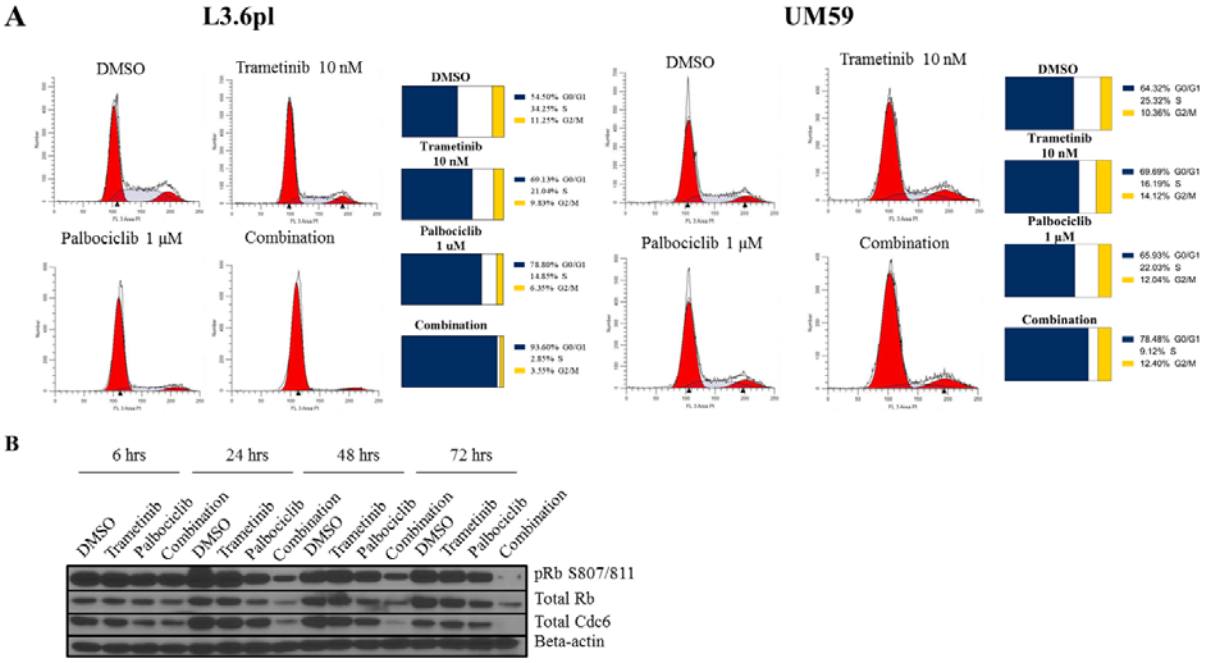

Figure 2.2 : Cell cycle effects of CDK4/6 inhibition are enhanced by MEK inhibition in L3.6pl and UM59 cells. (A) Cell cycle analysis shows evidence for G1 arrest in cells treated with palbociclib and trametinib for 48 hours. (B) Cells were treated with 10 nM trametinib or 1 µM palbociclib, alone or in combination for the indicated time period.

Figure 2.3

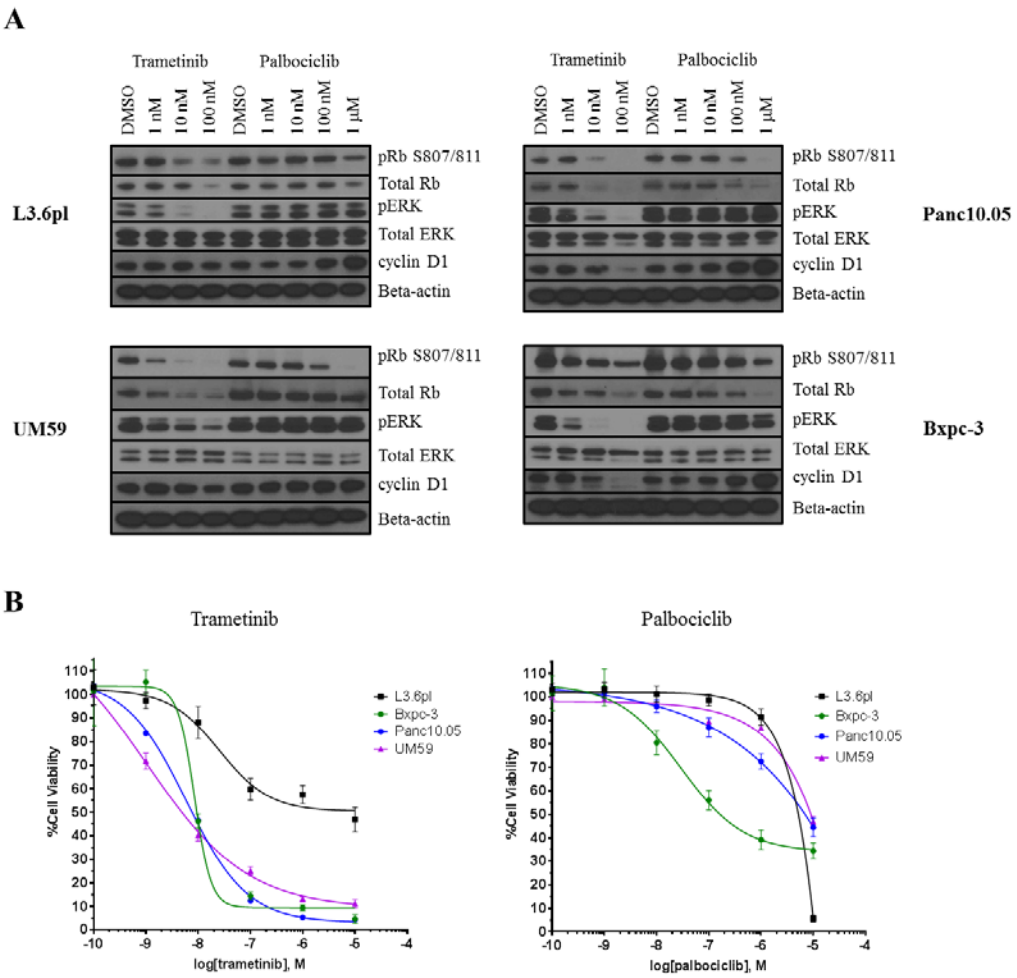

Figure 2.3: Single agent treatment with trametinib and palbociclib inhibits phosphorylation of Rb and ERK. (A) Concentration response of the effects of trametinib and palbociclib on Rb, ERK and cyclin D1 after 5 days of treatment. (B) Concentration response curves showing effects of trametinib and palbociclib on the proliferation of two cell lines with high synergy score (L3.6pl & UM59) and two with the low synergy score (Panc10.05 & Bxpc-3). Data are representative of multiple experiments and expressed as mean +/- SEM, n = 4 per point, treatment duration of 5 days. (C) Concentration response curves showing effects of trametinib and palbociclib on the proliferation of two cell lines with high synergy score (L3.6pl & UM59) and two with the low synergy score (Panc10.05 & Bxpc-3). Data are representative of multiple experiments and expressed as mean +/- SEM, n = 4 per point, treatment duration of 5 days.

Figure 2.4

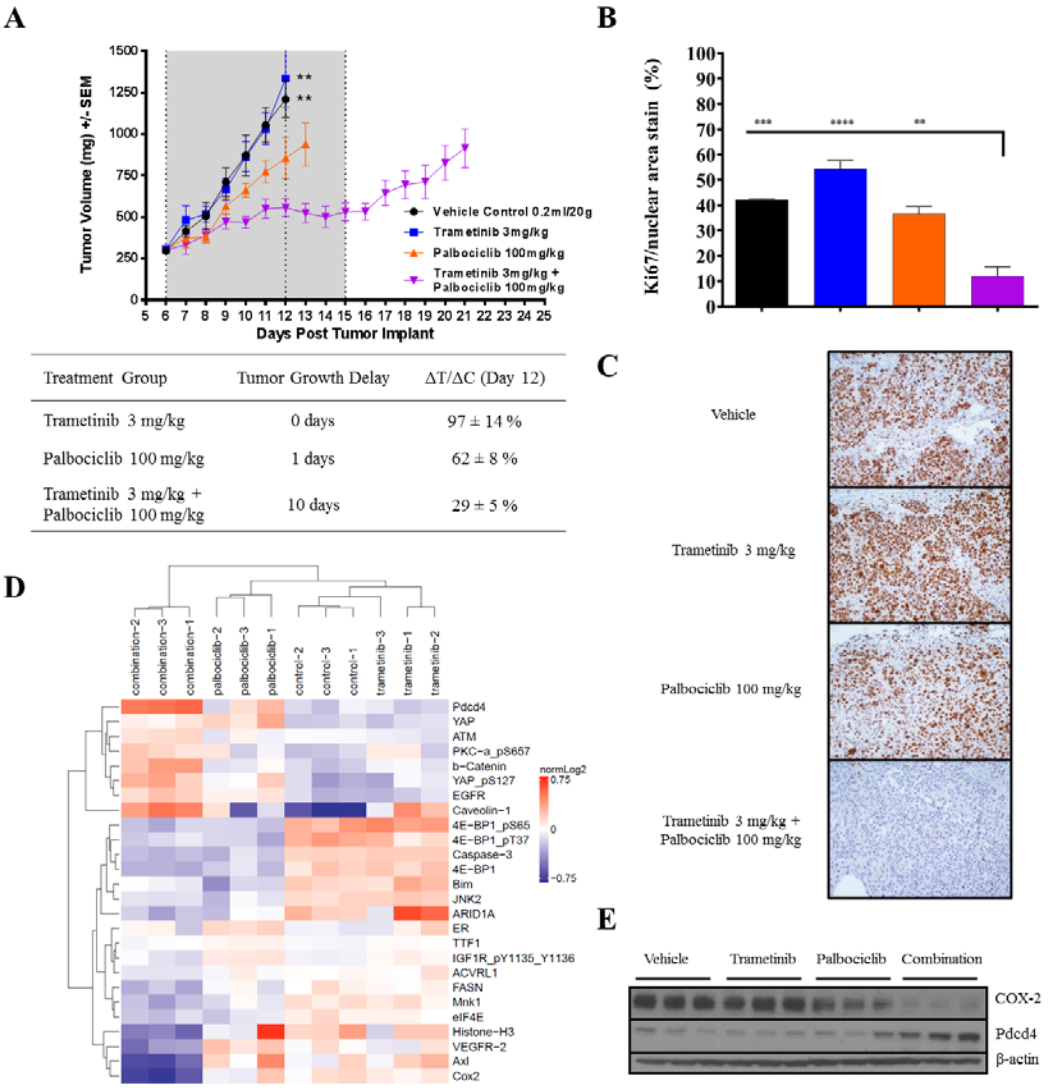

Treatment Group	Tumor Growth Delay	ΔT/ΔC (Day 12)
Trametinib 3 mg/kg	0 days	97 ± 14 %
Palbociclib 100 mg/kg	1 days	62 ± 8 %
Trametinib 3 mg/kg + Palbociclib 100 mg/kg	10 days	29 ± 5 %

Figure 2.4: Combination treatment is efficacious *in vivo* and correlates with decreased COX-2 expression. (A) L3.6pl cells were implanted subcutaneously and treatment was administered once daily via oral gavage for 10 days (shaded region) or until the group mean reached 1000 mm^3 (n = 5 per group). Tumors were harvested from a separate cohort on Day 7 (dotted line) for pharmacodynamic analysis. (B and C) Immunohistochemistry for Ki67 was performed and quantified (Immunoratio) in Figure B as a ratio between Ki67 stained nuclei and total nuclear area, while C shows representative images of treated tumors. (D) Heatmap generated from RPPA analysis of tumor lysates showing changes in protein expression. (E) RPPA results were verified via immunoblotting analysis for COX-2 and Pdcd4 expression. ** indicates $p < 0.005$, *** $p < 0.0005$, **** $p < 0.0001$, in comparison to combination arm.

Figure 2.5

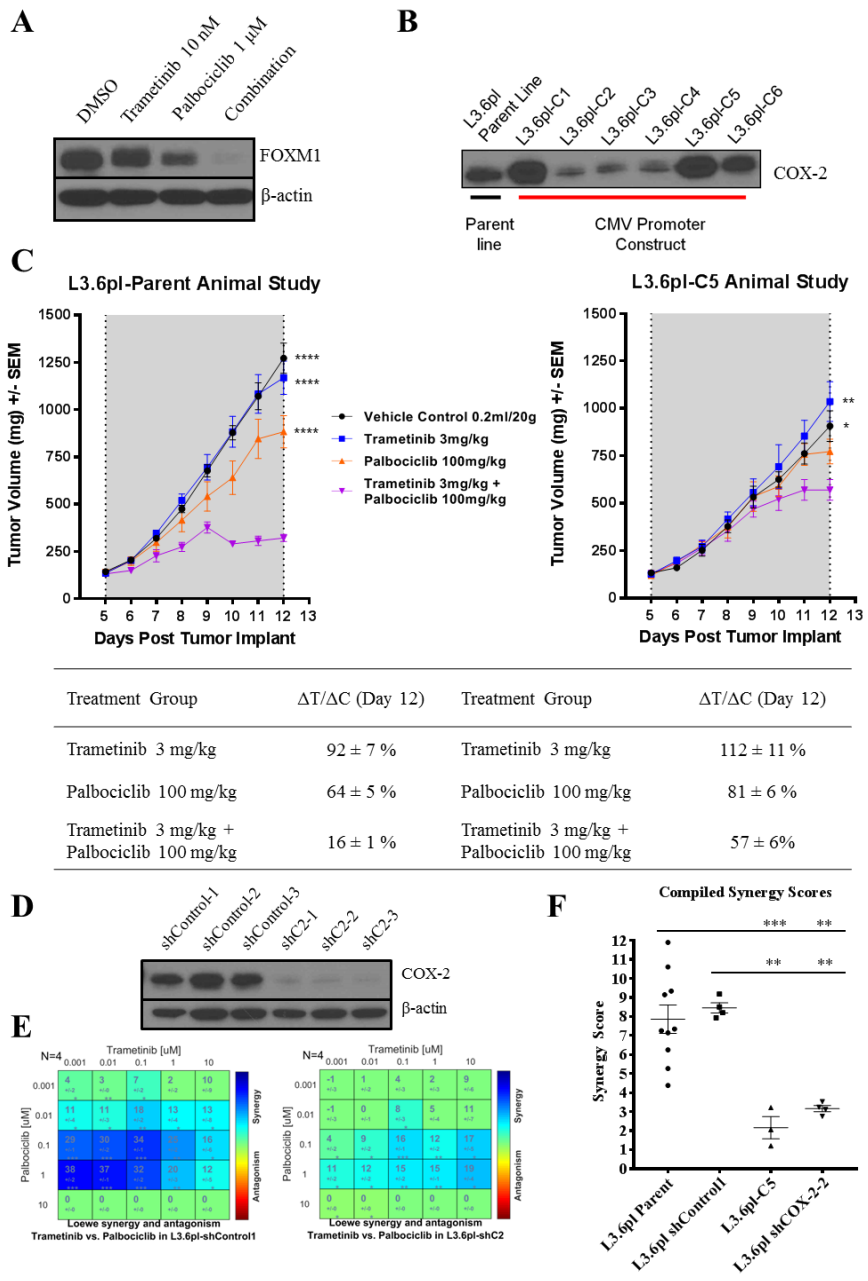

Treatment Group	ΔT/ΔC (Day 12)	Treatment Group	ΔT/ΔC (Day 12)
Trametinib 3 mg/kg	92 ± 7 %	Trametinib 3 mg/kg	112 ± 11 %
Palbociclib 100 mg/kg	64 ± 5 %	Palbociclib 100 mg/kg	81 ± 6 %
Trametinib 3 mg/kg + Palbociclib 100 mg/kg	16 ± 1 %	Trametinib 3 mg/kg + Palbociclib 100 mg/kg	57 ± 6%

Figure 2.5: COX-2 expression is implicated in sensitivity to co-targeting of MEK and CDK4/6. (A) Immunoblotting analysis of FOXM1 expression in L3.6pl cells harvested after a 5-day treatment with the indicated conditions. (B) Six clones expressing the CMV driven hCOX-2 construct were compared to the parent L3.6pl cell line for expression of COX-2. (C) A clone shown to express constitutively high levels of COX-2 (C5) was compared to the parent line in a head-to-head *in vivo* study (n = 5 per treatment condition, treatment period is shaded). Tumor burden was monitored during treatment and T/C values are shown for all treatment conditions. (D) Lysates were collected multiple times from L3.6pl cells expressing either a control shRNA plasmid or COX-2 shRNA to confirm COX-2 knockdown. (E) Combenefit graphs showing a reduced synergistic response of L3.6pl cells expressing COX-2 shRNA. (F) This chart lists the mean synergy scores +/- SEM of each cell line derived from L3.6pl to test the role of COX-2. ns indicates $p > 0.05$, * $p < 0.05$, ** $p < 0.005$, *** $p < 0.0005$, **** $p < 0.0001$, in comparison to combination arm.

Figure 2.6

A

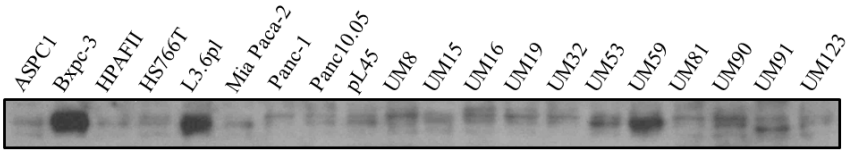

B

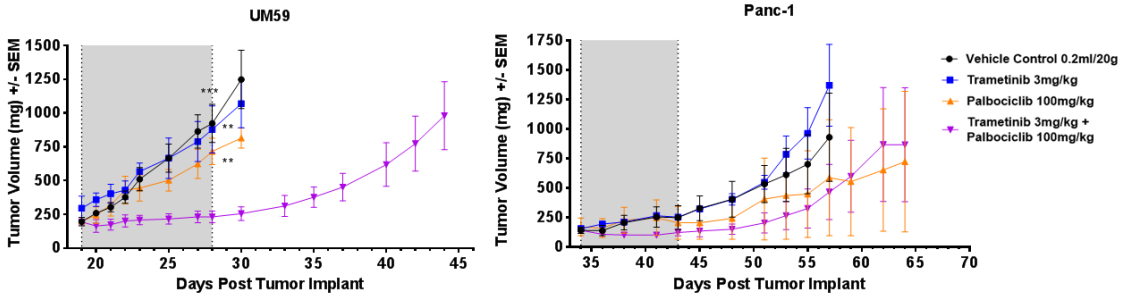

Treatment Group	Tumor Growth Delay	ΔT/ΔC (Day 28)	Treatment Group	Tumor Growth Delay	ΔT/ΔC (Day 43)
Trametinib 3 mg/kg	1 days	81 ± 12 %	Trametinib 3 mg/kg	0 days	54 ± 14 %
Palbociclib 100 mg/kg	3 days	71 ± 10 %	Palbociclib 100 mg/kg	9 days	41 ± 46 %
Trametinib 3 mg/kg + Palbociclib 100 mg/kg	16 days	5 ± 4 %	Trametinib 3 mg/kg + Palbociclib 100 mg/kg	5 days	14 ± 12 %

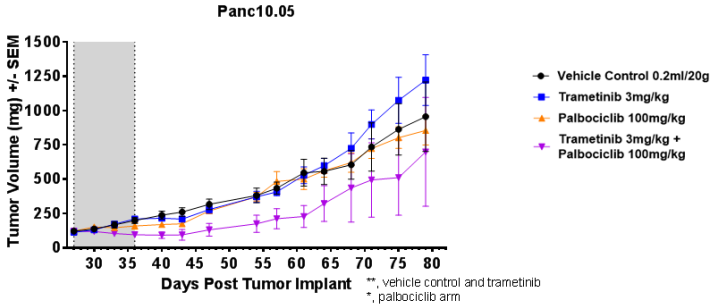

Treatment Group	Tumor Growth Delay	ΔT/ΔC (Day 36)	Percent Regression
Trametinib 3 mg/kg	0 days	126 ± 20 %	
Palbociclib 100 mg/kg	0 days	49 ± 24 %	
Trametinib 3 mg/kg + Palbociclib 100 mg/kg	9 days	N/A	21%

Figure 2.6: High expression of COX-2 correlates with greater relative benefit in the *in vitro* synergy screen and in tumor-bearing animals. (A) Expression of COX-2 in the panel of pancreatic cancer cell lines tested in the synergy screen. (B) *In vivo* studies were conducted in mice subcutaneously implanted with either UM59 (n = 4 per group), Panc-1 (n = 3 per group) or Panc10.05 (n = 5 per group) cells. Drugs were administered once daily via oral gavage for 10 days (shaded region) once tumors reached roughly 150-200 mm^3. The percent treatment/control (%T/C) and ΔT/ΔC on the last day of treatment as well as tumor growth delay (calculated at 750 mm^3 for UM59 and Panc-1, and 700 mm^3 for Panc10.05) are shown for each *in vivo* experiment. * indicates $p < 0.05$, ** $p < 0.005$, in comparison to combination arm on last day of treatment. Panc10.05 p values indicated on lower right of graph and were calculated based on T/C values, as a negative ΔT/ΔC cannot be calculated accurately. If no p values were indicated, differences are not statistically significant.

Figure 2.7: Supplementary Figure 1

A

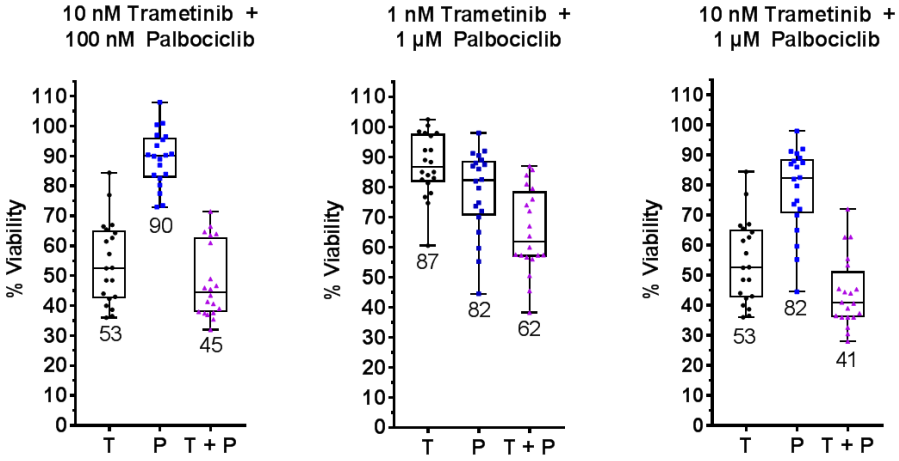

B

L3.6pl	Synergy Score
Trametinib + Palbociclib	7.26
Trametinib + LEE011	7.36
MEK162 + Palbociclib	4.84
MEK162 + LEE011	5.60

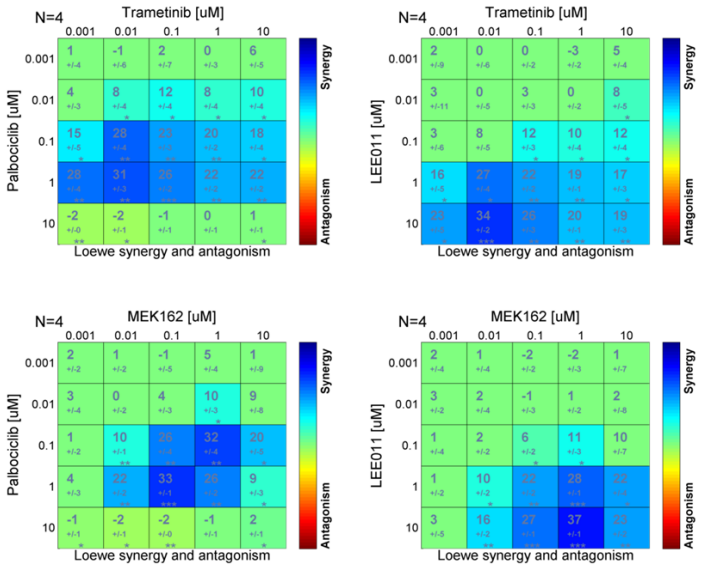

Figure 2.7: Supplementary Figure S1: Impact of drug concentration and kinase inhibitor selection on synergistic response (L3.6pl model). (A) Gross sensitivity of the pancreatic cancer cell line data set to combination treatment at the indicated concentrations is represented with box plots. The median of the cell line panel is shown by a line with the corresponding number below the line. The whiskers represent the minimum and maximum points. Each point in the boxes represents the percent viability of one cell line to the indicated drug treatment and is representative of replicate experiments. (B) Synergy scores and Combenefit graphs are shown for L3.6pl cells treated with different MEK and CDK4/6 inhibitors.

Figure 2.8: Supplementary Figure 2

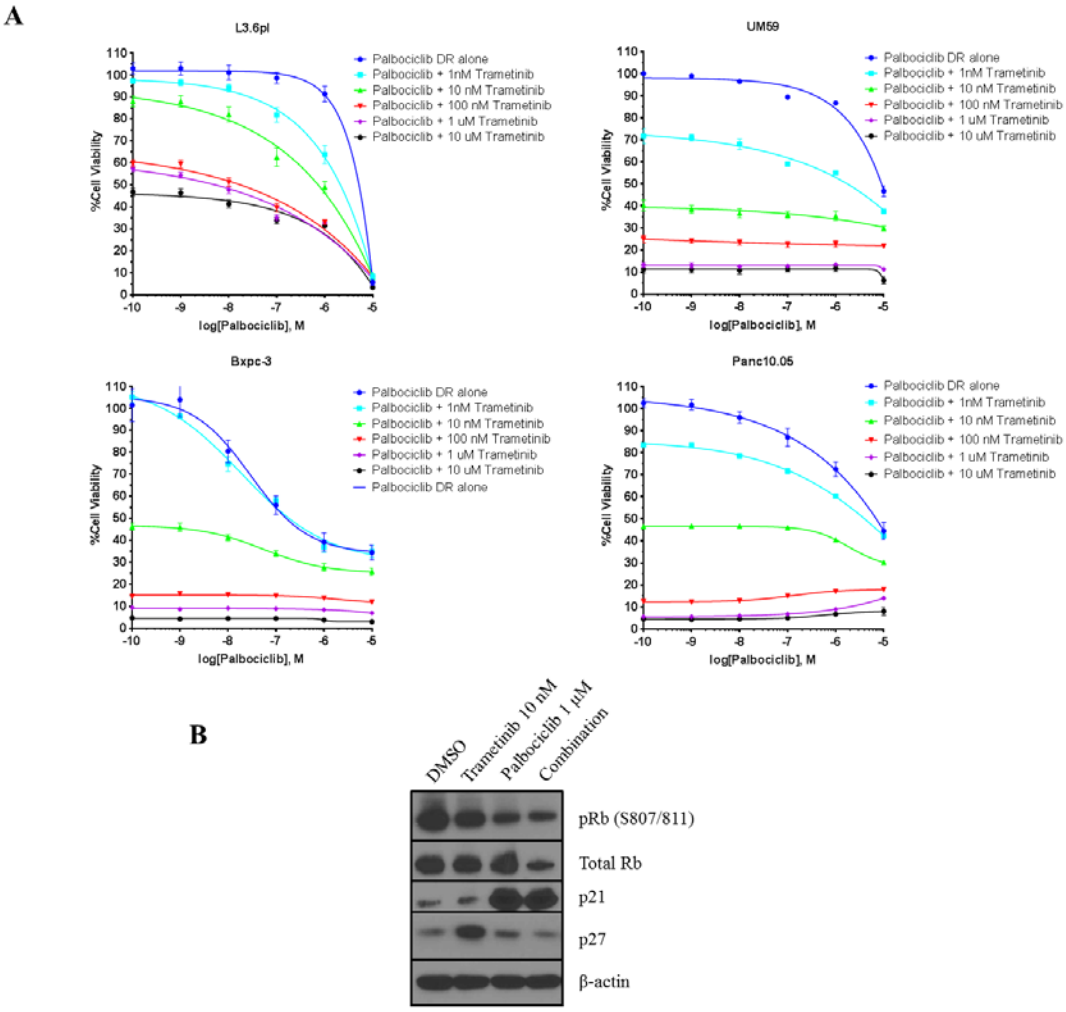

Figure 2.8: Supplementary Figure S2: Effect of combination treatment on growth and protein expression in models eliciting high and low synergy scores. (A) Palbociclib concentration response curves for L3.6pl, UM59, Panc10.05 and Bxpc-3 (mean +/- SEM, n = 4 per point) with indicated concentrations of trametinib added to show potency of combination treatment. (B) Immunoblotting analysis of various proteins using lysates harvested from L3.6pl cells treated for 5 days.

Figure 2.9: Supplementary Figure 3

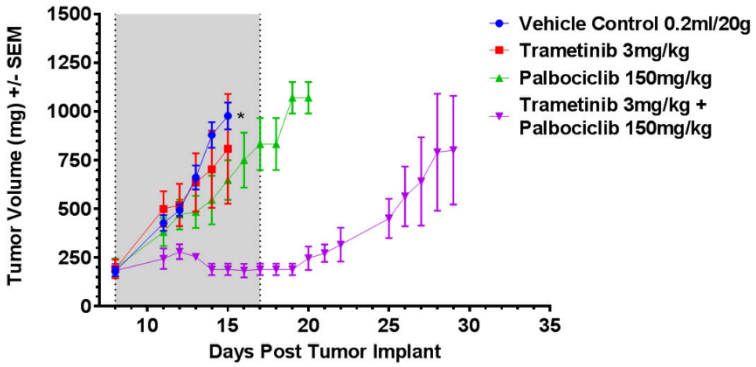

Treatment Group	Tumor Growth Delay (750 mm^3)	ΔT/ΔC (Day 15)
Trametinib 3 mg/kg	1 day	77 ± 24 %
Palbociclib 100 mg/kg	2 days	57 ± 5 %
Trametinib 3 mg/kg + Palbociclib 100 mg/kg	15 days	1 ± 3 %

Figure 2.9: Supplementary Figure S3: Evaluation of *in vivo* efficacy to the combination of trametinib and palbociclib in L3.6pl tumor-bearing animals. L3.6pl cells were implanted subcutaneously into the flank of nude mice (n = 3 per group) and once tumors reached ~150-200 mm^3, animals were treated via oral gavage once daily with the indicated doses. Each point represents the mean +/- SEM of the group. T/C values were calculated on day 15. Vehicle vs Combination $p < 0.05$, all other groups not statistically significant (combination versus palbociclib $p = 0.23$, combination versus trametinib $p = 0.08$).

Figure 2.10: Supplementary Figure 4

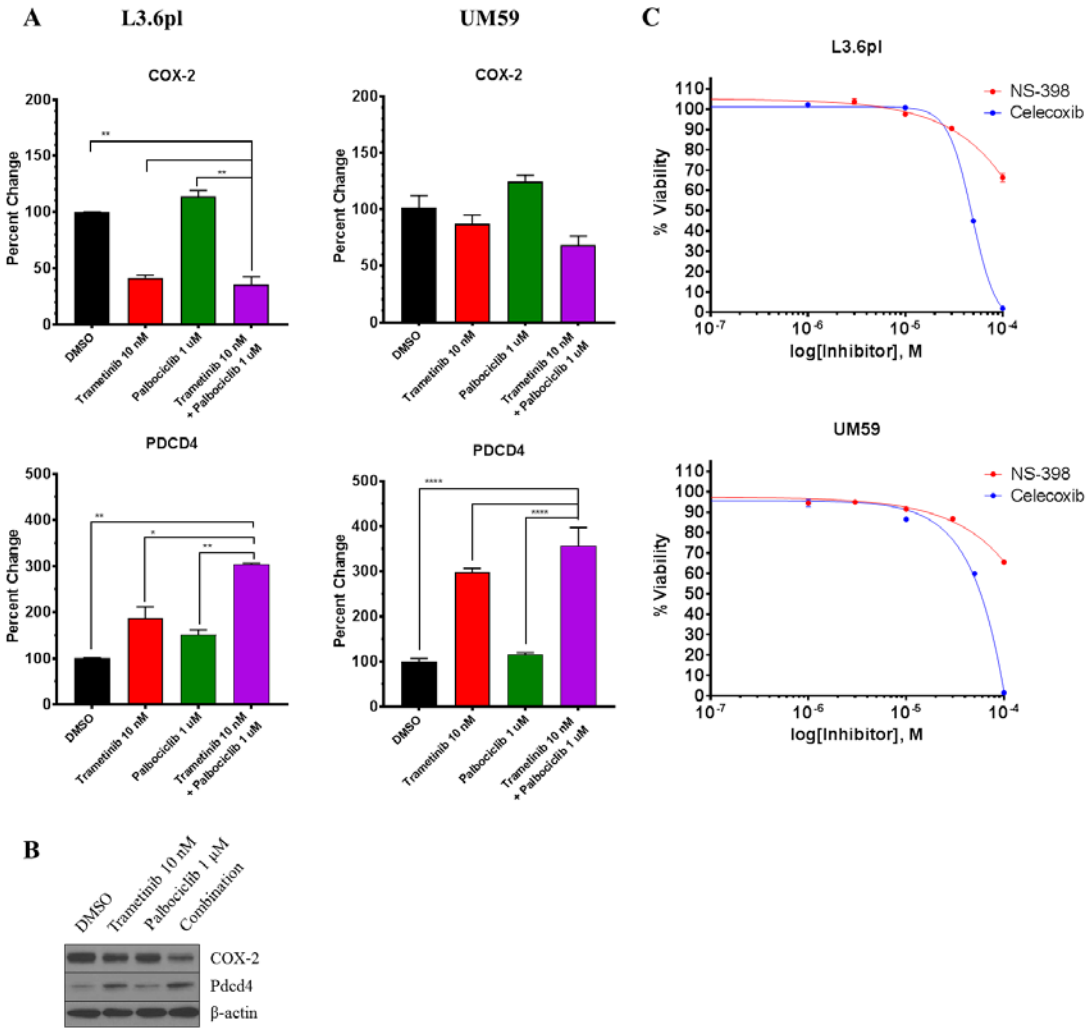

Figure 2.10: Supplementary Figure S4: Effect of combination treatment on COX-2 and Pdcd4 expression. (A) RT-qPCR of COX-2 and Pdcd4 transcripts from treated L3.6pl and UM59 cells, expressed as mean +/- SEM (n = 4 per group, results combined from two separate experiments) relative to DMSO treated cells. (B) Protein expression changes in lysates collected from treated UM59 cells (5 days). (C) L3.6pl and UM59 cells were treated with both celecoxib and NS-398 over a wide range of concentrations. Data are expressed as mean +/- SEM (n = 8). Data are representative of two additional experiments.

Figure 2.11: Supplementary Figure 5

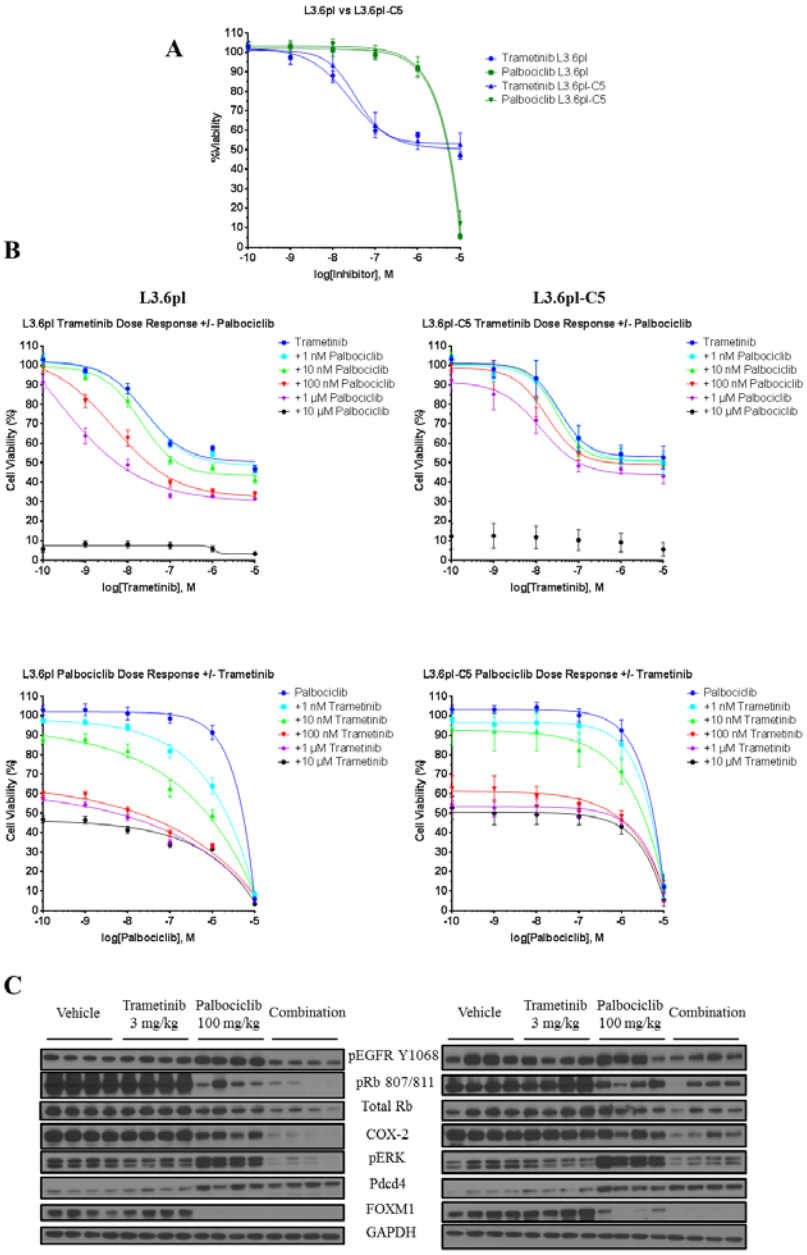

Figure 2.11: Supplementary Figure S5: Effects of trametinib and palbociclib alone and in combination on growth and expression of various signaling proteins. (A) Concentration response curves for both L3.6pl and L3.6pl-C5 in response to trametinib and palbociclib (mean +/- SEM, n = 4 per point). (B) Trametinib concentration response curves for L3.6pl and L3.6pl-C5 (mean +/- SEM, n = 4 per point) with indicated concentrations of palbociclib. Data for both (A) and (B) are representative of three additional experiments. (C) Lysates were harvested from tumors of the animal study in Figure 5C on the last day of treatment and immunoblots of indicated proteins are shown**.**

Figure 2.12: Supplementary Figure 6

A

Cell Line	Relative Expression (%)
Bxpc-3	100.1 ± 2.09
UM59	40.6 ± 0.65
L3.6pl	17.4 ± 0.14
UM90	6.2 ± 0.96
UM53	3.8 ± 0.10
UM15	2.9 ± 0.13
pL45	2.7 ± 0.04
HS766T	1.9 ± 0.01
Panc10.05	0.5 ± 0.01
HPAFII	0.3 ± 0.01
UM16	0.3 ± 0.00
UM81	0.3 ± 0.01
UM123	0.1 ± 0.00
UM91	0.1 ± 0.00
Panc-1	0.0 ± 0.00
ASPC1	0.0 ± 0.00
Mia Paca-2	0.0 ± 0.00
UM19	0.0 ± 0.00
UM32	0.0 ± 0.00
UM8	0.0 ± 0.00

B

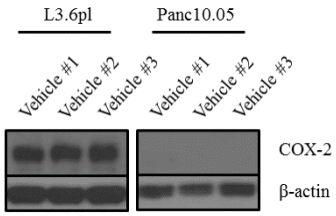

Figure 2.12: Supplementary Figure S6: COX-2 expression at the RNA and protein level. (A) RT-qPCR of COX-2 in RNA harvested from the pancreatic cancer panel, showing expression of the panel in relation to Bxpc-3 which had the highest expression (mean +/- SEM, n = 3 per point). (B) Comparison of COX-2 expression in tumors harvested from vehicle control animals in L3.6pl (Fig. 4) and Panc10.05 (Fig. 6). Each band represents a tumor from a separate animal.

Appendix B

Many people have contributed to the research studies presented in this chapter and their corresponding contributions are listed below.

Conception and design: Maust, JM, Sebolt-Leopold, JS

Methodology: Maust, JM, Frankowski-McGregor, CL

RPPA analysis: Bankhead III, A, Maust, JM

PDX models source: Crawford, H, Simeone, DM

Synergy screening: Maust, JM

Acquisition of data: Maust, JM, Frankowski-McGregor, CL

Molecular biology: Maust, JM, Frankowski-McGregor, CL

COX-2 pcDNA source: Smith. W

Writing, review and/or revisions of manuscript: Maust, JM, Sebolt-Leopold, JS

At the time of submission, Chapter 2 has been accepted to Molecular Cancer Therapeutics for publication.

> Maust, J.D., Frankowski-McGregor, C.L., Bankhead III, A., Simeone, D.M., Sebolt-Leopold, J.S. (2018). Cyclooxygenase-2 Influences Response to Co-Targeting of MEK and CDK4/6 in a Subpopulation of Pancreatic Cancers. Molecular Cancer Therapeutics.

Data presented in Chapter 2 were preceded by the evaluation of MEK and CDK4/6 co-inhibition in colorectal cancer and was published in Clinical Cancer Research.

> Ziemke, E.K., Dosch, J.S., Maust, J.D., Shettigar, A., Sen, A., Welling, T.H., Hardiman, K.M., Sebolt-Leopold, J.S. (2016). Sensitivity of KRAS-Mutant Colorectal Cancers to Combination Therapy that Co-targets MEK and CDK4/6. Clinical Cancer Research. doi: 10.1158/1078-0432.CCR-15-0829

Chapter 3: Designing Experimental Therapeutics to Treat KRAS and BRAF Mutant Colorectal Cancer

Abstract

Agents targeting epidermal growth factor receptor (EGFR) have met with limited success in the clinical management of colorectal cancer (CRC). Mutations in KRAS, BRAF, and PIK3CA are important drivers of resistance to EGFR-targeted therapy. Conversely, EGFR-mediated feedback mechanisms promote resistance to MEK inhibitor-based treatment of CRC by reactivating MAP kinase signaling. Our central hypothesis is that a dual small molecule inhibitor that potently and selectively targets only EGFR and PI3K, when combined with a MEK inhibitor, will be highly efficacious against subpopulations of BRAF mutant or KRAS mutant colorectal cancers that are dependent upon these kinase molecules to drive tumor progression. Employing a computational modeling approach, we exploited the known binding modes of structurally related ATP binding site inhibitors of EGFR and PI3K to design small molecules that simultaneously inhibit both kinases in a selective manner. To the best of our knowledge, the lead compound MTX-211, whose binding mode is flipped in PI3K compared to EGFR, represents a first in class selective inhibitor of these two critical oncogenic kinases. MTX-211 exhibits a favorable pharmaceutical and selectivity profile, possessing sub- to low nanomolar potency against both targets, >70% oral bioavailability, strong pharmacodynamic modulation of both

EGFR and PI3K signaling, and strong *in vivo* single agent efficacy against multiple $BRAF^{mt}$ and $KRAS^{mt}$ colorectal cancer models.

Introduction

Agents targeting EGFR have met with limited success in the clinical management of colorectal cancer (CRC) and are limited to treatment of those patients whose tumors do not harbor mutations in KRAS or BRAF (Amado et al, JCO 2008; De Roock et al, Lancet Oncol, 2011; Karapetis et al, NEJM 2008). Approximately 50% of colorectal malignancies are known to possess either a KRAS or BRAF mutation, conferring a poor prognosis. The co-occurrence of PIK3CA mutations or loss of expression of the tumor suppressor PTEN further contribute to the inability of EGFR inhibitors to effectively treat these tumors (Atreya et al, Cancer Med, 2013; Jhawer et al, Cancer Res 2008; Liao et al, Clin Cancer Res 2012; Sawai et al, BMC Gastroenterol 2008). Both EGFR and PI3K signaling have also been implicated in the resistance of KRAS mutant cancers to MEK inhibitor monotherapy (Caunt et al, Nature Rev Cancer, 2015; Mirzoeva et al, MCT 2013; Turke et al, Cancer Res 2012). Thus, the design of a single molecule that could target both EGFR and PI3K compensatory signaling in response to MEK inhibition would be an attractive alternative to triple drug combination treatment strategies. This chapter explores the evaluation of MTX-211, a rationally designed small molecule inhibitor of EGFR and PI3K, two kinases that are importantly linked to KRAS signaling.

Materials and Methods

Cell Culture and Inhibitors

HCT-116 and RKO cells were obtained from the American Type Culture Collection ATCC). HCT-116 cells were maintained in McCoy's 5A media (Invitrogen) supplemented with 10% FBS (HyClone), 1% GlutaMax, (Invitrogen) and 1% Penicillin Streptomycin (Invitrogen). RKO cells were maintained in EMEM media (Lonza) supplemented with 10% FBS (HyClone), 1% GlutaMax, (Invitrogen) and 1% Penicillin Streptomycin (Invitrogen). All cells were incubated at 37°C in 5% CO_2. Cell line validation was performed by the University of Michigan DNA Sequencing Core using short tandem repeat analysis.

Drugs

MTX-211 was synthesized by Cayman Chemicals and trametinib was purchased from LC Laboratories. For cellular studies, drugs were dissolved in DMSO at a concentration of 10 mmol/L and stock solutions were stored at -20°C.

Cell Viability Assay

For growth inhibition analysis, cells were seeded in whitewalled/clear-bottom tissue culture treated 96-well plates and allowed to adhere for 24 hours followed by addition of growth media containing serial dilutions of MTX-211, trametinib, or both drugs in combination. Control wells received DMSO at a final concentration of 0.2%. Cells were incubated for 3 days in the continuous presence of drug or DMSO and viability was measured using CellTiter-Glo (Promega). Viability was calculated as a percentage of the

DMSO-treated cells. Four replicates were performed for each of the different drug treatment conditions. Data were modeled using a nonlinear regression curve fit with a sigmoidal dose–response using GraphPad Prism 6 (GraphPad Software). Synergy calculations were performed using Combenefit software (Cancer Research UK Cambridge Institute).

Clonogenic Assay

For each cell line, 500 cells were plated per well into 6-well plates, with six replicates per treatment condition. The cells were allowed to attach overnight. Cells were treated with MTX-211, trametinib, or the combination at the concentrations indicated in the figure legends. Ten days later, the cells were fixed with 10% neutral buffered formalin (NBF) and the stained using 0.1% crystal violet. The colonies were counted using OpenCFU open-access software (insert reference number). Quantification is presented as mean ± SEM. In assessing the different treatment conditions, a one-way ANOVA test was used for statistical analysis.

Western Blots

Cells or tumors were lysed in NP-40 lysis buffer [25 mmol/L Tris-HCl (pH 7.6), 150 mmol/L NaCl, 1% Nonidet P-40, 10% glycerol, 1 mmol/L EDTA, 1 mmol/L dithiothreitol, and protease and phosphatase inhibitors], rocked for 30 minutes at 4°C, and centrifuged at 13,200 rpm for 20 minutes at 4°C. Protein concentration was determined by BioRad Protein Assays and lysates were subsequently subjected to SDS gel electrophoresis. Proteins were transferred to polyvinylidene fluoride (PVDF) membranes and probed with primary antibodies recognizing p-EGFR tyr1068), EGFR, p-HER2 (tyr1248), HER2, p-AKT

(ser473), p-AKT (thr308), AKT, pERK1/2 (thr202/tyr204), ERK1/2, pS6K (ser235/236), S6K, and cleaved PARP (all from Cell Signaling Technology) and beta actin (Abcam). After incubation with anti-rabbit HRP-linked secondary antibody (Jackson ImmunoResearch Laboratories, Inc.), proteins were detected using chemiluminescence (GE Healthcare).

Xenograft Studies

The colorectal PDX models were established as described previously (Ziemke et al., 2015). For the xenograft studies established from the PDX models, female 6- to 7-week-old NCR nude mice (CrTac:NCr-Foxn1nu from Taconic) were implanted subcutaneously with low-passage PDX tumor fragments (30 mg) into the region of the right axilla. For the xenograft studies established from cell lines, the HCT-116 or RKO cells were injected (1 X 10^6 cells per injection) into the flanks of female 6- to 7-week old NCR nude mice. In both cases, the mice were randomized into treatment groups and treatments initiated when tumors reached 100 to 200 mg. MTX-211 and trametinib were administered daily by oral gavage as a solution in 5% dimethyl sulfoxide and 95% polyethylene glycol and a fine suspension in 0.5% HPMC with 0.2% Tween-80, respectively, based upon individual animal body weight (0.2 mL/20 g). Subcutaneous tumor volume and body weights were measured two to three times a week. Tumor volumes were calculated by measuring two perpendicular diameters with calipers and using the formula: tumor volume ¼ (length x width^2)/2. For the single agent screening studies, mice were treated for the time period as indicated in the figure and euthanized following the last treatment. Percent treated/control (%T/C) was calculated by dividing the median treated tumor weight by the median control tumor weight and multiplying by 100 on the last day of treatment. A one-sided unpaired T-test was used

to assess differences between the vehicle control and the MTX-211 treated mice. For the lifespan assays, the mice were treated daily as indicated until their individual tumor burdens surpassed 1000 mg at which point the mice were euthanized. Increase in lifespan was calculated by dividing the median increase in lifespan (days) by the median survival time of the vehicle control group. A log-rank (Mantel-Cox) test was run to compare the difference in survival between the treatment groups. All procedures related to the handling, care, and treatment of animals were conducted in accordance with University of Michigan's Institutional Animal Care and Use Committee guidelines.

Immunohistochemistry

Tissues were fixed in 10% NBF, embedded in paraffin, and sectioned in accordance with standard procedures. Samples were processed by Daniel Long in the Crawford Lab at University of Michigan. The Ki67 antibody was obtained from Abcam (ab15580). The slides were scanned using a 3D Histotech Panoramic SCAN II. Images were captured using CaseViewer software. Images were taken with a Nikon E-800 microscope, Olympus DP71 digital camera, and DP Controller software. For quantification of staining, representative images were obtained from the stained slides at ×40 objective magnification for ImmunoRatio analysis. For each treatment condition (vehicle, trametinib, palbociclib, and combination), five representative fields of view from four individual tumors were analyzed. The images were analyzed using the basic mode in the ImmunoRatio software. Quantification is presented as mean ± SEM. In assessing the different treatment conditions, a one-way ANOVA test was used for statistical analysis.

Results

MTX-211 binds to EGFR and PI3K in a flipped binding mode fashion

MTX-211 emerged from a drug design campaign in the Leopold laboratory employing computational modeling to design small molecules that would selectively and simultaneously inhibit EGFR and PI3K. The design of MTX-211 and structurally related analogs was based upon analysis of the known binding modes of closely related ATP binding site inhibitors of these kinases. The x-ray crystal structure of erlotinib bound to EGFR (Stamos et al., 2002) shows the nitrogen at the 1-position of the quinazoline moiety forming a hydrogen bond with the amide nitrogen of MET793 (Fig. 3.1A). Residues Leu792 and Gln791 form the backbone of the erlotinib binding pocket. In contrast, omipalisib (GSK2126458) bound to PI3Kγ (Knight et al., 2010) is flipped relative to the way in which erlotinib binds to EGFR with the nitrogen at the 1-position of the quinoline moiety forming a hydrogen bond with the hinge backbone of VAL882. Whereas the 6-position of the quinazoline ring of erlotinib points out towards solvent, the 6-position of omipalisib points towards the back of the ATP pocket of PI3Kγ towards a hydrophilic PI3K specificity pocket. The flipped binding mode of the quinazoline core between EGFR and PI3Kγ was leveraged to computationally design potent and selective dual inhibitors of both enzyme families, which lead to the discovery of MTX-211 (Figure 3.1B). Crystallization studies carried out with purified EGFR and PI3Kgamma have confirmed the postulated flipped binding mode of MTX-211 between these two targets (Figure 3.1C).

Biochemical profiling: MTX-211 is highly potent and selective against EGFR and PI3K

MTX-211 possesses low or sub- nanomolar potency against purified EGFR and PI3Kα as reflected by IC_{50}'s of 3.6 and 0.6 nM, respectively (Supplementary Fig. 3.5/1A). Expanded testing against other HER and PI3K family members showed that MTX-211 also exhibits significant, albeit reduced, potency against HER2 and HER4, similar to the profile of erlotinib. Furthermore, the ability of MTX-211 to strongly inhibit all PI3K isoforms as well as mTOR leads to a biochemical profile strikingly similar to that of copanlisib (Scott et al., 2016). MTX-211 is highly selective for HER and PI3K family members as revealed by screening of a broad panel of >100 kinases, encompassing a diverse array of tyrosine, serine/threonine, and lipid kinases (Supplementary Table 3.1).

Biological profiling of MTX-211 reveals strong activity in colorectal cancer models

The anti-proliferative activity of MTX-211 against the NCI-60 panel was most pronounced for colorectal cancer models, where KRAS or BRAF is mutated in 5 of 6 cases and the median IC_{50} was 1110 nM (Fig. 3.2A; Supplemental Fig. 3.5/1B). In accordance with the strong activity of MTX-211 towards PI3K, PIK3CA was the only gene mutated in the NCI-60 panel that correlated with sensitivity to MTX-211, with the most responsive half of the cohort containing all the PIK3CA mutations (Supplementary Fig. 3.5/1C). Evidence for dual cellular inhibition of EGFR and PI3K signaling was generated in both BRAF mutant RKO and KRAS mutant HCT-116 colorectal cells (Fig. 3.2B). In both models, autophosphorylation of $EGFR_{Y1068}$ is effectively suppressed by MTX-211. Consistent with

its biochemical profile, MTX-211 more strongly inhibits PI3K than EGFR as reflected by reduced pAKT expression at concentrations as low as 1 to 10 nM.

Since the PI3K pathway is a major regulator of cyclin D1, cell cycle entry and has been reported extensively to inhibit apoptosis (Klein and Assoian, 2008; Li et al., 2008a; Liu et al., 2013; She et al., 2005; Shimura et al., 2012; Will et al., 2014), we anticipated that MTX-211 treatment would lead to cell cycle arrest and/or apoptosis. A significant sub-G1 population was induced in HCT-116 cells in response to MTX-211, indicative of apoptosis. This was confirmed by a time-dependent induction of cleaved PARP expression, which was also a concentration-dependent response (Fig. 3.2C; Supplementary Fig. 3.6/2A). The cell cycle effects of MTX-211 mirrored those seen in response to the combination of omipalisib and erlotinib, consistent with its on-target effects. Pan-caspase inhibitor Z-VAD-FMK prevented the emergence of the sub-G1 population and also cell death caused by MTX-211 over a 24 hour treatment. This suggests that the sub-G1 population predates apoptosis and cell death (Supplementary Fig. 3.6/2B). Z-VAD-FMK left cells arrested in G2/M phase, indicating that a G2/M arrest possibly forms a transition state into apoptosis in response to MTX-211. Importantly, these results are consistent with cells treated with comparator compounds omipalisib and erlotinib at equimolar concentrations.

Pharmacodynamic profiling of MTX-211 confirms its dual inhibitory properties in vivo

Treatment of mice with a single oral dose of MTX-211 results in an exposure (≈20 μM) that is roughly 2 logs higher than the cellular EC_{50}'s required to impair EGFR and PI3K signaling (Supplementary Table 3.2). In HCT-116 tumor-bearing animals, a single oral dose of 50 mg/kg MTX-211 was sufficient to strongly inhibit expression of activated EGFR

and AKT, indicative of its dual kinase inhibitory profile (Fig. 3.2D). This experiment further substantiated the induction of apoptosis seen *in vitro*, with a significant induction of cleaved PARP (Fig. 3.2D)

MTX-211 is synergistic in combination with a MEK inhibitor

The ability of MTX-211 to inhibit both EGFR and PI3K family members makes it an ideal candidate for combination with agents targeting the ERK pathway. Resistance to MEK inhibition has been shown to be mediated by reactivation of HER family members, enabled in part by loss of an ERK-mediated inhibitory feedback phosphorylation on EGFR (T669) leading to activation of the PI3K/AKT pathway (Li et al., 2008b; Turke et al., 2012a). The ineffectiveness of MEK inhibitor monotherapy is fueled by strong induction of AKT activation, which is driven by increased phosphorylation and transcription of HER3 as well as the loss of feedback inhibition of EGFR.

We hypothesized that MTX-211, by virtue of its dual ability to inhibit HER and PI3K family members, would target the multiple escape routes that lead to resistance to ERK pathway intervention (Fig. 3.3A). We found that expression of phosphorylated HER3 is effectively suppressed by 1 μM MTX-211 in both $KRAS^{MT}$ and $BRAF^{MT}$ cells (Fig. 3.3B). MTX-211 also ablates upregulation of pHER3 expression that occurs in response to MEK inhibition in $KRAS^{MT}$ cells (Fig. 3.3B, Supplementary Fig. 3.6/2C). Consequently, MTX-211 acts to blunt the activation of AKT that ensues in response to trametinib treatment. Consistent with the observations of others (Turke et al., 2012b), we find that MEK inhibited $KRAS^{MT}$ cells exhibit a reduction in the degree of phosphorylation of the T_{669} regulatory

site on EGFR (Fig. 3.3B), and further find that this reduction can be reversed by MTX-211.

Apoptosis occurring in response to MTX-211 increases upon co-treatment with trametinib, inversely correlating with the degree of phosphorylation of the serine112 site of the propapoptotic protein BAD (Fig. 3.3C). A published study by She et al. presents support for this site being EGFR/MEK/ERK dependent, in contrast to the serine136 site, which is PI3K/AKT dependent (Fang et al., 1999; She et al., 2005). This finding led to the prediction that MTX-211 would prove synergistic in combination with ERK pathway intervention, which was borne out in clonogenic assays conducted with HCT-116 and RKO cells treated with MTX-211 and a number of MEK or ERK inhibitors (Fig. 3.3C, Supplementary Fig. 2.7/3A).

These data were further corroborated by the emergence of PI-/Annexin V+ and PI+/Annexin V+ populations in cells treated with MTX-211. Comparator compounds omipalisib and erlotinib elicited a similar response at concentrations that inhibit pAKT and pEGFR equally (Supplementary Fig. 3.7/3B).

MTX-211 in combination with trametinib is highly efficacious in patient-derived colorectal cancer models

Preclinical proof-of-concept for the clinical advancement of MTX-211 emerged from a pilot mouse trial of a diverse panel of $KRAS^{MT}$ colorectal cancer patient-derived xenografts. Five models were selected to provide heterogeneity of KRAS mutations (G12D, G13D and G12C) and included one $BRAF^{MT}$ model, UM CRC 14-929 (Supplemental Table 3.3). Cohorts were included to evaluate *in vivo* efficacy of MTX-211

alone and in combination with trametinib. Only one model received no benefit from MTX-211 treatment and one model responded equally well to MTX-211 and the combination (Fig. 3.4).

The remaining three models all responded favorably to the combination of MTX-211 and trametinib, as evidenced by the incidence of objective responses or an increase in progression free survival (PFS) >100% (Fig. 3.4). Trametinib as a single agent was mostly inactive in all five models. No significant body weight loss was observed in response to the combination of MTX-211 and trametinib over the course of these studies, exceeding 120 days of daily dosing in some cases (Supplementary Fig. 3.8/4). MTX-211 was also efficacious in combination with trametinib in fully immune competent animals implanted with $KRAS^{MT}$ CT-26 tumors (Supplemental Fig. 3.9/5). Furthermore, MTX-211 was found to be highly efficacious in combination with trametinib against the $BRAF^{MT}$ CRC model. UM CRC 14-929 displayed a 285% increase of lifespan in animals treated with combination therapy, a noteworthy decrease in Ki67 staining and favorable target potency (Supplementary Fig. 3.10/6A, B, C). In addition, comparing MTX-211 and trametinib to MTX-211 and binimetinib (MEK) or alpelisib (PI3K), cetuximab (EGFR) and trametinib showed that MTX-211 and trametinib/binimetinib led to substantially better activity than the comparator compounds (Supplementary Fig. 3.10/6D). This forms the basis for preclinical proof-of-concept in comparison to current clinical candidates and approved agents targeting EGFR and PI3K.

Discussion

The rationale for targeted therapy rests upon the assumption that certain signaling nodes or kinases are critical for growth. Preclinical and clinical findings have shown that, while this may be true, critical adaptive signaling methods exist to enforce redundancy in these pathways. The emergence of dual and even triple combination studies foreshadow a field that relies upon inhibiting several kinases that in sum inhibit signaling and bypass feedback mechanisms. While employing several inhibitors would fulfill this requirement, balancing adverse events in the clinic precludes many of these combinations. In this study, we report a dual inhibitor of EGFR and PI3K, two critical growth kinases that have and are a part of adaptive signaling. Inhibition of both targets with a single molecule decreases the risk of adverse drug-drug interactions and offers the attractiveness of a single pharmacokinetic profile for optimization of a dosing regimen.

MTX-211 was computationally designed based off the known binding nodes of closely related ATP binding site inhibitors omipalisib and erlotinib. These inhibitors share a common quinazoline core that are spatially flipped within their respective kinase. Crystallization studies confirmed the flipped binding mode of MTX-211 to its two targets. Low to sub- nanomolar potency is observed against EGFR and PI3K (3.6 and 0.6 nM).

MTX-211 displays broad activity against cancer models from the NCI-60 panel, with the most potent median activity against colorectal cancer. While it is not expected for an EGFR-based therapy to directly show benefit in KRAS and BRAF mutant disease, it is a critical node through which adaptive signaling to MAPK pathway inhibition is directed (Corcoran et al., 2012; Li et al., 2008b; Turke et al., 2012a). We report that in combination

with MEK inhibition, not only is growth signaling inhibited and tumor growth inhibition observed, but anticipated and observed feedback activation is targeted. Reduction in $EGFR_{T669}$ is observed in response to MEK inhibition in CRC models, as well as upregulated transcription and phosphorylation of HER3. MTX-211, by inhibiting EGFR and PI3K activity, is poised to negate these acute adjustments in the growth signaling network.

EGFR-based therapies are also limited in their ability to target KRAS and BRAF mutant disease due to the common co-occurrence of PIK3CA mutations or loss of tumor suppressor PTEN. Dual inhibition of EGFR and PI3K can therefore target downstream mutations that would normally preclude a patient from EGFR-based therapy. Circumstantial evidence supporting activity in PIK3CA mutant cells can be found in the mutational profile of the responsive NCI-60 panel models. Every model with a PIK3CA mutation was more responsive than the median of the panel, while no other mutation correlated with activity in the panel.

MTX-211 displays anti-tumor activity in models in this report, primarily through the induction of apoptosis. Importantly, the anti-tumor effect of MTX-211 is predicated upon its ability to induce apoptosis, as a pan-caspase inhibitor Z-VAD-FMK was able to negate its effects. Furthermore, a G2/M arrest appears to be an important transition state to an apoptotic state. If the effects of this agent were purely growth inhibitory, a prolonged G1 or G2/M arrested state would be expected. Instead, a dual-arrested G1-G2/M transitory state precedes induction of sub-G1, PI-/Annexin V+ and PI+/Annexin V+ populations. These characteristics raise the possibility that additional suitable combination agents that target the cell cycle in G1 or G2/M could prove synergistic with MTX-211.

The pharmacokinetic profile of MTX-211 is favorable, with exposures *in vivo* exceeding cellular EC_{50}'s required to inhibit EGFR and PI3K. These doses also elicit favorable pharmacodynamics, with a single, tolerated oral dose inducing cleaved PARP and inhibiting pAKT and pEGFR. *In vivo* activity also demonstrates substantial preclinical proof-of-concept in six CRC PDX models.

Figures

Figure 3.1

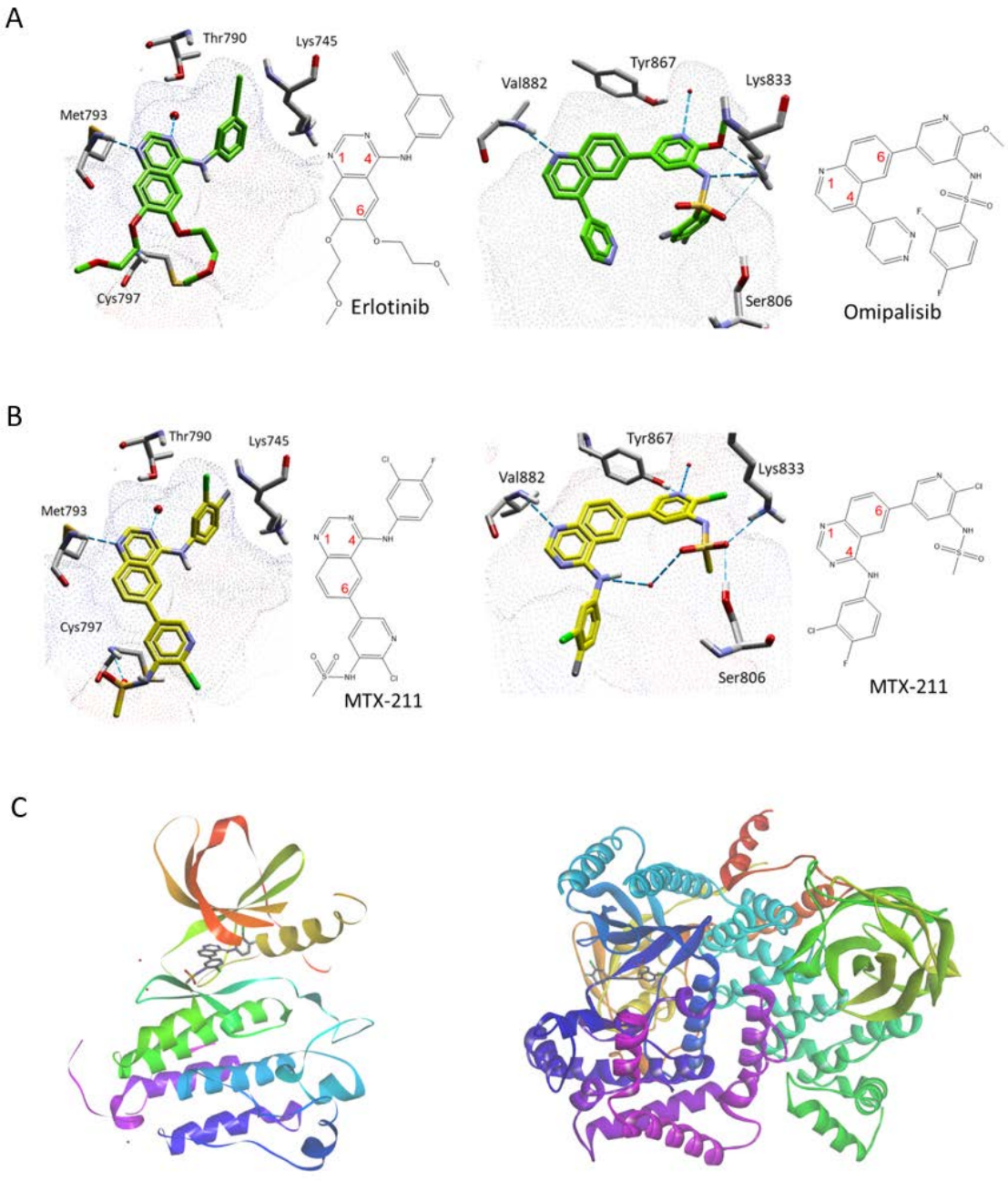

Figure 3.1: X-ray crystal structure of MTX-211 bound to EGFR and PI3K. (A) X-ray crystal structures of erlotinib bound to the EGFR kinase domain (1M17) and omipalisib bound to PI3K gamma (3L08) left and right respectively. Figure 1B, x-ray crystal structures of MTX-211 bound to the kinase domain of EGFR (left) and PI3K gamma (right). Figure 1c ribbon diagram of MTX-211 bound to kinase domain EGFR (left) and PI3K gamma (right).

Figure 3.2

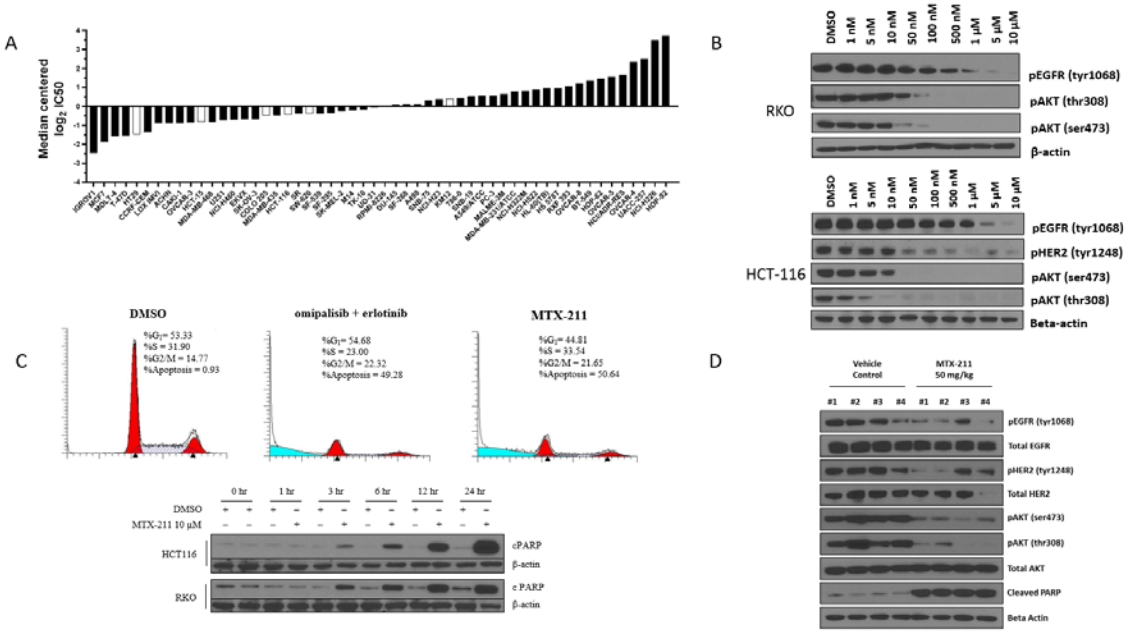

Figure 3.2: Response of the NCI-60 panel to MTX-211 and the effects of MTX-211 *in vitro*. (A) The NCI-60 panel response to MTX-211 median centered by the logIC_{50}. (B) Immunoblots of various proteins related to MTX-211 mode of action and their response to MTX-211 treatment in BRAF mutant model RKO and KRAS mutant model HCT-116. (C) Cell cycle effects of MTX-211 and comparator compounds in HCT116. Below this, time dependent apoptosis study. (D) Single oral dose of MTX-211 in nude mice implanted with HCT-116 cells. Tumors were harvested 2 hours after single oral dose and immunoblotted for various proteins to examine pharmacodynamics of MTX-211.

Figure 3.3

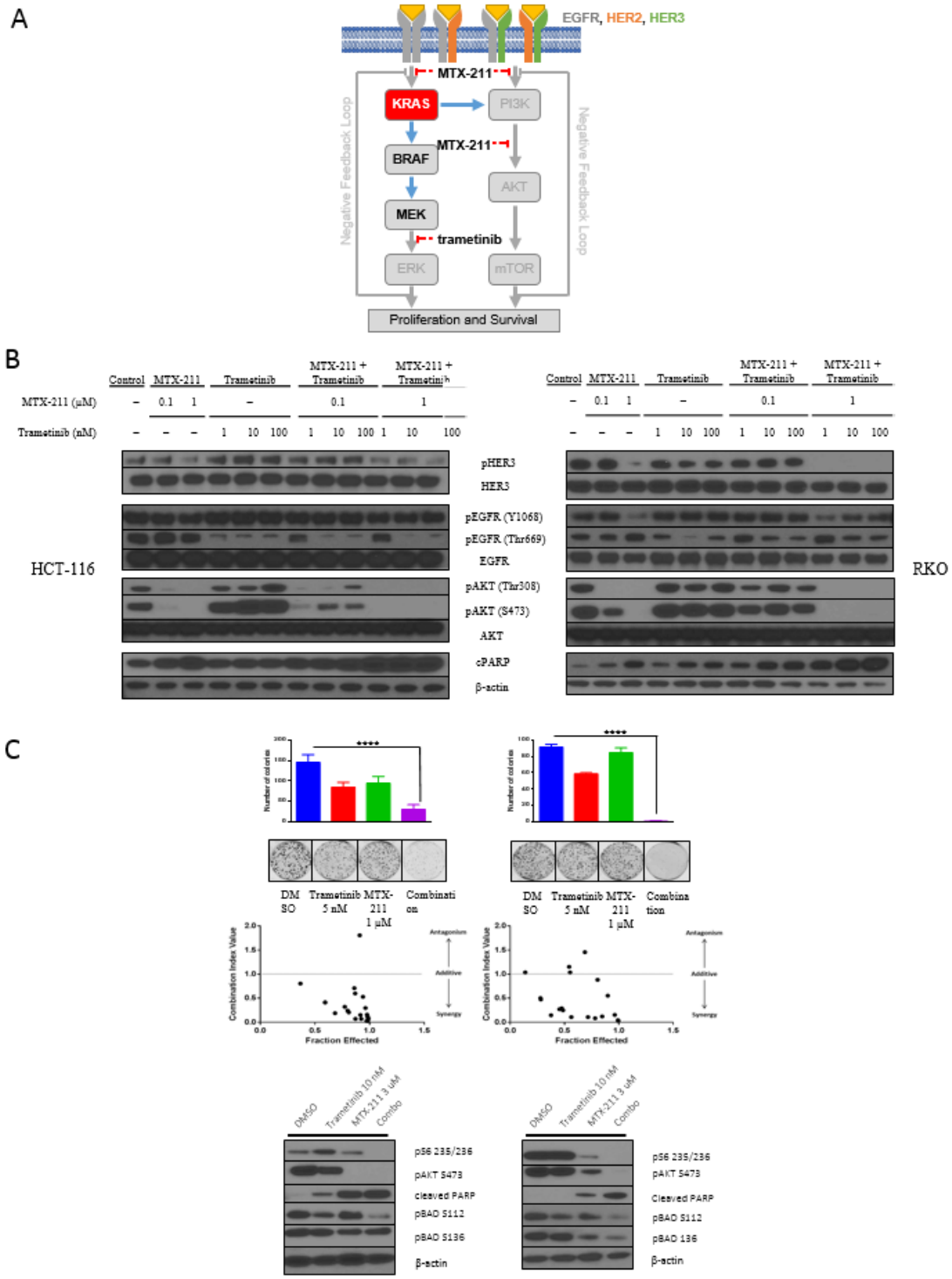

Figure 3.5: Effects of MTX-211 in combination with MEK inhibition. (A) Signaling diagram showcasing common adaptive signaling in response to MEK and MTOR signaling and how MTX-211 can target these mechanisms. (B) Immunoblots showcasing the ability of MTX-211 to target these resistance mechanisms, namely HER3 and pEGFR T669. (C) Clonogenic assays and immunoblots of HCT-116 and RKO cells treated with MTX-211, trametinib and a combination of the two.

Figure 3.4

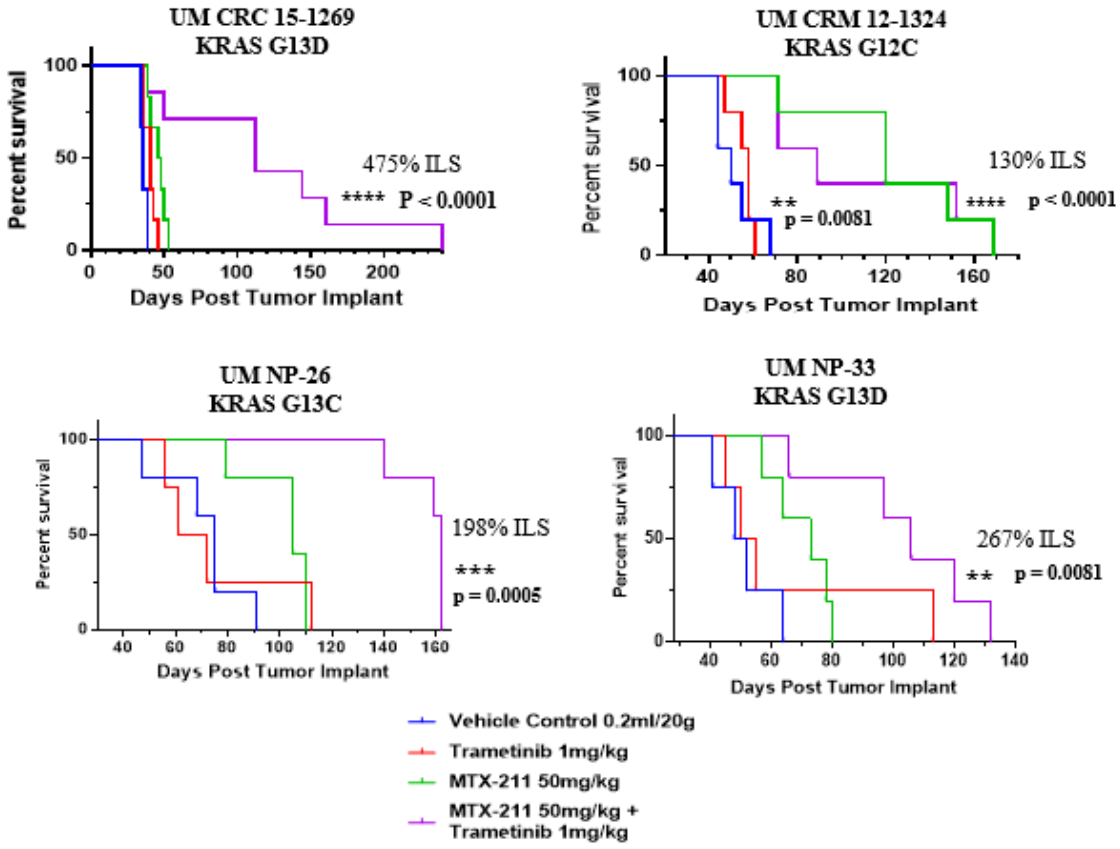

Figure 3.6: ***In vivo*** **activity of combination therapy.** Four UM CRC PDX models were evaluated for activity against trametinib, MTX-211 and combination therapy. Tumors were implanted subcutaneously and treated via oral gavage at the indicated doses once tumors reached ~150 mm^3, with cohorts consisting of at least five animals in each treatment group. Efficacy was evaluated by an increase in lifespan (ILS) and statistics are shown on graph.

Figure 3.5 / Supplementary Figure 1

A

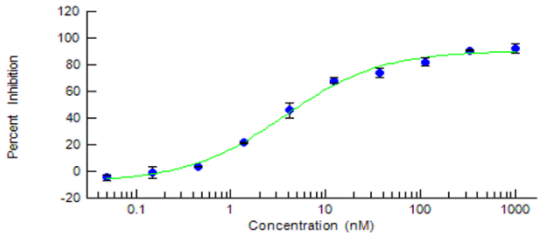

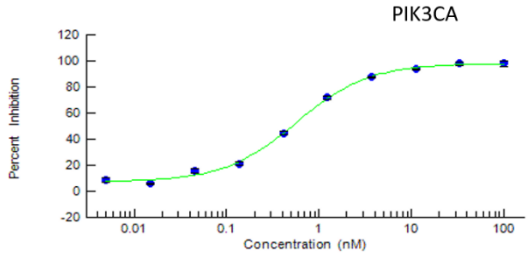

B

Tumor Subtype	Median IC50
Colon Cancer	1.11
Leukemia	1.17
Melanoma	1.29
CNS Cancer	1.43
Renal Cancer	1.45
Breast Cancer	1.75
Prostate Cancer	1.93
Non-Small Cell Lung Cancer	2.69
Ovarian Cancer	3.47

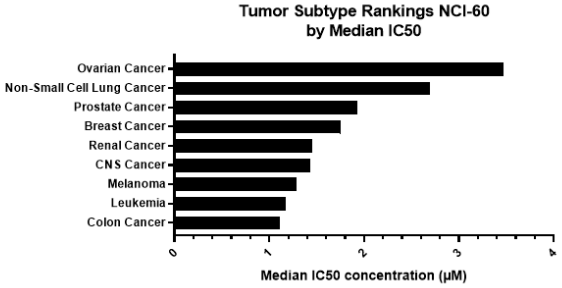

C

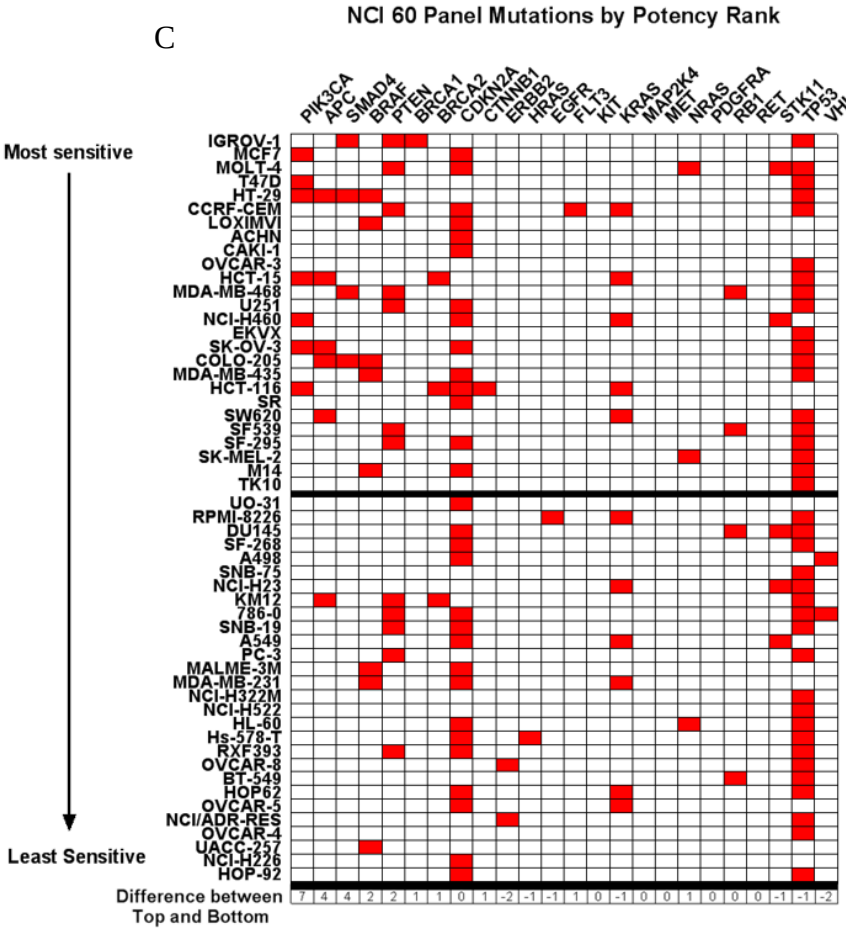

Figure 3.8: Target potency and response of NCI-60 panel to MTX-211 treatment. (A) Concentration response curves showing target potency against PI3K and EGFR in purified enzyme assays. (B) The NCI-60 panel was sorted by tumor subtype and the median IC_{50} of MTX-211. (C) NCI-60 panel sorted by sensitivity to MTX-211 with listed gene mutations.

Figure 3.6 / Supplementary Figure 2

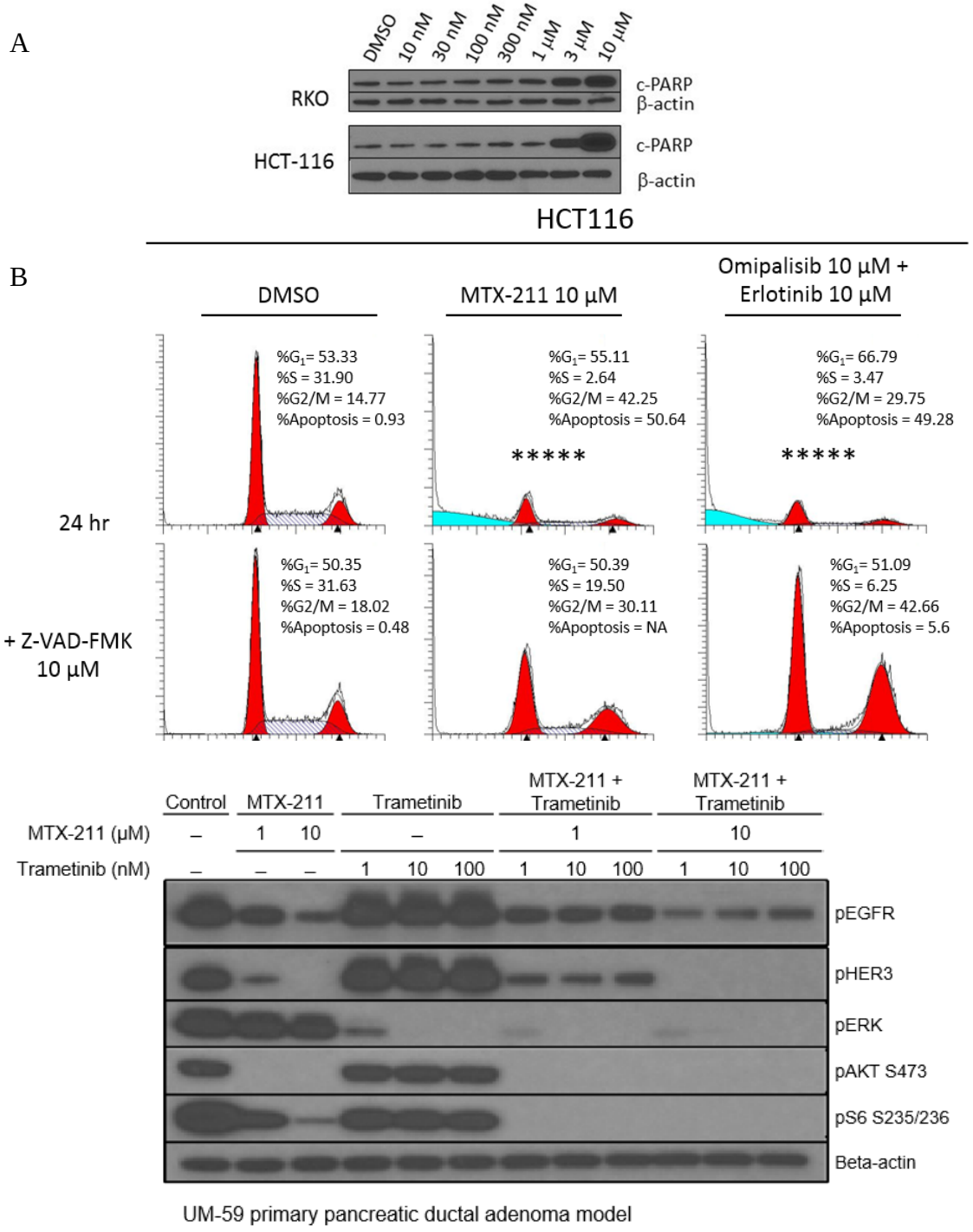

Figure 3.6: MTX-211 induces apoptosis in cells and blocks reactivation of pHER3 in response trametinib treatment. (A) Concentration-dependent titration of cleaved PARP induction in HCT-116 and RKO cells. (B) Cell cycle analysis of MTX-211 and comparator compounds show a similar induction of a sub-G1 population which is blocked by pan-caspase inhibitor Z-VAD-FMK. (C) $KRAS^{MT}$ pancreatic adenocarcinoma PDX model UM59 treated with trametinib and MTX-211, with immunoblots showcasing reactivation of pHER3 and pAKT by trametinib treatment.

Figure 3.7 / Supplementary Figure 3

A

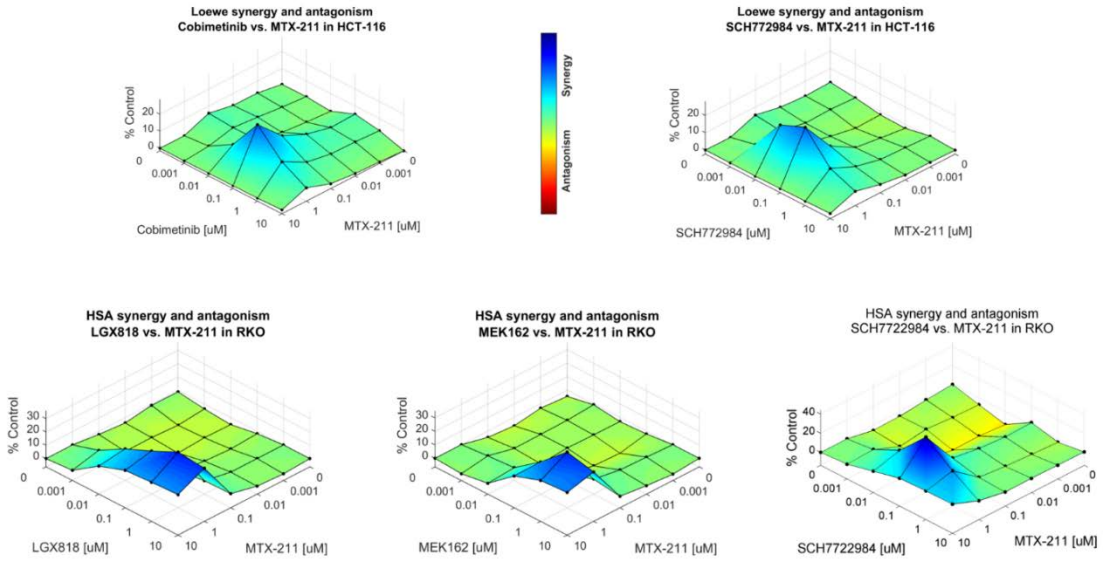

B

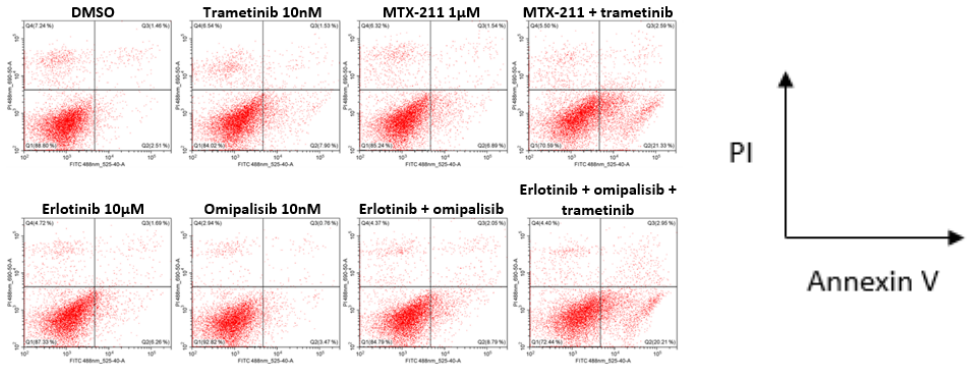

Treatment	PI- / Annexin V- (Live cells)	PI- / Annexin V+ (Early Apoptotic)	PI+ / Annexin V+ (Late Apoptotic)	PI+ / Annexin V- (Necrotic)
DMSO	88.80%	2.51%	1.46%	7.24%
Trametinib 10nM	84.02%	7.90%	1.53%	6.54%
MTX-211 1µM	85.24%	6.89%	1.54%	6.32%
MTX-211 + trametinib	70.59%	21.33%	2.59%	5.50%
Erlotinib 10µM	87.33%	6.26%	1.69%	4.72%
Omipalisib 10nM	92.82%	3.47%	0.76%	2.94%
Erlotinib + omipalisib	84.79%	8.79%	2.05%	4.37%
Erlotinib + omipalisib + trametinib	72.44%	20.21%	2.95%	4.40%

C

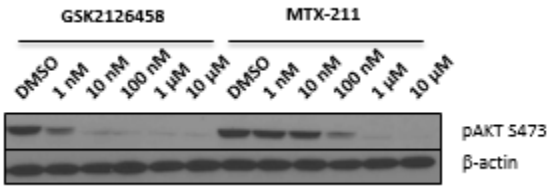

Figure 3.7: Discovery of synergy between MTX-211 and trametinib. (A) Synergy between MAPK pathway inhibitors and MTX-211 shown with synergy heatmaps generated with Comebenefit. (B & C) PI/Annexin V staining in HCT-116 cells examining the effects of trametinib and MTX-211 in comparison to erlotinib, omipalisib and trametinib at bioequivalent concentrations. Similar apoptosis is observed at these concentrations, consistent with the shared mechanistic basis of these inhibitors.

Figure 3.8 / Supplementary Figure 4

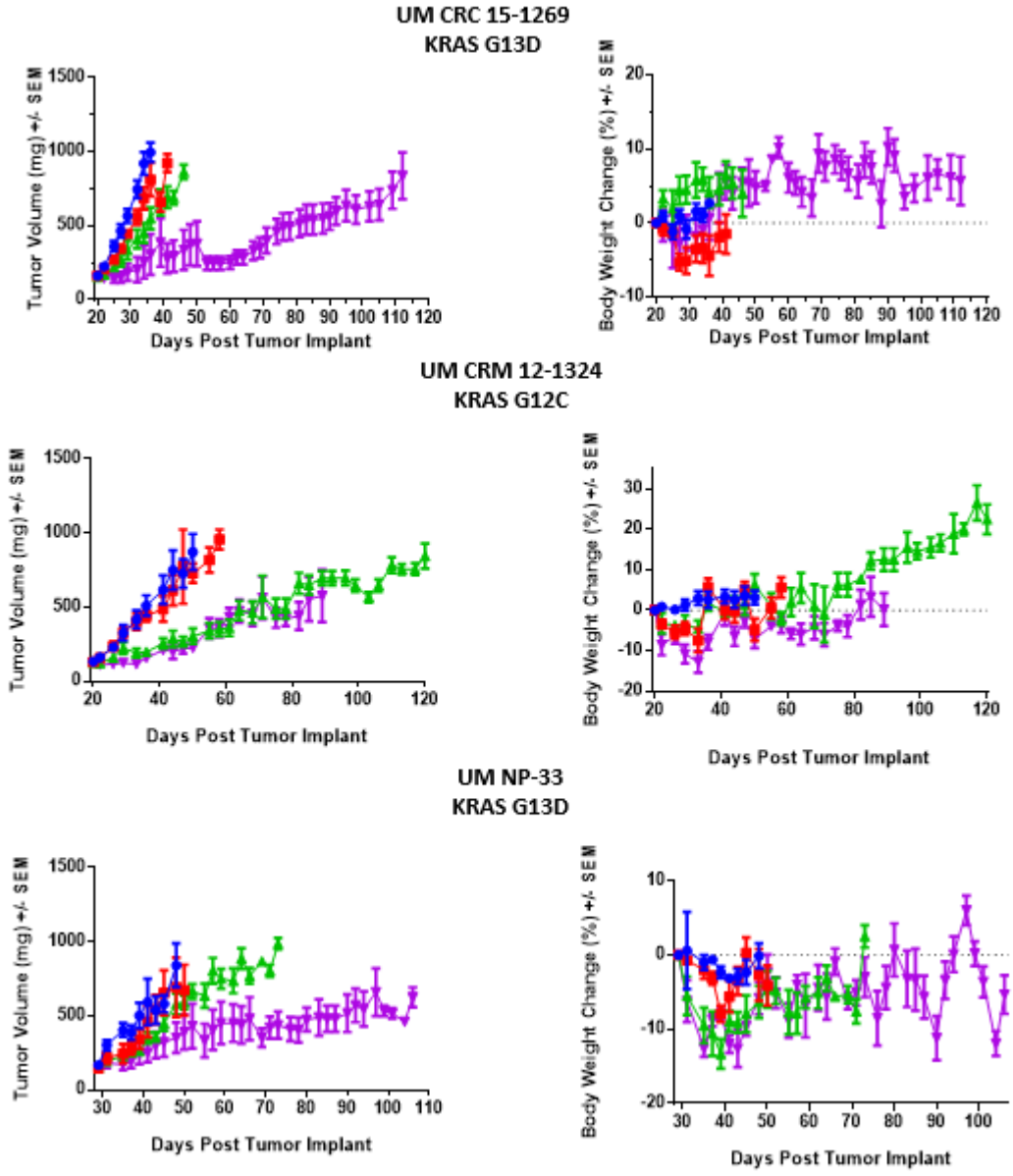

Figure 3.8: *In vivo* efficacy and safety plots of combination therapy. Trametinib and MTX-211 were evaluated as single agents and in combination for efficacy and dose tolerance. These plots are an alternate way of visualizing the *in vivo* graphs presented in Fig. 3.4. No significant body weight loss was observed in these studies as shown in the second column.

Figure 3.9 / Supplementary Figure 5

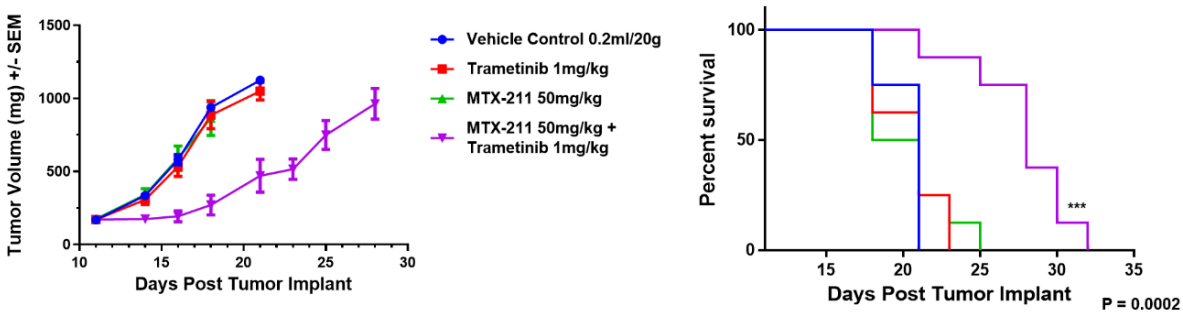

Figure 3.9: *In vivo* efficacy of MEK and MTX-211 combinatorial treatment in immune competent mice of KRAS^{MT} mouse model CT-26.

Figure 3.10 / Supplementary Figure 6

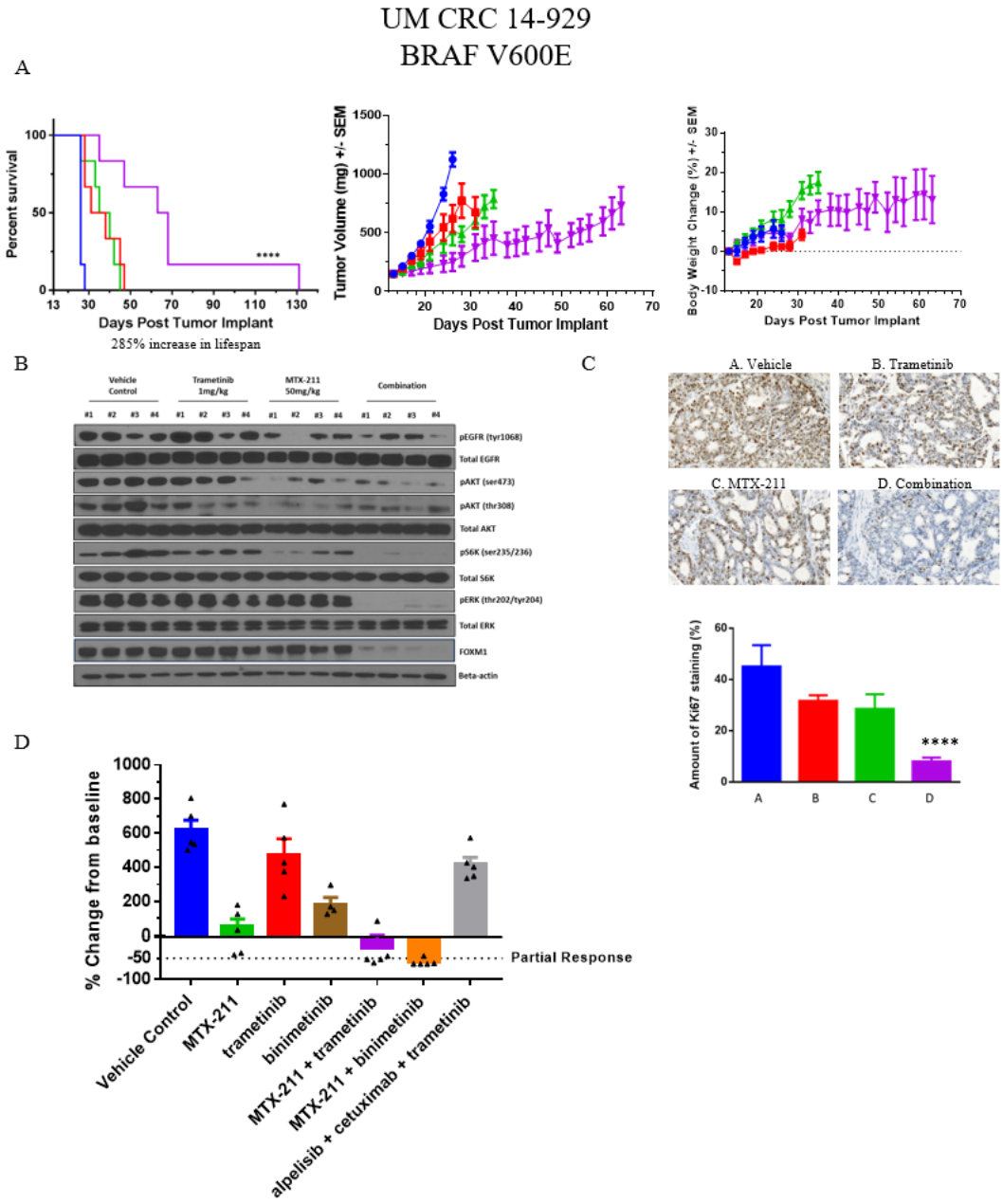

Figure 3.10: Activity of combination treatment of BRAF V600E model UM CRC 14-929. (A) Combination treatment showed substantial *in vivo* activity in this model, with a 285% ILS. Treatment was tolerated well by animals. (B) Immunoblots of lysates generated from harvested tumors show combination treatment decreases MAPK and PI3K signaling effectively, as well as ERK downstream target FOXM1. (C) Ki67 staining from the same harvested tumors mirrored the efficacy measurements. (D) *In vivo* comparator study in the UM CRC 14-929 model show equal if not better activity of MTX-211 and trametinib in comparison to similar compounds.

Supplementary Table 3.1

Kinase	% inhibition (10 μ M)	Kinase	% inhibition (10 μ M)	Kinase	% inhibition (10 μ M)	Kinase	% inhibition (10 μ M)	Kinase	% inhibition (10 μ M)	Kinase	% inhibition (10 μ M)	Kinase	% inhibition (10 μ M)
ABL1	81	CDK9	6	FES	10	IKBKE	1	MAPK8	3	PRKCA	7	SYK	52
ABL2	65	CHEK1	-3	FGFR1	-3	JAK1	-2	MATK	10	PRKCB2	22	TBK1	18
AKT1	4	CHEK2	12	FGFR3	1	JAK2	3	MET	27	PTK2	14	TEK	9
AKT2	8	CSF1R	5	FGFR4	15	JAK3	19	MST1R	4	PTK2B	-2	TNK2	16
ALK	8	CSNK1E	42	FGR	81	KDR	51	NEK2	-9	PTK6	39	TTK	91
AURA	72	CSNK2A1	8	FLT1	15	KIT	-8	NTRK1	12	RAF1	48	TYRO3	49
AURB	31	DNA-PK	**102**	FLT3	35	KSR2	11	PAK4	7	RET1	81	WEE1	8
AURC	7	EGFR	**102**	FLT4	44	LCK	42	PDGFRA	20	ROCK1	3		
AXL	69	EPHA1	66	FRAP1	**99**	LYN	61	PDGFRB	-1	ROS1	-1		
BRAF	-7	EPHA2	44	FYN	17	MAP2K1	8	PDK1	-5	RPS6KA1	16		
BTK	77	EPHA3	8	GSG2	89	MAP3K14	5	PIK3CA	**100**	RPS6KB1	-2		
CDC42	0	EPHB2	66	GSK3A	40	MAP3K8	18	PIK3CD	**98**	SGK	50		
CDK1	47	EPHB4	63	GSK3B	35	MAP4K4	57	PIK3CG	**99**	SGKL	5		
CDK2	7	ERBB2	**94**	HCK	43	MAPK1	-4	PIM1	19	SPHK1	-50		
CDK5	7	ERBB4	**95**	IGF1R	8	MAPK14	18	PLK1	6	SRC	10		
CDK7	-2	FER	7	IKBKB	7	MAPK3	-1	PLK3	21	STK33	11		

Table 3.1: Inhibition of a general kinase panel by MTX-211.

Supplementary Table 3.2

Route	Dose (mg/kg)	$T_{1/2}$ (hr)	AUC_{INF_obs} (hr*ng/ml)	Cl_{obs} (ml/hr/kg)	$AUMC_{INF\_obs}$ (hr*hr*ng/ml)	MRT_{INF_obs} (hr)	V_{ss_obs} (ml/kg)	C_{max} (ng/ml)	T_{max} (hr)	Bioavailability (%)
IV	10	2 ± 0.1	22263 ± 1159	450 ± 24	38128 ± 6000	1.7 ± 0.27	312 ± 18	N/A	N/A	N/A
PO	20	6.68± 3.3	34431 ± 3498	593 ± 111	288690 ± 136905	8.13 ± 3.04	N/A	8683 ± 969	0.55 ± 0.42	77.3

Table 3.2: Pharmacokinetics of MTX-211.

Supplementary Table 3.3

Model	Gender	Age	Prior Chemotherapy	Location	Histopathology				Mutational Status			Microsatellite Instability
					Type	TNM	Stage	Degree of Tumor Differentation (Grade)	KRAS	BRAF	PIK3CA	
UM-CRM 12-1324	M	54	Unkn	Liver	ADC	Unkn	Unkn	Poor	G12D	WT	WT	Unkn
UM-CRC 14-929	F	77	No	Transverse Colon	ADC	pT3N0	IIA	Moderate	WT	V600E	WT	Microsatellite unstable
UM-CRC 15-1269	F	78	No	Cecum	ADC	pT2N1a	IIIA	Moderate	G13D	WT	WT	Microsatellite stable (MSS)
NP-26	M	45	No	Rectum	ADC	pT3N2	IIIB	Moderate	G13D	WT	WT	Microsatellite stable (MSS)
NP-33	F	51	No	Rectum	ADC	pT4N2	IIIC	Moderate	G13D	WT	WT	Microsatellite stable (MSS)

Abbreviations: ADC = adenocarcinoma; MUC = Mucinous; WT = Wild type; Unkn = Unknown

Table 3.3: PDX models from University of Michigan used in this report.

Appendix B

Many people have contributed to the research studies presented in this chapter and their corresponding contributions are listed below.

Conception and design: Maust, JM, Sebolt-Leopold, JS, Whitehead, CE, Ziemke, EK

Computational chemistry: Whitehead, CE

Animal studies: Mumby, RM, Ziemke, EK

PDX models source: Hardiman, JM, Sebolt-Leopold, JS

Acquisition of data: Frankowski-McGregor, CL, Ku, JB, Maust, JM, Mumby, RM, Whitehead, CE, Ziemke, EK

X-ray crystallography: Ohren, JF, Viola, R, Whitehead, CE, Young, M

Writing, review and/or revisions of manuscript: Maust, JM, Sebolt-Leopold, JS, Whitehead, CE, Ziemke, EK

Chapter 4: Discussion and Future Directions

Prior to 1975, cytotoxic agents were all that was available for cancer therapy. Tamoxifen was the first hormonal anti-cancer drug, and hormonal agents have grown since then to account for approximately 20% of all cancer treatment drugs (Savage, 2012; Savage, 2013). The time range from 1980-2000 saw an increasing amount of diversity in the content of approved drugs and the most prolific period of drug approval, with introduction of hormonal agents, new cytotoxics, and a few targeted therapies. It wasn't until after 2000 that a new era of drug discovery came, with the introduction of monoclonal antibodies, kinase inhibitors and other targeted therapies. In fact, from 2010-2014, the largest increase in novel drugs were kinase inhibitors, with 13 new inhibitors introduced to the market (Savage and Mahmoud, 2015).

Following the introduction of these novel targeted therapies, the field began to think of cancer treatment not only in terms of tissue of origin, but the genetic background of cancer and the mutations driving oncogenesis. This in turn led to the concept of precision medicine, wherein individualized treatment plans are tailored to the mutations present in a particular tumor, regardless of tissue of origin (2017; Mateo et al., 2018). This has become more prevalent due to the significant decrease in costs of genomic sequencing, as well as an increase in "big data" projects that emphasize the power of bioinformatics in discovering trends in large patient datasets and in informing treatment decisions. These precision

medicine approaches de-emphasize subjective treatment decisions and aim to place decision making that is based on similar data from large patient cohorts.

RAS mutations occur in 30-40% of all cancer and are a prime target for precision medicine approaches, although they have proven especially difficult to treat due to the absence of direct inhibitors and the lack of efficacy in inhibiting downstream effectors. Therefore, novel therapies for the treatment of RAS mutant disease are needed to help inform precision medicine approaches.

Historically, while inhibition of RAS signaling has focused on inhibition of downstream effectors as single agents, inhibition of multiple different downstream effectors in combination has emerged as essential for addressing the compensatory signaling that arises in response to monotherapies. The design of combination treatment approaches have been empowered by a better understanding of the feedback regulatory mechanisms that govern pathway output.

MAPK pathway inhibitors have been approved in melanoma and include vemurafenib (BRAF), dabrafenib (BRAF) and trametinib (MEK). However, many of these agents prolong rather than ensure survival. For indications such as colorectal, MAPK pathway inhibitors have not been as successful, with approved therapies limited to EGFR-based inhibitors cetuximab and panitumumab. While these MAPK pathway inhibitors have been approved, they are contraindicated in patients with KRAS mutations, as EGFR inhibitors have shown a lack of efficacy in a $KRAS^{mt}$ setting (Douillard et al., 2013). These agents are therefore limited to the treatment of EGFR-expressing, metastatic colorectal cancer that are $KRAS^{wt}$. The situation is similar for pancreatic cancer, where erlotinib, an EGFR inhibitor, was approved for the treatment of pancreatic cancer in combination with

gemcitabine. It was approved based on clinical trial results showing that median overall survival improved from 5.91 to 6.24 months with gemcitabine alone compared to gemcitabine and erlotinib in combination, respectively (Amanam and Chung, 2018). These modest improvements in outcome highlight the need for better therapeutics, as erlotinib was only improved based on this improvement due to the critical lack of effective therapeutics in the area.

Co-targeting MEK and CDK4/6

The lack of agents for the treatment of $KRAS^{mt}$ colorectal and pancreatic cancer forms the rationale for MAPK-based combination therapies discussed in this dissertation. The first of these discussed was co-targeting MEK and CDK4/6 for the treatment of pancreatic cancer. The rationale for evaluating this combination was based on several factors outlined in the introduction of Chapter 2. Briefly, the high mutation rate of KRAS and CDKN2A is conducive to a combination therapy targeting the signaling consequences of these mutations (Figure 4.1 and Figure 4.2). Furthermore, additional evidence for this combination has been shown in studies showing synthetic lethality between KRAS and CDK4/6 (Mao et al., 2014; Puyol et al., 2010). CDK4 was also identified as a key driver of an alternative phenotype when comparing genetic ablation of mutant NRAS to the same cells treated with a MEK inhibitor instead (Kwong et al., 2012).

A synergy-based screen was carried out in order to evaluate the efficacy of this dual-targeted therapy in pancreatic cancer. A high degree of synergy was found in two adenosquamous carcinoma pancreatic cell lines, L3.6pl and UM59. This synergy was accompanied by high expression of COX-2, which was ablated by the introduction of

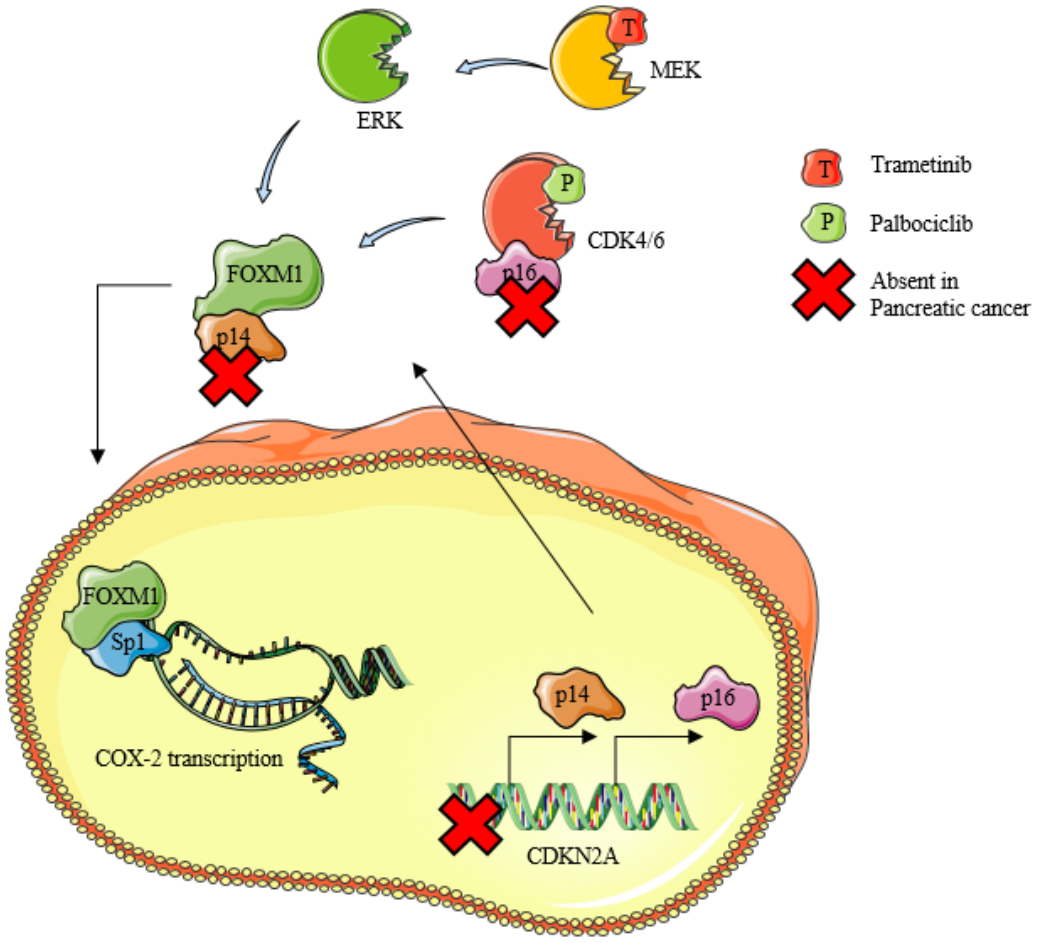

Figure 4.1: Genetic aberrations predisposing pancreatic cancer to dual inhibition of MEK and CDK4/6 and the signaling implications of these mutations.

CMV-driven COX-2 gene expression as well as shRNA targeting COX-2. This led to the conclusion that high levels of COX-2 expression could potentially serve as a biomarker of exceptional response to combination therapy in pancreatic cancer. COX-2 has been extensively studied for its role in driving inflammation and carcinogenesis in pancreatic cancer as well as other cancers (Hawk et al., 2002; Hill et al., 2012; Ogino et al., 2008; Okami et al., 1999). It appears that pancreatic cancer cell lines in which COX-2 expression is elevated indicates a cellular context which is particularly sensitive to the effects of co-targeting MEK and CDK4/6.

The exact reason for these results is unclear, although we hypothesize that transcriptional control of COX-2 by MEK and CDK4/6 occurs through their direct control of the COX-2 transcriptional regulator FOXM1. CDK4/6 phosphorylation controls stability of FOXM1 (Anders et al., 2011) and activity and cellular localization is controlled by ERK phosphorylation as well (Ma et al., 2005b). In addition to these data, CDKN2A, which encodes for endogenous inhibitor CDK4/6 p16, also encodes p14. CDKN2A is deleted in the majority of cases of pancreatic cancer, which means loss of both these proteins. p14, has a role in regulating E3 ubiquitin-protein ligase MDM2 which itself regulates p53 protein levels (Kumamoto et al., 2004; Lohrum et al., 2000). In addition, it has also been shown to directly bind and regulate FOXM1 due to the presence of two independent MDM2 binding domains (Pandit and Gartel, 2015; Quan et al., 2013). Therefore, in pancreatic cancer, not only do ERK and CDK4/6 play a role in regulating FOXM1, but there is an additional role for p14, which is itself not present in the majority of cases due to the deletion of CDKN2A. These considerations serve as suggestive circumstantial evidence for the ostensible role of combination therapy in targeting and reducing expression of FOXM1 and in turn COX-2.

While FOXM1 is potentially implicated in the activity of MEK and CDK4/6 combination therapy, there exist other potential mechanisms of regulation behind COX-2. Reports indicate that COX-2 co-localizes at the plasma membrane with caveolin-1, a component critical for formation of plasma membrane caveolae (Liou et al., 2001; Perrone et al., 2007). These caveolae can function as signaling hubs, wherein they can be critical for the formation of lipid rafts as well as entry of signaling pathway components into these caveolae invaginations (Boscher and Nabi, 2012; Quest et al., 2008). In this way, close

proximity of the components of various signaling pathways can modulate pathway expression as well as gate potential directions for that signaling. Furthermore, localization to lipid rafts and plasma membrane location can modulate proximity to membrane bound tyrosine kinase receptors and gate signaling further in this way. It is possible that co-localization MAPK-pathway components with COX-2 and its effector prostaglandins and in turn their effectors can form a signaling loop. COX-2 leads to the production of

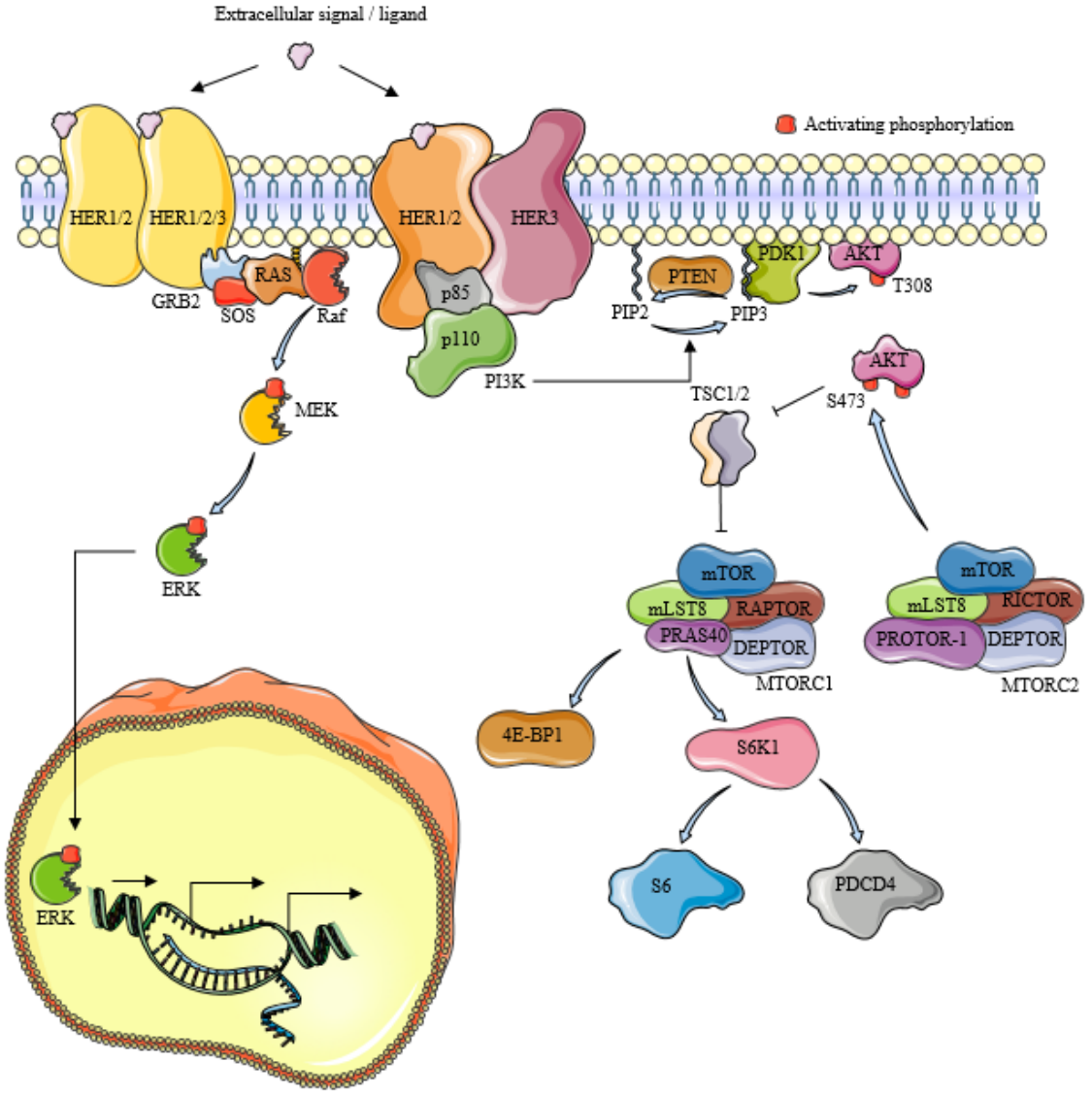

Figure 4.2: Extracellular growth signals are required for activation of MAPK and PI3K signaling in a normal setting. Mutation and overexpression of HER family members and RAS leads to malignant growth, which leads to gene expression and growth changes.

prostaglandins, which themselves activate the EP1-4 family of receptors. EP4 signaling has been shown to transactivate EGFR through Src-mediated phosphorylation minutes following treatment of cells with PGE_2, which was blocked by an EGFR inhibitor or an EP4 inhibitor, with other studies corroborating these results (Buchanan et al., 2003; Kim et al., 2010; Pai et al., 2002).

Furthermore, the role of COX-2 in angiogenesis has been noted (Huang et al., 2013). Given the downregulation seen, it is possible that combination treatment leads to activity partly through inhibition of angiogenesis in the developing tumors. I have anecdotal evidence from the L3.6pl animal study, in which tumors were harvested for RPPA analysis. The tumors from combination treated animals were paler than tumors from control and single agent groups and appeared to have less blood vessel innervation. However, at the time, pictures were not taken, as it did not appear important.

Caveolin-1

Caveolin-1 has been implicated in protein degradation of COX-2 (Chen et al., 2010). Caveolin-1 null mice showed higher expression of COX-2 and deletion of the C-terminus of COX-2 (which is distinct from COX-1), decreased both binding between the two and the ability of caveolin-1 to reduce COX-2 expression. In the studies in Chapter 2 showing CMV-driven COX-2 decreased activity of combination therapy, there still existed significant decreases in COX-2 expression, presumably both from endogenous COX-2 still present as well as the ability of caveolin-1 to decrease COX-2 protein. Considering that the RPPA dataset showed a modest increase in caveolin-1 in combination treated tumors (Chapter 2), the role of caveolin-1 and signaling caveolae cannot be discounted and should be considered for future studies. The significance of this possibility is that efficacy of

combination therapy could be dependent on co-localization of COX-2 with MEK, CDK4/6 and/or kinase suppressor of RAS (KSR), a complex needed for MAPK signaling (Morrison, 2001; Nguyen et al., 2002; Razidlo et al., 2009; Roskoski, 2012). While signaling between all of these distinct pathways is assumed to occur in disparate locations of the cell, emerging evidence suggests that there may be more to regulation of these pathways than simple protein partners and linear signaling.

Pdcd4

In addition to regulation of COX-2, Pdcd4 was the other protein found to be most regulated by combination therapy upon RPPA analyses. This protein was recently discovered and the complete function is unknown, although a role in inhibiting progression of cancer and regulation by AKT has been discovered (Afonja et al., 2004; Kang et al., 2002; Leupold et al., 2007; Palamarchuk et al., 2005; Zhang and DuBois, 2001; Zhen et al., 2016). Among these studies, it was found that decreased expression of this protein correlated with increased invasiveness and progression of cancer. It is telling that an increase in protein expression of Pdcd4 was found in the tumors of animals treated with combination therapy, suggesting the initiation of cell death signaling and a possible tumor suppressor role. However, no increase in apoptotic proteins PARP, caspase-3, 7 or 8 was observed concurrently. As mentioned in Chapter 2, this tumor suppressor has been found to be in part responsible for the anti-cancer effects of COX-2 inhibitor NS-398 in a study looking at colorectal cancer, suggesting a possible link to the current study, wherein Pdcd4 expression was increased alongside a decrease in COX-2 (Zhang and DuBois, 2001). To further strengthen this correlation, Pdcd4 has also been shown to negatively regulate gene expression by inhibiting Sp1/Sp3 binding at important motifs, which has implications for

the current study seeing as FOXM1 cooperates with Sp1 to promote COX-2 expression (Leupold et al., 2007). While no conclusive mechanistic insights come from these observations, many of these proteins have roles suggestive of mutual regulation.

Emerging observations in the field

In a manuscript published in 2014, Franco et al. conducted studies to screen for pathway selective inhibitors that show favorable activity in combination with CDK4/6 inhibitors (Franco et al., 2014). In this study, the observation was made that cyclin E expression was increased in cells treated with CDK4/6 inhibitors. At the time, aberrant induction of cyclin E was considered a targeted symptom of CDK4/6 inhibition and it was observed that shRNA knockdown of cyclin E and inhibitors that blocked induction of cyclin E showed synergy with CDK4/6 inhibitors. Beyond this observation, this group has not published any additional insights concerning this phenomenon. In fact, in 2016, Franco et al. reported the upregulation of cyclin D in response to CDK4/6 inhibition, with no mention of cyclin E (Franco et al., 2016). Both studies were conducted in models of pancreatic cancer, and the group collaborates with a surgeon at their institution for the establishment of PDX models of pancreatic cancer, in which they've identified CDK4/6 inhibition as a viable therapy for pancreatic cancer (Witkiewicz et al., 2015a; Witkiewicz et al., 2015b). Other than these two studies, there is a gap in the literature concerning the paradoxical upregulation of cyclin D/E in response to CDK4/6 inhibition.

Palbociclib (Ibrance®) was given accelerated approval by the FDA in 2015 based on results from PALOMA-1, a phase 2 randomized, open-label clinical trial evaluating palbociclib in combination with letrozole for the treatment of postmenopausal, ER+, HER2- breast cancer (Finn et al.). PALOMA-2 and PALOMA-3 were phase 3 double-

blind, randomized, clinical trials evaluating palbociclib in combination with letrozole (Finn et al., 2016) or fulvestrant (Cristofanilli et al., 2016), respectively. PALOMA-1 and PALOMA-2 both had biomarker cohorts, wherein certain predicted biomarkers were analyzed for their predictive ability. In PALOMA-1, a cohort of patients was required to contain amplification of cyclin D1, loss of p16 (CDKN2A), or both. In PALOMA-2, ER, Rb, p16, cyclin D1 and Ki67 were the biomarkers selected. In both studies, no significant predictive ability of cyclin D1 amplification or p16 loss was found, which runs counter to the fundamental assumption that these genetic alterations are necessary for activity of CDK4/6 inhibition. These negative results in biomarker analyses cause some confusion due to the fact that rational design of CDK4/6 inhibitors was predicated on its ability to restore functionality of p16 loss, which is the second-most mutated gene in human cancer (Liggett and Sidransky, 1998; Yarbrough et al., 1999).

While neither cyclin D1 amplification or p16 loss can predict activity of CDK4/6-based combination therapy, emerging evidence from the PALOMA-3 trial revealed that high cyclin E expression can help predict response to palbociclib in metastatic breast cancer (Turner et al., 2018). Therefore, the only biomarker to date determined to predict for activity to palbociclib other than the presence of Rb is cyclin E, not p16 loss or cyclin D amplification. This fact brings us back to the phenomenon observed in pancreatic cancer in response to palbociclib treatment which upregulates cyclin D and E. It is important to first note that cyclin E is dispensable for mouse development and is not necessarily required for proliferation of all cell types, as commonly assumed (Geng et al., 2003). In fact, cyclin E deficient cells lack the ability to exit G_0 to S, presumably due to the ability of cyclin E-CDK2 complex to load mini-chromosome maintenance (MCM) proteins at origins of

replication (ORC). Furthermore, cyclin E-deficient cells resist oncogenic transformation. It would follow that overexpression of cyclin E promotes oncogenic transformation, as has been observed, notably in breast cancer (Furstenthal et al., 2001; Gao et al., 2013; Lunn et al., 2010; Matsumoto and Maller, 2004; Skalicky et al., 2006).

The most likely explanation for the increase in expression of cyclin D and E in response to CDK4/6 inhibition is the loss of transcriptional regulator FOXM1, as was seen in Chapter 2 upon treatment with CDK4/6 inhibition as well as combination therapy. FOXM1 is a critical regulator of cell cycle genes Skp2 and Cks1, which form part of the SCF ubiquitin ligase complex that degrades the G_1 cyclins as well as the cyclin dependent kinase inhibitor (CKI) proteins p21 and p27 (Vodermaier, 2004; Wang et al., 2005). The lack of SCF complex degradation capacity likely leads to an accumulation of cyclin D/E and CKIs p21 and p27. In addition to this, CKIs p21 and p27 are not only inhibitors of the complex activity, but are also critical for activation of the cyclin D-CDK4/6 and cyclin E-CDK2 complexes due to the nuclear localization sequences on p21 and p27 which are not present

on CDK4/6 and CDK2 (Bockstaele et al., 2006; Cheng et al., 1999; Child and Mann, 2006). Therefore, the accumulation of cyclins D and E as well as p21/p27 is likely caused by an inability of the cell to generate the necessary components to degrade them, as the cell is permanently stuck in late G_1 due to the presence of CDK4/6 inhibition. Increases in p21 and p27 can be seen in Chapter 2 in response to treatment, and unpublished data generated in the Leopold Lab point not only to increases in cyclins D and E but also an increased association with their cognate CDKs in immunoprecipitation experiments. An increased association between cyclin D and CDK4 and cyclin D and p21 is also observed. This lends credence to the hypothesis that cells are permanently stuck in G_1 due to the presence of

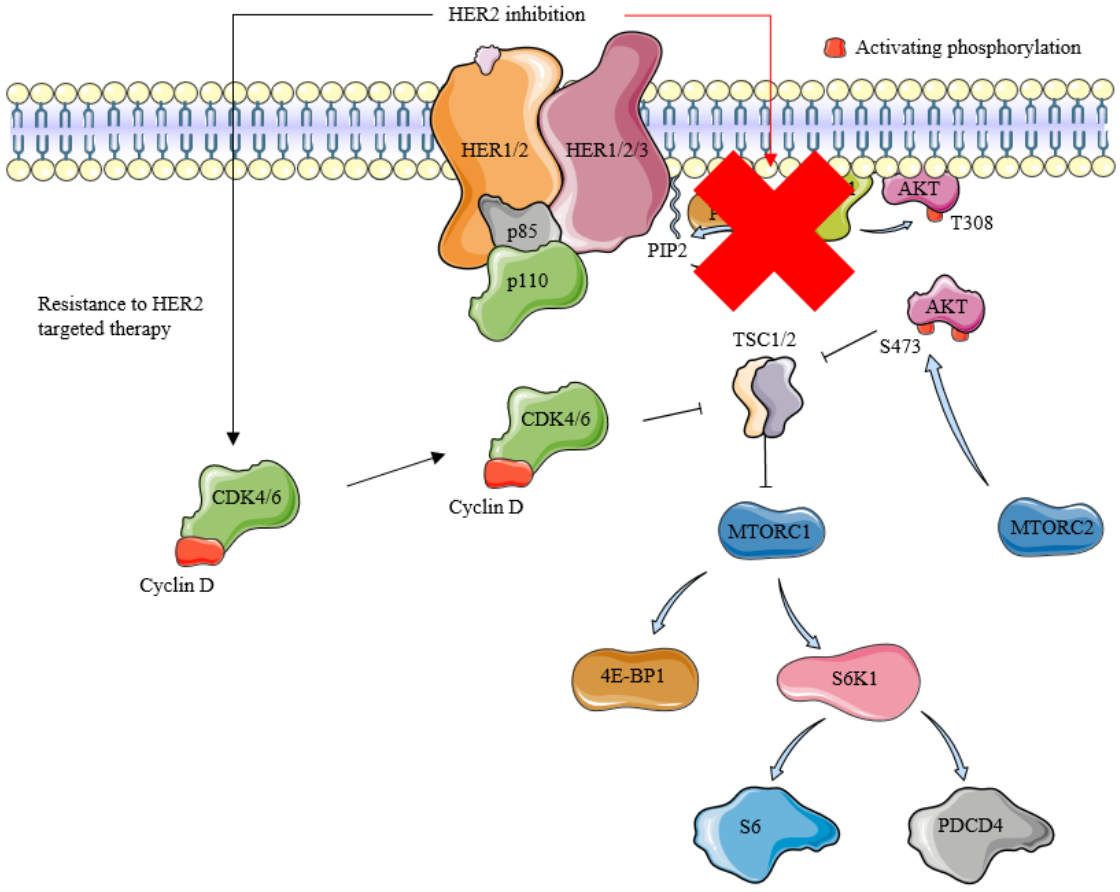

Figure 4.3: CDK4/6-cyclin D complex signaling has been implicated in resistance to HER2-targeted therapies. Resistance through this complex leads to inhibition of TSC1/TSC2 and activates MTOR signaling, which HER2 normally activates.

these associated and inhibited complexes and the inability of the cell to degrade them and progress to S phase.

The observation that increased expression of cyclin E could predict for sensitivity to palbociclib in PALOMA-3 may or may not be related to the previous observations made regarding accumulation of cyclin E. The most likely explanation is that they are unrelated to each other. Cyclin E is the last critical regulator of the $G_1 \rightarrow$ S transition, as cyclin E mediates the transition past the G_1 restriction point and further regulates MCM loading and ORC formation (Ferguson and Maller, 2008; Geng et al., 2007; Geng et al., 2003; Liu et al., 2000; Lunn et al., 2010). Higher expression of cyclin E likely forces DNA replication through phosphorylation and inactivation of Rb in cells that would otherwise senesce or stall at the G_1 DNA damage checkpoint. This is consistent with reports that low molecular weight isoforms of cyclin E in breast cancer lead to increased genomic instability and tumorigenesis due to the higher affinity of LMW cyclin E for CDK2 (Duong et al., 2012; Loeb and Chen, 2012; Nanos-Webb et al., 2012; Wingate et al., 2009). It seems that the ability of cyclin E to predict for palbociclib activity therefore arises from the ability of CDK4/6 inhibition to interrupt this uncontrolled cell division at the checkpoint immediately prior to cyclin E-CDK2, or to force cells into G_0. The ability of cyclin E to promote tumorigenesis is further supported by elegant studies showing CDK2 to be a critical mediator of the cell decision in mitosis to continue proliferating or to enter a state of quiescence (Spencer et al., 2013).

Tuberin Sclerosis Complex (TSC1/TSC2)

CDK4/6 inhibition has been extensively studied for the treatment of breast cancer in combination with letrozole and fulvestrant, as covered in the previous section. Recently

however, it was reported that resistance to HER2 targeted therapy in breast cancer was mediated by cyclin D-CDK4 (Goel et al., 2016). This group showed that CDK4/6 not only suppresses Rb phosphorylation, but also plays a role in de-activating TSC1/TSC2 through phosphorylation, which has been known for some time (Franco et al., 2016; Huang and Manning, 2008). Inhibition of CDK4/6 through use of clinical inhibitors therefore led to activation of TSC1/TSC2, which in turn attenuates mTOR activity (Ma et al., 2005a). With EGFR/HER2 inhibition, CDK4/6 inhibition therefore increases activity by participating in reduction of TSC1/TSC2 phosphorylation, which attenuates mTOR activity further and consequently helps relieve feedback inhibition of the HER family members.

In relation to the current project, the possibility that co-targeting MEK and CDK4/6 modulates the AKT-MTOR axis is interesting. It has been reported that cyclin D by itself regulates the TSC complex, irrespective of CDK4/6 binding (Zacharek et al., 2005). A mutant cyclin D protein that is unable to bind the CDK complex negatively regulates TSC expression (Zacharek et al., 2005). Therefore, the previously mentioned finding that cyclin D and cyclin E expression is increased in response to CDK4/6 inhibition suggests that a regulatory role in the AKT-MTOR axis exists. This role could lead to negative regulation of TSC1/TSC2 expression, thereby activating the pathway. This suggests a mechanism of resistance to CDK4/6 inhibition in activating mTOR. Activation of mTOR explains the observation that cells treated with CDK4/6 inhibitors show aberrant cell size growth (Franco et al., 2016; Franco et al., 2014; Witkiewicz et al., 2015a). In fact, Franco et al. report that while MEK and CDK4/6 co-inhibition leads to cell cycle exit in pancreatic cancer, co-inhibition of mTOR and CDK4/6 results in superior activity by suppressing cell growth and metabolism, leading to apoptosis reduction in tumor growth (Franco et al.,

2016). This group claims that CDK4/6 inhibition elicits metabolic reprogramming by stimulating glycolytic and oxidative phosphorylation metabolism, increasing mitochondrial numbers and reactive oxygen species (ROS).

Discovery of small molecule inhibitor MTX-211

Chapter 3 outlined the discovery of MTX-211, a dual inhibitor of EGFR and PI3K. The rational design of MTX-211 was based on known binding small molecule inhibitors of PI3K and EGFR omipalisib and erlotinib, respectively. Omipalisib bound to PI3K is flipped relative to how erlotinib binds EGFR. Therefore, while sharing a common core, they share similarities that enabled the design and synthesis of a dual inhibitor by assimilating features of both. Crystallization studies confirmed the flipped binding orientation of MTX-211, and *in vitro* kinase assays show potency against PI3K and EGFR at 0.6 and 3.6 nM, respectively. More expansive assays studying potency against other family members showed that MTX-211 possesses potent inhibitor activity against HER2/HER4 and mTOR.

The rationale and computational design of MTX-211 form the basis of its novelty, as it is the first reported highly selective inhibitor of both a tyrosine and lipid kinase. However, it remains unclear which patient population would derive the greatest benefit. The utility of MTX-211 as a single agent is being explored in various indications that show mutation or overexpression of EGFR to exploit MTX-211's ability to target EGFR-altered cancers. Glioblastoma, colorectal cancer, lung cancer and pancreatic cancer are a few indications with a significant percentage of EGFR mutant tumors, which form part of the rationale for the application of MTX-211. In addition to EGFR-altered cancers, PI3K mutant tumors

(either PIK3CA or PTEN mutations or HER overexpression) are another component of the development portfolio for MTX-211.

While MTX-211 would be expected to exhibit single agent activity in a defined population of patients, the greater utility of MTX-211 in combination with other inhibitors is being investigated. Combination-based therapies increase the chance of successful treatment given the wide variety of regulatory feedback pathways and signal redundancy that lead to resistance. A prime target for a combination-based therapy is MEK, given the reports that have implicated MEK in resistance to HER-based therapies.

MEK as a target for combination therapy with MTX-211 was explored in Chapter 3, and the rationale has been covered in Chapter 1. Briefly, ERK-induced feedback inhibition of EGFR is decreased upon inhibition of MEK and other MAPK pathway kinases, which leads to reactivation signaling through the MAPK and PI3K-AKT pathways (Corcoran et al., 2012; Li et al., 2008b; Lito et al., 2012; Morris et al., 2013; Nissan et al., 2013). MEK inhibition has also been shown to lead to increased transcription and phosphorylation of HER3, an activator of EGFR and HER2 and thus several different growth pathways, which we have shown occurs in Chapter 3 (Kitai et al., 2016; Montero-Conde et al., 2013; Sergina et al., 2007; Sun et al., 2014; Turke et al., 2012a). In Chapter 3, a decrease in phosphorylation of T669 on EGFR was seen with MEK inhibition, which confirms the rationale for combining MTX-211 with a MEK inhibitor, in order to target the reactivation of EGFR as well as PI3K. At the same time, increased phosphorylation of HER3 was also seen in the models tested, leading to an increase in AKT activation in response to MEK inhibition. This activation of AKT was also targeted by MTX-211, which led to impressive synergy upon co-inhibition with trametinib and MTX-211. The data shown in Chapter 3

therefore establish precedent for this combination therapy in colorectal cancer. On the same track, in addition to MEK, it is expected that MTX-211 would be comparably effective in combination with BRAF inhibitors, as these have led to similar relief of feedback inhibition.

The ability of signal transduction pathways to inhibit proapoptotic proteins such as BAD has been explored (Bonni et al., 1999; Fang et al., 1999; She et al., 2005). EGFR and PI3K signaling were shown to contribute to the phosphorylation of BAD on Ser112 and Ser136, respectively. Increased signaling through these growth pathways in cancer therefore prevents initiation of apoptosis (Chen et al., 2001; Mebratu and Tesfaigzi, 2009; Roskoski, 2012; Will et al., 2014). MTX-211 inhibits both phosphorylation sites through MAPK and PI3K pathway inhibition, which accounts in part for increased apoptosis observed in cells treated with MTX-211. This agent, both as a single agent and in combination with a MEK inhibitor causes significant induction of apoptosis through the loss of S112/S136 phosphorylation on BAD and induction of cleaved PARP and caspase-3 expression, consistent with an increase in the population of stained cells that are PI-/Annexin V+ and PI+/Annexin V+ (Chapter 3). The primary mechanism by which MTX-211 contributes to tumor growth inhibition appears to be through induction of apoptosis, by itself and in combination with MEK inhibition. The extent of this effect in tumors as a single agent and in combination is likely mutation dependent, as the activity of MTX-211 decreases in the presence of RAS or RAF mutations, necessitating the addition of a MEK inhibitor.

In addition to the inhibition of EGFR and PI3K by MTX-211, some activity is observed in the inhibition of mTOR. This is favorable considering that inhibition of AKT activation has been shown affect regulatory feedback loops surrounding MTORC1 (Chandarlapaty et

al., 2011). Inhibition of AKT causes upregulation of a specific set of RTKs (HER3, IGF-1R, insulin receptor) in a wide spectrum of tumor types in response to typical PI3K inhibitors. The ability of MTX-211 to inhibit mTOR therefore adds an additional layer protecting against tumor adaption to drug treatment.

Colorectal Cancer and Pancreatic Cancer

MTX-211 was evaluated for activity against a panel of 60 standardized cell lines curated by the NCI (NCI-60), of various tissue origins. However, the panel is not exhaustive for all tissues. The data showed that colorectal was, on average, the most responsive tissue of origin. As mentioned in Chapter 1, the predominance of KRAS and BRAF mutations in colorectal cancer and the introduction of novel therapies that preclude MAPK-altered, metastatic patients from receiving recently approved EGFR inhibitors introduces the need for novel therapies for these patients. This was the rationale for the application of MTX-211 in colorectal cancer.

While the majority of work done so far has been performed in colorectal cancer models, MTX-211 also shows promise in pancreatic cancer in early studies. As previously mentioned, erlotinib was recently approved for the treatment of pancreatic cancer in combination with gemcitabine (Amanam and Chung, 2018). Despite only modest improvements in outcome, the requirement for novel therapies is critical. MTX-211 was in part designed after erlotinib, which provides some support for the application of MTX-211 in pancreatic cancer. Unpublished work I've performed in pancreatic cancer primary models showed an average IC_{50} of around 5 μM, which is in the middle of the therapeutic range of MTX-211 in colorectal cancer. These data are promising and are being investigated further to establish a potential role in treating pancreatic cancer.

Future Directions

Expanding upon the findings summarized in Chapter 2, establishing the roles of caveolin-1 and Pdcd4 in the degradation of COX-2 will be critical going forward. Elucidation of the mechanistic role that these proteins play in a $KRAS^{mt}$/CDKN2A null background will be enlightening. Further strengthening of the data presented with a larger panel of pancreatic cancer models will be required to conclusively decipher the role of COX-2 as a prognostic biomarker of response. It is currently unknown if COX-2 is an indication of another feature, such as an expressed marker of pancreatic adenosquamous carcinoma histology exhibited by the top two responders. Along these same lines, histology is considered less accurate by some who favor gene profiling as a more accurate representation of subpopulation of cancers. Reports have shown the power of molecular subtypes. Collisson et al. divide pancreatic cancer into classical, quasimesenchymal and exocrine-like (Collisson et al., 2011). Bailey et al. divides them into squamous, pancreatic progenitor, immunogenic and aberrantly differentiated endocrine exocrine (Bailey et al., 2016). Moffitt et al. divide them based on stromal characteristics into basal-like, normal and activated stromal subtypes (Moffitt et al., 2015). While there may be common ground between these various classifications, the field of molecular subtyping of pancreatic is growing, and establishing the responder models into a molecular subtype may be informative and enable the discovery of additional responder models.

Expanding upon the findings described in Chapter 3, further work with MTX-211 in colorectal cancer should focus on discovery of prognostic biomarkers. Mechanistic studies have shown conclusively the potential for this compound, but it remains to be determined where best to employ it. Precision medicine has become much more focused on similar

features between responders rather than a gross anatomical location. Elucidation of a molecular subtype or prognostic biomarker will be important in establishing a niche for MTX-211. Furthermore, MTX-211 showed activity in pancreatic cancer and could possibly be applied to many other subtypes of cancer, such as lung and neurological cancers which exhibit overexpression of EGFR or KRAS activation.

Ending thoughts

In this dissertation, the lack of treatment options for KRAS mutant disease has been addressed by exploring potential new therapies. Chapters 2 and 3 focused on developing novel therapies for the treatment of $KRAS^{mt}$ pancreatic and colorectal cancers, respectively. In pancreatic cancer (Chapter 2), focus was placed on developing a novel combination therapy that leverages the mutation profile of pancreatic cancer through the inhibition of MEK and CDK4/6, targeting KRAS and CDKN2A mutations. In colorectal cancer (Chapter 3), instead of developing a therapy based on approved agents in combination, a project delineating the discovery process of MTX-211, a dual inhibitor of EGFR and PI3K in a single molecule, was described. While it is known that utility exists for kinase inhibitors in the clinic, the ideal indication for these agents needs to be optimal as resistance occurs rapidly. The chapters presented were based in part on the knowledge of existing kinase inhibitors and their lack of durable anti-tumor activity as single agents. The results of previous preclinical and clinical studies guided the rational design of novel combination therapies presented here that overcome adaptive signaling and increase activity in tandem.

There are a number of pharmaceutically attractive agents that have failed in monotherapy trials. Looking forward, the design of rational combination approaches that build upon the

knowledge gained from these failed trials is imperative. The reports outlined in Chapters 2 and 3 approach the problem in this manner. They leverage both recently approved drugs and knowledge from failed clinical trials to design novel polypharmacology approaches to treat cancer.

Bilbiography

(2017). AACR Project GENIE: Powering Precision Medicine through an International Consortium. Cancer discovery *7*, 818-831.

Afonja, O., Juste, D., Das, S., Matsuhashi, S., and Samuels, H.H. (2004). Induction of PDCD4 tumor suppressor gene expression by RAR agonists, antiestrogen and HER-2//neu antagonist in breast cancer cells. Evidence for a role in apoptosis. Oncogene *23*, 8135-8145.

Ahmed, M., Hussain, A.R., Siraj, A.K., Uddin, S., Al-Sanea, N., Al-Dayel, F., Al-Assiri, M., Beg, S., and Al-Kuraya, K.S. (2015). Co-targeting of Cyclooxygenase-2 and FoxM1 is a viable strategy in inducing anticancer effects in colorectal cancer cells. Molecular cancer *14*, 131.

Allen, L.F., Sebolt-Leopold, J., and Meyer, M.B. (2003). CI-1040 (PD184352), a targeted signal transduction inhibitor of MEK (MAPKK). Seminars in oncology *30*, 105-116.

Amanam, I., and Chung, V. (2018). Targeted Therapies for Pancreatic Cancer. Cancers *10*.

Anders, L., Ke, N., Hydbring, P., Choi, Y.J., Widlund, H.R., Chick, J.M., Zhai, H., Vidal, M., Gygi, S.P., Braun, P., *et al.* (2011). A systematic screen for CDK4/6 substrates links FOXM1 phosphorylation to senescence suppression in cancer cells. Cancer cell *20*, 620-634.

Athuluri-Divakar, S.K., Vasquez-Del Carpio, R., Dutta, K., Baker, S.J., Cosenza, S.C., Basu, I., Gupta, Y.K., Reddy, M.V., Ueno, L., Hart, J.R., *et al.* (2016). A Small Molecule RAS-Mimetic Disrupts RAS Association with Effector Proteins to Block Signaling. Cell *165*, 643-655.

Bailey, P., Chang, D.K., Nones, K., Johns, A.L., Patch, A.-M., Gingras, M.-C., Miller, D.K., Christ, A.N., Bruxner, T.J.C., Quinn, M.C., *et al.* (2016). Genomic analyses identify molecular subtypes of pancreatic cancer. Nature *531*, 47.

Bardeesy, N., Aguirre, A.J., Chu, G.C., Cheng, K.H., Lopez, L.V., Hezel, A.F., Feng, B., Brennan, C., Weissleder, R., Mahmood, U., *et al.* (2006). Both p16(Ink4a) and the p19(Arf)-p53 pathway constrain progression of pancreatic adenocarcinoma in the mouse. Proceedings of the National Academy of Sciences of the United States of America *103*, 5947-5952.

Basile, K.J., Le, K., Hartsough, E.J., and Aplin, A.E. (2014). Inhibition of mutant BRAF splice variant signaling by next-generation, selective RAF inhibitors. Pigment cell & melanoma research *27*, 479-484.

Biankin, A.V., Waddell, N., Kassahn, K.S., Gingras, M.C., Muthuswamy, L.B., Johns, A.L., Miller, D.K., Wilson, P.J., Patch, A.M., Wu, J., *et al.* (2012). Pancreatic cancer genomes reveal aberrations in axon guidance pathway genes. Nature *491*, 399-405.

Blagosklonny, M.V., and Pardee, A.B. (2002). The Restriction Point of the Cell Cycle. Cell cycle (Georgetown, Tex) *1*, 102-109.

Bockstaele, L., Coulonval, K., Kooken, H., Paternot, S., and Roger, P.P. (2006). Regulation of CDK4. Cell Division *1*, 25.

Bollag, G., Hirth, P., Tsai, J., Zhang, J., Ibrahim, P.N., Cho, H., Spevak, W., Zhang, C., Zhang, Y., Habets, G., *et al.* (2010). Clinical efficacy of a RAF inhibitor needs broad target blockade in BRAF-mutant melanoma. Nature *467*, 596-599.

Bollag, G., Tsai, J., Zhang, J., Zhang, C., Ibrahim, P., Nolop, K., and Hirth, P. (2012). Vemurafenib: the first drug approved for BRAF-mutant cancer. Nature reviews Drug discovery *11*, 873-886.

Bonni, A., Brunet, A., West, A.E., Datta, S.R., Takasu, M.A., and Greenberg, M.E. (1999). Cell survival promoted by the Ras-MAPK signaling pathway by transcription-dependent and -independent mechanisms. Science (New York, NY) *286*, 1358-1362.

Bos, J.L., Rehmann, H., and Wittinghofer, A. (2007). GEFs and GAPs: Critical Elements in the Control of Small G Proteins. Cell *129*, 865-877.

Boscher, C., and Nabi, I.R. (2012). Caveolin-1: role in cell signaling. Advances in experimental medicine and biology *729*, 29-50.

Braden, W.A., McClendon, A.K., and Knudsen, E.S. (2008). Cyclin-dependent kinase 4/6 activity is a critical determinant of pre-replication complex assembly. Oncogene *27*, 7083-7093.

Brewer, M.R., Choi, S.H., Alvarado, D., Moravcevic, K., Pozzi, A., Lemmon, M.A., and Carpenter, G. (2009). The Juxtamembrane Region of the EGF Receptor Functions as an Activation Domain. Mol Cell *34*, 641-651.

Brody, J.R., Costantino, C.L., Potoczek, M., Cozzitorto, J., McCue, P., Yeo, C.J., Hruban, R.H., and Witkiewicz, A.K. (2009). Adenosquamous carcinoma of the pancreas harbors KRAS2, DPC4 and TP53 molecular alterations similar to pancreatic ductal adenocarcinoma. Modern pathology : an official journal of the United States and Canadian Academy of Pathology, Inc *22*, 651-659.

Buchanan, F.G., Wang, D., Bargiacchi, F., and DuBois, R.N. (2003). Prostaglandin E2 regulates cell migration via the intracellular activation of the epidermal growth factor receptor. The Journal of biological chemistry *278*, 35451-35457.

Burgess, A.W., Cho, H.S., Eigenbrot, C., Ferguson, K.M., Garrett, T.P., Leahy, D.J., Lemmon, M.A., Sliwkowski, M.X., Ward, C.W., and Yokoyama, S. (2003). An open-and-shut case? Recent insights into the activation of EGF/ErbB receptors. Mol Cell *12*, 541-552.

Calbo, J., Marotta, M., Cascallo, M., Roig, J.M., Gelpi, J.L., Fueyo, J., and Mazo, A. (2001). Adenovirus-mediated wt-p16 reintroduction induces cell cycle arrest or apoptosis in pancreatic cancer. Cancer gene therapy *8*, 740-750.

Callahan, M.K., Rampal, R., Harding, J.J., Klimek, V.M., Chung, Y.R., Merghoub, T., Wolchok, J.D., Solit, D.B., Rosen, N., Abdel-Wahab, O., *et al.* (2012). Progression of RAS-mutant leukemia during RAF inhibitor treatment. The New England journal of medicine *367*, 2316-2321.

Carrato, A., Falcone, A., Ducreux, M., Valle, J.W., Parnaby, A., Djazouli, K., Alnwick-Allu, K., Hutchings, A., Palaska, C., and Parthenaki, I. (2015). A Systematic Review of the Burden of Pancreatic Cancer in Europe: Real-World Impact on Survival, Quality of Life and Costs. Journal of gastrointestinal cancer *46*, 201-211.

Cascinu, S., Scartozzi, M., Carbonari, G., Pierantoni, C., Verdecchia, L., Mariani, C., Squadroni, M., Antognoli, S., Silva, R.R., Giampieri, R., *et al.* (2007). COX-2 and NF-KB overexpression is common in pancreatic cancer but does not predict for COX-2 inhibitors

activity in combination with gemcitabine and oxaliplatin. American journal of clinical oncology *30*, 526-530.

Castellano, E., and Downward, J. (2011). RAS Interaction with PI3K: More Than Just Another Effector Pathway. Genes & cancer *2*, 261-274.

Chandarlapaty, S., Sawai, A., Scaltriti, M., Rodrik-Outmezguine, V., Grbovic-Huezo, O., Serra, V., Majumder, P.K., Baselga, J., and Rosen, N. (2011). AKT inhibition relieves feedback suppression of receptor tyrosine kinase expression and activity. Cancer cell *19*, 58-71.

Chen, J., Fujii, K., Zhang, L., Roberts, T., and Fu, H. (2001). Raf-1 promotes cell survival by antagonizing apoptosis signal-regulating kinase 1 through a MEK–ERK independent mechanism. Proceedings of the National Academy of Sciences *98*, 7783-7788.

Chen, S.F., Liou, J.Y., Huang, T.Y., Lin, Y.S., Yeh, A.L., Tam, K., Tsai, T.H., Wu, K.K., and Shyue, S.K. (2010). Caveolin-1 facilitates cyclooxygenase-2 protein degradation. Journal of cellular biochemistry *109*, 356-362.

Cheng, M., Olivier, P., Diehl, J.A., Fero, M., Roussel, M.F., Roberts, J.M., and Sherr, C.J. (1999). The p21(Cip1) and p27(Kip1) CDK 'inhibitors' are essential activators of cyclin D-dependent kinases in murine fibroblasts. The EMBO journal *18*, 1571-1583.

Cheng, Y., and Tian, H. (2017). Current Development Status of MEK Inhibitors. Molecules *22*, 1551.

Cherfils, J., and Zeghouf, M. (2013). Regulation of Small GTPases by GEFs, GAPs, and GDIs. Physiological Reviews *93*, 269-309.

Child, E.S., and Mann, D.J. (2006). The intricacies of p21 phosphorylation: protein/protein interactions, subcellular localization and stability. Cell cycle (Georgetown, Tex) *5*, 1313-1319.

Collisson, E.A., Sadanandam, A., Olson, P., Gibb, W.J., Truitt, M., Gu, S., Cooc, J., Weinkle, J., Kim, G.E., Jakkula, L., *et al.* (2011). Subtypes of pancreatic ductal adenocarcinoma and their differing responses to therapy. Nature medicine *17*, 500-503.

Corcoran, R.B., Ebi, H., Turke, A.B., Coffee, E.M., Nishino, M., Cogdill, A.P., Brown, R.D., Della Pelle, P., Dias-Santagata, D., Hung, K.E., *et al.* (2012). EGFR-mediated re-

activation of MAPK signaling contributes to insensitivity of BRAF mutant colorectal cancers to RAF inhibition with vemurafenib. Cancer discovery *2*, 227-235.

Cox, A.D., Der, C.J., and Philips, M.R. (2015). Targeting RAS Membrane Association: Back to the Future for Anti-RAS Drug Discovery? Clinical Cancer Research *21*, 1819-1827.

Cox, A.D., Fesik, S.W., Kimmelman, A.C., Luo, J., and Der, C.J. (2014). Drugging the undruggable RAS: Mission Possible? Nature Reviews Drug Discovery *13*, 828.

Cristofanilli, M., Turner, N.C., Bondarenko, I., Ro, J., Im, S.A., Masuda, N., Colleoni, M., DeMichele, A., Loi, S., Verma, S., *et al.* (2016). Fulvestrant plus palbociclib versus fulvestrant plus placebo for treatment of hormone-receptor-positive, HER2-negative metastatic breast cancer that progressed on previous endocrine therapy (PALOMA-3): final analysis of the multicentre, double-blind, phase 3 randomised controlled trial. The Lancet Oncology *17*, 425-439.

Cunningham, D., Humblet, Y., Siena, S., Khayat, D., Bleiberg, H., Santoro, A., Bets, D., Mueser, M., Harstrick, A., Verslype, C., *et al.* (2004). Cetuximab monotherapy and cetuximab plus irinotecan in irinotecan-refractory metastatic colorectal cancer. The New England journal of medicine *351*, 337-345.

Davies, N.M., McLachlan, A.J., Day, R.O., and Williams, K.M. (2000). Clinical Pharmacokinetics and Pharmacodynamics of Celecoxib. Clinical Pharmacokinetics *38*, 225-242.

Domchek, S.M., Auger, K.R., Chatterjee, S., Burke, T.R., and Shoelson, S.E. (1992). Inhibition of SH2 domain/phosphoprotein association by a nonhydrolyzable phosphonopeptide. Biochemistry *31*, 9865-9870.

Douillard, J.Y., Oliner, K.S., Siena, S., Tabernero, J., Burkes, R., Barugel, M., Humblet, Y., Bodoky, G., Cunningham, D., Jassem, J., *et al.* (2013). Panitumumab-FOLFOX4 treatment and RAS mutations in colorectal cancer. The New England journal of medicine *369*, 1023-1034.

Duncan, J.S., Whittle, M.C., Nakamura, K., Abell, A.N., Midland, A.A., Zawistowski, J.S., Johnson, N.L., Granger, D.A., Jordan, N.V., Darr, D.B., *et al.* (2012). Dynamic reprogramming of the kinome in response to targeted MEK inhibition in triple-negative breast cancer. Cell *149*, 307-321.

Duong, M.T., Akli, S., Wei, C., Wingate, H.F., Liu, W., Lu, Y., Yi, M., Mills, G.B., Hunt, K.K., and Keyomarsi, K. (2012). LMW-E/CDK2 deregulates acinar morphogenesis, induces tumorigenesis, and associates with the activated b-Raf-ERK1/2-mTOR pathway in breast cancer patients. PLoS genetics *8*, e1002538.

Duso, B.A., Trapani, D., Viale, G., Criscitiello, C., D'Amico, P., Belli, C., Mazzarella, L., Locatelli, M., Minchella, I., and Curigliano, G. (2018). Clinical efficacy of ribociclib as a first-line therapy for HR-positive, advanced breast cancer. Expert opinion on pharmacotherapy *19*, 299-305.

Eberhart, C.E., Coffey, R.J., Radhika, A., Giardiello, F.M., Ferrenbach, S., and DuBois, R.N. (1994). Up-regulation of cyclooxygenase 2 gene expression in human colorectal adenomas and adenocarcinomas. Gastroenterology *107*, 1183-1188.

Ebi, H., Corcoran, R.B., Singh, A., Chen, Z., Song, Y., Lifshits, E., Ryan, D.P., Meyerhardt, J.A., Benes, C., Settleman, J., *et al.* (2011). Receptor tyrosine kinases exert dominant control over PI3K signaling in human KRAS mutant colorectal cancers. The Journal of clinical investigation *121*, 4311-4321.

Elder, D.J., Halton, D.E., Playle, L.C., and Paraskeva, C. (2002). The MEK/ERK pathway mediates COX-2-selective NSAID-induced apoptosis and induced COX-2 protein expression in colorectal carcinoma cells. International journal of cancer Journal international du cancer *99*, 323-327.

Fang, X., Yu, S., Eder, A., Mao, M., Bast, R.C., Jr., Boyd, D., and Mills, G.B. (1999). Regulation of BAD phosphorylation at serine 112 by the Ras-mitogen-activated protein kinase pathway. Oncogene *18*, 6635-6640.

FDA FDA approves dabrafenib plus trametinib for adjuvant treatment of melanoma with BRAF V600E or V600K mutations.

FDA (2018). FDA approves encorafenib and binimetinib in combination for unresectable or metastatic melanoma with BRAF mutations.

Ferguson, R.L., and Maller, J.L. (2008). Cyclin E-dependent localization of MCM5 regulates centrosome duplication. Journal of cell science *121*, 3224-3232.

Ferguson, S., Hebert, R.L., and Laneuville, O. (1999). NS-398 upregulates constitutive cyclooxygenase-2 expression in the M-1 cortical collecting duct cell line. Journal of the American Society of Nephrology : JASN *10*, 2261-2271.

Finn, R., Jiang, Y., Rugo, H., Moulder, S.L., Im, S.A., Gelmon, K.A., Dieras, V., Martin, M., Joy, A.A., Toi, M., *et al.* (2016). Biomarker analyses from the phase 3 PALOMA-2 trial of palbociclib (P) with letrozole (L) compared with placebo (PLB) plus L in postmenopausal women with ER + /HER2– advanced breast cancer (ABC). Annals of Oncology *27*, LBA15-LBA15.

Finn, R.S., Crown, J.P., Lang, I., Boer, K., Bondarenko, I.M., Kulyk, S.O., Ettl, J., Patel, R., Pinter, T., Schmidt, M., *et al.* The cyclin-dependent kinase 4/6 inhibitor palbociclib in combination with letrozole versus letrozole alone as first-line treatment of oestrogen receptor-positive, HER2-negative, advanced breast cancer (PALOMA-1/TRIO-18): a randomised phase 2 study. The Lancet Oncology *16*, 25-35.

Fiorucci, G., and Hall, A. (1988). All three human ras genes are expressed in a wide range of tissues. Biochimica et biophysica acta *950*, 81-83.

Fiskus, W., and Mitsiades, N. (2016). B-Raf Inhibition in the Clinic: Present and Future. Annual review of medicine *67*, 29-43.

Forbes, S.A., Tang, G., Bindal, N., Bamford, S., Dawson, E., Cole, C., Kok, C.Y., Jia, M., Ewing, R., Menzies, A., *et al.* (2010). COSMIC (the Catalogue of Somatic Mutations in Cancer): a resource to investigate acquired mutations in human cancer. Nucleic acids research *38*, D652-657.

Franco, J., Balaji, U., Freinkman, E., Witkiewicz, A.K., and Knudsen, E.S. (2016). Metabolic Reprogramming of Pancreatic Cancer Mediated by CDK4/6 Inhibition Elicits Unique Vulnerabilities. Cell reports *14*, 979-990.

Franco, J., Witkiewicz, A.K., and Knudsen, E.S. (2014). CDK4/6 inhibitors have potent activity in combination with pathway selective therapeutic agents in models of pancreatic cancer. Oncotarget.

Frémin, C., and Meloche, S. (2010). From basic research to clinical development of MEK1/2 inhibitors for cancer therapy. Journal of Hematology & Oncology *3*, 8.

Furstenthal, L., Kaiser, B.K., Swanson, C., and Jackson, P.K. (2001). Cyclin E Uses Cdc6 as a Chromatin-Associated Receptor Required for DNA Replication. The Journal of Cell Biology *152*, 1267-1278.

Furth, M.E., Aldrich, T.H., and Cordon-Cardo, C. (1987). Expression of ras proto-oncogene proteins in normal human tissues. Oncogene *1*, 47-58.

Gao, S., Ma, J.J., and Lu, C. (2013). Prognostic value of cyclin E expression in breast cancer: a meta-analysis. Tumour biology : the journal of the International Society for Oncodevelopmental Biology and Medicine *34*, 3423-3430.

Gao, Y., Chang, M.T., McKay, D., Na, N., Zhou, B., Yaeger, R., Torres, N.M., Muniz, K., Drosten, M., Barbacid, M., *et al.* (2018). Allele-Specific Mechanisms of Activation of MEK1 Mutants Determine Their Properties. Cancer discovery *8*, 648-661.

Garrett, T.P., McKern, N.M., Lou, M., Elleman, T.C., Adams, T.E., Lovrecz, G.O., Kofler, M., Jorissen, R.N., Nice, E.C., Burgess, A.W., *et al.* (2003). The crystal structure of a truncated ErbB2 ectodomain reveals an active conformation, poised to interact with other ErbB receptors. Mol Cell *11*, 495-505.

Geng, Y., Lee, Y.M., Welcker, M., Swanger, J., Zagozdzon, A., Winer, J.D., Roberts, J.M., Kaldis, P., Clurman, B.E., and Sicinski, P. (2007). Kinase-independent function of cyclin E. Mol Cell *25*, 127-139.

Geng, Y., Yu, Q., Sicinska, E., Das, M., Schneider, J.E., Bhattacharya, S., Rideout, W.M., Bronson, R.T., Gardner, H., and Sicinski, P. (2003). Cyclin E ablation in the mouse. Cell *114*, 431-443.

Goel, S., Wang, Q., Watt, A.C., Tolaney, S.M., Dillon, D.A., Li, W., Ramm, S., Palmer, A.C., Yuzugullu, H., Varadan, V., *et al.* (2016). Overcoming Therapeutic Resistance in HER2-Positive Breast Cancers with CDK4/6 Inhibitors. Cancer cell *29*, 255-269.

Hawk, E.T., Viner, J.L., Dannenberg, A., and DuBois, R.N. (2002). COX-2 in Cancer—A Player That's Defining the Rules. JNCI: Journal of the National Cancer Institute *94*, 545-546.

Heisermann, G.J., Wiley, H.S., Walsh, B.J., Ingraham, H.A., Fiol, C.J., and Gill, G.N. (1990). Mutational removal of the Thr669 and Ser671 phosphorylation sites alters substrate specificity and ligand-induced internalization of the epidermal growth factor receptor. The Journal of biological chemistry *265*, 12820-12827.

Hill, R., Li, Y., Tran, L.M., Dry, S., Calvopina, J.H., Garcia, A., Kim, C., Wang, Y., Donahue, T.R., Herschman, H.R., *et al.* (2012). Cell intrinsic role of COX-2 in pancreatic cancer development. Molecular cancer therapeutics *11*, 2127-2137.

Huang, F., Cao, J., Liu, Q., Zou, Y., Li, H., and Yin, T. (2013). MAPK/ERK signal pathway involved expression of COX-2 and VEGF by IL-1β induced in human endometriosis

stromal cells in vitro. International Journal of Clinical and Experimental Pathology *6*, 2129-2136.

Huang, J., and Manning, B.D. (2008). The TSC1–TSC2 complex: a molecular switchboard controlling cell growth. The Biochemical journal *412*, 179-190.

Jaffee, E.M., Hruban, R.H., Canto, M., and Kern, S.E. (2002). Focus on pancreas cancer. Cancer cell *2*, 25-28.

Janes, M.R., Zhang, J., Li, L.S., Hansen, R., Peters, U., Guo, X., Chen, Y., Babbar, A., Firdaus, S.J., Darjania, L., *et al.* (2018). Targeting KRAS Mutant Cancers with a Covalent G12C-Specific Inhibitor. Cell *172*, 578-589.e517.

Janku, F. (2017). Phosphoinositide 3-kinase (PI3K) pathway inhibitors in solid tumors: From laboratory to patients. Cancer treatment reviews *59*, 93-101.

Jemal, A., Bray, F., Center, M.M., Ferlay, J., Ward, E., and Forman, D. (2011). Global cancer statistics. CA Cancer J Clin *61*, 69-90.

Jones, R.B., Gordus, A., Krall, J.A., and MacBeath, G. (2006). A quantitative protein interaction network for the ErbB receptors using protein microarrays. Nature *439*, 168-174.

Jonker, D.J., O'Callaghan, C.J., Karapetis, C.S., Zalcberg, J.R., Tu, D., Au, H.J., Berry, S.R., Krahn, M., Price, T., Simes, R.J., *et al.* (2007). Cetuximab for the treatment of colorectal cancer. The New England journal of medicine *357*, 2040-2048.

Kang, M.J., Ahn, H.S., Lee, J.Y., Matsuhashi, S., and Park, W.Y. (2002). Up-regulation of PDCD4 in senescent human diploid fibroblasts. Biochem Biophys Res Commun *293*, 617-621.

Karoulia, Z., Wu, Y., Ahmed, T.A., Xin, Q., Bollard, J., Krepler, C., Wu, X., Zhang, C., Bollag, G., Herlyn, M., *et al.* (2016). An Integrated Model of RAF Inhibitor Action Predicts Inhibitor Activity against Oncogenic BRAF Signaling. Cancer cell *30*, 485-498.

Katz, M.H., Taylor, T.H., Al-Refaie, W.B., Hanna, M.H., Imagawa, D.K., Anton-Culver, H., and Zell, J.A. (2011). Adenosquamous versus adenocarcinoma of the pancreas: a population-based outcomes analysis. Journal of gastrointestinal surgery : official journal of the Society for Surgery of the Alimentary Tract *15*, 165-174.

Kern, S.E. The Genetics of Pancreatic Cancer.

Kidger, A.M., Sipthorp, J., and Cook, S.J. (2018). ERK1/2 inhibitors: New weapons to inhibit the RAS-regulated RAF-MEK1/2-ERK1/2 pathway. Pharmacology & therapeutics *187*, 45-60.

Kim, J.I., Lakshmikanthan, V., Frilot, N., and Daaka, Y. (2010). Prostaglandin E2 Promotes Lung Cancer Cell Migration Via EP4-βArrestin1-c-Src Signalsome. Mol Cancer Res *8*, 569-577.

Kitai, H., Ebi, H., Tomida, S., Floros, K.V., Kotani, H., Adachi, Y., Oizumi, S., Nishimura, M., Faber, A.C., and Yano, S. (2016). Epithelial-to-mesenchymal transition defines feedback activation of receptor tyrosine kinase signaling induced by MEK inhibition in KRAS mutant lung cancer. Cancer discovery *6*, 754-769.

Klein, E.A., and Assoian, R.K. (2008). Transcriptional regulation of the cyclin D1 gene at a glance. Journal of cell science *121*, 3853-3857.

Knight, S.D., Adams, N.D., Burgess, J.L., Chaudhari, A.M., Darcy, M.G., Donatelli, C.A., Luengo, J.I., Newlander, K.A., Parrish, C.A., Ridgers, L.H., *et al.* (2010). Discovery of GSK2126458, a Highly Potent Inhibitor of PI3K and the Mammalian Target of Rapamycin. ACS Med Chem Lett *1*, 39-43.

Kovacs, E., Zorn, J.A., Huang, Y., Barros, T., and Kuriyan, J. (2015). A Structural Perspective on the Regulation of the EGF Receptor. Annual review of biochemistry *84*, 739-764.

Kumamoto, H., Izutsu, T., Ohki, K., Takahashi, N., and Ooya, K. (2004). p53 gene status and expression of p53, MDM2, and p14 proteins in ameloblastomas. Journal of oral pathology & medicine : official publication of the International Association of Oral Pathologists and the American Academy of Oral Pathology *33*, 292-299.

Kwong, L.N., Costello, J.C., Liu, H., Jiang, S., Helms, T.L., Langsdorf, A.E., Jakubosky, D., Genovese, G., Muller, F.L., Jeong, J.H., *et al.* (2012). Oncogenic NRAS signaling differentially regulates survival and proliferation in melanoma. Nature medicine *18*, 1503-1510.

Lake, D., Corrêa, S.A.L., and Müller, J. (2016). Negative feedback regulation of the ERK1/2 MAPK pathway. Cellular and Molecular Life Sciences *73*, 4397-4413.

Lavoie, J.N., L'Allemain, G., Brunet, A., Müller, R., and Pouysségur, J. (1996). Cyclin D1 Expression Is Regulated Positively by the p42/p44MAPK and Negatively by the p38/HOGMAPK Pathway. Journal of Biological Chemistry *271*, 20608-20616.

Lee, M.S., Helms, T.L., Feng, N., Gay, J., Chang, Q.E., Tian, F., Wu, J.Y., Toniatti, C., Heffernan, T.P., Powis, G., *et al.* (2016). Efficacy of the combination of MEK and CDK4/6 inhibitors in vitro and in vivo in KRAS mutant colorectal cancer models. Oncotarget *7*, 39595-39608.

Leupold, J.H., Yang, H.S., Colburn, N.H., Asangani, I., Post, S., and Allgayer, H. (2007). Tumor suppressor Pdcd4 inhibits invasion/intravasation and regulates urokinase receptor (u-PAR) gene expression via Sp-transcription factors. Oncogene *26*, 4550-4562.

Li, C., Xing, T., Tang, M., Yong, W., Yan, D., Deng, H., Wang, H., Wang, M., Chen, J., and Ruan, D. (2008a). Involvement of cyclin D1/CDK4 and pRb mediated by PI3K/AKT pathway activation in Pb2+ -induced neuronal death in cultured hippocampal neurons. Toxicology and applied pharmacology *229*, 351-361.

Li, X., Huang, Y., Jiang, J., and Frank, S.J. (2008b). ERK-dependent threonine phosphorylation of EGF receptor modulates receptor downregulation and signaling. Cellular signalling *20*, 2145-2155.

Lidsky, M., Antoun, G., Speicher, P., Adams, B., Turley, R., Augustine, C., Tyler, D., and Ali-Osman, F. (2014). Mitogen-activated protein kinase (MAPK) hyperactivation and enhanced NRAS expression drive acquired vemurafenib resistance in V600E BRAF melanoma cells. The Journal of biological chemistry *289*, 27714-27726.

Lievre, A., Bachet, J.B., Le Corre, D., Boige, V., Landi, B., Emile, J.F., Cote, J.F., Tomasic, G., Penna, C., Ducreux, M., *et al.* (2006). KRAS mutation status is predictive of response to cetuximab therapy in colorectal cancer. Cancer research *66*, 3992-3995.

Liggett, W.H., and Sidransky, D. (1998). Role of the p16 tumor suppressor gene in cancer. Journal of Clinical Oncology *16*, 1197-1206.

Liou, J.Y., Deng, W.G., Gilroy, D.W., Shyue, S.K., and Wu, K.K. (2001). Colocalization and interaction of cyclooxygenase-2 with caveolin-1 in human fibroblasts. The Journal of biological chemistry *276*, 34975-34982.

Lito, P., Pratilas, C.A., Joseph, E.W., Tadi, M., Halilovic, E., Zubrowski, M., Huang, A., Wong, W.L., Callahan, M.K., Merghoub, T., *et al.* (2012). Relief of profound feedback

inhibition of mitogenic signaling by RAF inhibitors attenuates their activity in BRAFV600E melanomas. Cancer cell *22*, 668-682.

Little, A.S., Balmanno, K., Sale, M.J., Newman, S., Dry, J.R., Hampson, M., Edwards, P.A.W., Smith, P.D., and Cook, S.J. (2011). Amplification of the Driving Oncogene, KRAS or BRAF, Underpins Acquired Resistance to MEK1/2 Inhibitors in Colorectal Cancer Cells, Vol 4.

Liu, J., Smith, C.L., DeRyckere, D., DeAngelis, K., Martin, G.S., and Berger, J.M. (2000). Structure and function of Cdc6/Cdc18: implications for origin recognition and checkpoint control. Mol Cell *6*, 637-648.

Liu, W., Ren, H., Ren, J., Yin, T., Hu, B., Xie, S., Dai, Y., Wu, W., Xiao, Z., Yang, X., *et al.* (2013). The role of EGFR/PI3K/Akt/cyclinD1 signaling pathway in acquired middle ear cholesteatoma. Mediators of inflammation *2013*, 651207.

Loeb, K.R., and Chen, X. (2012). Too much cleavage of cyclin E promotes breast tumorigenesis. PLoS genetics *8*, e1002623.

Lohrum, M.A., Ashcroft, M., Kubbutat, M.H., and Vousden, K.H. (2000). Contribution of two independent MDM2-binding domains in p14(ARF) to p53 stabilization. Curr Biol *10*, 539-542.

Lu, S., Jang, H., Gu, S., Zhang, J., and Nussinov, R. (2016). Drugging Ras GTPase: a comprehensive mechanistic and signaling structural view. Chemical Society Reviews *45*, 4929-4952.

Lunn, C.L., Chrivia, J.C., and Baldassare, J.J. (2010). Activation of Cdk2/Cyclin E complexes is dependent on the origin of replication licensing factor Cdc6 in mammalian cells. Cell cycle (Georgetown, Tex) *9*, 4533-4541.

Ma, L., Chen, Z., Erdjument-Bromage, H., Tempst, P., and Pandolfi, P.P. (2005a). Phosphorylation and functional inactivation of TSC2 by Erk implications for tuberous sclerosis and cancer pathogenesis. Cell *121*, 179-193.

Ma, R.Y., Tong, T.H., Cheung, A.M., Tsang, A.C., Leung, W.Y., and Yao, K.M. (2005b). Raf/MEK/MAPK signaling stimulates the nuclear translocation and transactivating activity of FOXM1c. Journal of cell science *118*, 795-806.

Maitra, A., and Hruban, R.H. (2008). Pancreatic cancer. Annual review of pathology *3*, 157-188.

Mao, C.Q., Xiong, M.H., Liu, Y., Shen, S., Du, X.J., Yang, X.Z., Dou, S., Zhang, P.Z., and Wang, J. (2014). Synthetic lethal therapy for KRAS mutant non-small-cell lung carcinoma with nanoparticle-mediated CDK4 siRNA delivery. Molecular therapy : the journal of the American Society of Gene Therapy *22*, 964-973.

Mateo, J., Chakravarty, D., Dienstmann, R., Jezdic, S., Gonzalez-Perez, A., Lopez-Bigas, N., Ng, C.K.Y., Bedard, P.L., Tortora, G., Douillard, J.Y., *et al.* (2018). A framework to rank genomic alterations as targets for cancer precision medicine: the ESMO Scale for Clinical Actionability of molecular Targets (ESCAT). Ann Oncol.

Matsumoto, Y., and Maller, J.L. (2004). A centrosomal localization signal in cyclin E required for Cdk2-independent S phase entry. Science (New York, NY) *306*, 885-888.

Maurer, T., Garrenton, L.S., Oh, A., Pitts, K., Anderson, D.J., Skelton, N.J., Fauber, B.P., Pan, B., Malek, S., Stokoe, D., *et al.* (2012). Small-molecule ligands bind to a distinct pocket in Ras and inhibit SOS-mediated nucleotide exchange activity. Proceedings of the National Academy of Sciences *109*, 5299-5304.

Mebratu, Y., and Tesfaigzi, Y. (2009). How ERK1/2 activation controls cell proliferation and cell death: Is subcellular localization the answer? Cell cycle (Georgetown, Tex) *8*, 1168-1175.

Meitner, P.A., Kajiji, S.M., LaPosta-Frazier, N., Bogaars, H.A., Jolly, G.A., Dexter, D.L., Calabresi, P., and Turner, M.D. (1983). "COLO 357," a human pancreatic adenosquamous carcinoma: growth in artificial capillary culture and in nude mice. Cancer research *43*, 5978-5985.

Moffitt, R.A., Marayati, R., Flate, E.L., Volmar, K.E., Loeza, S.G.H., Hoadley, K.A., Rashid, N.U., Williams, L.A., Eaton, S.C., Chung, A.H., *et al.* (2015). Virtual microdissection identifies distinct tumor- and stroma-specific subtypes of pancreatic ductal adenocarcinoma. Nature Genetics *47*, 1168.

Montero-Conde, C., Ruiz-Llorente, S., Dominguez, J.M., Knauf, J.A., Viale, A., Sherman, E.J., Ryder, M., Ghossein, R.A., Rosen, N., and Fagin, J.A. (2013). Relief of feedback inhibition of HER3 transcription by RAF and MEK inhibitors attenuates their antitumor effects in BRAF-mutant thyroid carcinomas. Cancer discovery *3*, 520-533.

Morris, E.J., Jha, S., Restaino, C.R., Dayananth, P., Zhu, H., Cooper, A., Carr, D., Deng, Y., Jin, W., Black, S., *et al.* (2013). Discovery of a novel ERK inhibitor with activity in models of acquired resistance to BRAF and MEK inhibitors. Cancer discovery *3*, 742-750.

Morrison, D.K. (2001). KSR: a MAPK scaffold of the Ras pathway? Journal of cell science *114*, 1609-1612.

Nanos-Webb, A., Jabbour, N.A., Multani, A.S., Wingate, H., Oumata, N., Galons, H., Joseph, B., Meijer, L., Hunt, K.K., and Keyomarsi, K. (2012). Targeting low molecular weight cyclin E (LMW-E) in breast cancer. Breast cancer research and treatment *132*, 575-588.

Nazarian, R., Shi, H., Wang, Q., Kong, X., Koya, R.C., Lee, H., Chen, Z., Lee, M.K., Attar, N., Sazegar, H., *et al.* (2010). Melanomas acquire resistance to B-RAF(V600E) inhibition by RTK or N-RAS upregulation. Nature *468*, 973-977.

Nguyen, A.C., Burack, W.R., Stock, J.L., Kortum, R., Chaika, O.V., Afkarian, M., Muller, W.J., Murphy, K.M., Morrison, D.K., Lewis, R.E., *et al.* (2002). Kinase Suppressor of Ras (KSR) Is a Scaffold Which Facilitates Mitogen-Activated Protein Kinase Activation In Vivo. Molecular and cellular biology *22*, 3035-3045.

Nissan, M.H., Rosen, N., and Solit, D.B. (2013). ERK pathway inhibitors: how low should we go? Cancer discovery *3*, 719-721.

Oberholzer, P.A., Kee, D., Dziunycz, P., Sucker, A., Kamsukom, N., Jones, R., Roden, C., Chalk, C.J., Ardlie, K., Palescandolo, E., *et al.* (2012). RAS mutations are associated with the development of cutaneous squamous cell tumors in patients treated with RAF inhibitors. Journal of clinical oncology : official journal of the American Society of Clinical Oncology *30*, 316-321.

Ogino, S., Kirkner, G.J., Nosho, K., Irahara, N., Kure, S., Shima, K., Hazra, A., Chan, A.T., Dehari, R., Giovannucci, E.L., *et al.* (2008). Cyclooxygenase-2 expression is an independent predictor of poor prognosis in colon cancer. Clinical cancer research : an official journal of the American Association for Cancer Research *14*, 8221-8227.

Ohren, J.F., Chen, H., Pavlovsky, A., Whitehead, C., Zhang, E., Kuffa, P., Yan, C., McConnell, P., Spessard, C., Banotai, C., *et al.* (2004). Structures of human MAP kinase kinase 1 (MEK1) and MEK2 describe novel noncompetitive kinase inhibition. Nature structural & molecular biology *11*, 1192-1197.

Okami, J., Yamamoto, H., Fujiwara, Y., Tsujie, M., Kondo, M., Noura, S., Oshima, S., Nagano, H., Dono, K., Umeshita, K., *et al.* (1999). Overexpression of cyclooxygenase-2 in carcinoma of the pancreas. Clinical cancer research : an official journal of the American Association for Cancer Research *5*, 2018-2024.

Onconova (2018). Onconova Moving Forward With Phase 3 INSPIRE Pivotal Trial With Increased Sample Size Following Promising Interim Analysis.

Ostrem, J.M., Peters, U., Sos, M.L., Wells, J.A., and Shokat, K.M. (2013). K-Ras(G12C) inhibitors allosterically control GTP affinity and effector interactions. Nature *503*, 548-551.

Pai, R., Soreghan, B., Szabo, I.L., Pavelka, M., Baatar, D., and Tarnawski, A.S. (2002). Prostaglandin E2 transactivates EGF receptor: a novel mechanism for promoting colon cancer growth and gastrointestinal hypertrophy. Nature medicine *8*, 289-293.

Palamarchuk, A., Efanov, A., Maximov, V., Aqeilan, R.I., Croce, C.M., and Pekarsky, Y. (2005). Akt phosphorylates and regulates Pdcd4 tumor suppressor protein. Cancer research *65*, 11282-11286.

Pandit, B., and Gartel, A.L. (2015). Mutual Regulation of FOXM1, NPM and ARF Proteins. Journal of Cancer *6*, 538-541.

Papke, B., and Der, C.J. (2017). Drugging RAS: Know the enemy. Science (New York, NY) *355*, 1158-1163.

Pawson, T. (2004). Specificity in Signal Transduction: From Phosphotyrosine-SH2 Domain Interactions to Complex Cellular Systems. Cell *116*, 191-203.

Pawson, T., and Nash, P. (2003). Assembly of Cell Regulatory Systems through Protein Interaction Domains. Science (New York, NY) *300*, 445-452.

Perrone, G., Zagami, M., Altomare, V., Battista, C., Morini, S., and Rabitti, C. (2007). COX-2 localization within plasma membrane caveolae-like structures in human lobular intraepithelial neoplasia of the breast. Virchows Archiv : an international journal of pathology *451*, 1039-1045.

Poulikakos, P.I., and Solit, D.B. (2011). Resistance to MEK Inhibitors: Should We Co-Target Upstream?, Vol 4.

Prenen, H., Tejpar, S., and Van Cutsem, E. (2010). New strategies for treatment of KRAS mutant metastatic colorectal cancer. Clinical cancer research : an official journal of the American Association for Cancer Research *16*, 2921-2926.

Prior, I.A., Lewis, P.D., and Mattos, C. (2012). A comprehensive survey of Ras mutations in cancer. Cancer research *72*, 2457-2467.

Puyol, M., Martin, A., Dubus, P., Mulero, F., Pizcueta, P., Khan, G., Guerra, C., Santamaria, D., and Barbacid, M. (2010). A synthetic lethal interaction between K-Ras oncogenes and Cdk4 unveils a therapeutic strategy for non-small cell lung carcinoma. Cancer cell *18*, 63-73.

Puyol, M., Martín, A., Dubus, P., Mulero, F., Pizcueta, P., Khan, G., Guerra, C., Santamaría, D., and Barbacid, M. A Synthetic Lethal Interaction between K-Ras Oncogenes and Cdk4 Unveils a Therapeutic Strategy for Non-small Cell Lung Carcinoma. Cancer cell *18*, 63-73.

Qin, G., Xu, F., Qin, T., Zheng, Q., Shi, D., Xia, W., Tian, Y., Tang, Y., Wang, J., Xiao, X., *et al.* (2015). Palbociclib inhibits epithelial-mesenchymal transition and metastasis in breast cancer via c-Jun/COX-2 signaling pathway. Oncotarget *6*, 41794-41808.

Quan, M., Wang, P., Cui, J., Gao, Y., and Xie, K. (2013). The roles of FOXM1 in pancreatic stem cells and carcinogenesis. Molecular cancer *12*, 159.

Quest, A.F.G., Gutierrez-Pajares, J.L., and Torres, V.A. (2008). Caveolin-1: an ambiguous partner in cell signalling and cancer. Journal of Cellular and Molecular Medicine *12*, 1130-1150.

Rahib, L., Smith, B.D., Aizenberg, R., Rosenzweig, A.B., Fleshman, J.M., and Matrisian, L.M. (2014). Projecting cancer incidence and deaths to 2030: the unexpected burden of thyroid, liver, and pancreas cancers in the United States. Cancer research *74*, 2913-2921.

Rahman, M.A., Salajegheh, A., Smith, R.A., and Lam, A.K. (2014). BRAF inhibitors: From the laboratory to clinical trials. Crit Rev Oncol Hematol *90*, 220-232.

Ray, A., James, M.K., Larochelle, S., Fisher, R.P., and Blain, S.W. (2009). p27(Kip1) Inhibits Cyclin D-Cyclin-Dependent Kinase 4 by Two Independent Modes. Molecular and cellular biology *29*, 986-999.

Razidlo, G.L., Johnson, H.J., Stoeger, S.M., Cowan, K.H., Bessho, T., and Lewis, R.E. (2009). KSR1 is required for cell cycle reinitiation following DNA damage. The Journal of biological chemistry *284*, 6705-6715.

Red Brewer, M., Choi, S.H., Alvarado, D., Moravcevic, K., Pozzi, A., Lemmon, M.A., and Carpenter, G. (2009). The juxtamembrane region of the EGF receptor functions as an activation domain. Mol Cell *34*, 641-651.

Roskoski, R., Jr. (2012). ERK1/2 MAP kinases: structure, function, and regulation. Pharmacological research *66*, 105-143.

Roux, P.P., and Blenis, J. (2004). ERK and p38 MAPK-Activated Protein Kinases: a Family of Protein Kinases with Diverse Biological Functions. Microbiology and Molecular Biology Reviews *68*, 320-344.

Rowell, C.A., Kowalczyk, J.J., Lewis, M.D., and Garcia, A.M. (1997). Direct Demonstration of Geranylgeranylation and Farnesylation of Ki-Ras in Vivo. Journal of Biological Chemistry *272*, 14093-14097.

Ryan, M.B., Der, C.J., Wang-Gillam, A., and Cox, A.D. (2015). Targeting RAS-mutant cancers: is ERK the key? Trends in cancer *1*, 183-198.

Saltz, L.B., Meropol, N.J., Sr, P.J.L., Needle, M.N., Kopit, J., and Mayer, R.J. (2004). Phase II Trial of Cetuximab in Patients With Refractory Colorectal Cancer That Expresses the Epidermal Growth Factor Receptor. Journal of Clinical Oncology *22*, 1201-1208.

Savage, P. (2012). Development and economic trends in cancer therapeutic drugs in the UK from 1955 to 2009. Journal of oncology pharmacy practice : official publication of the International Society of Oncology Pharmacy Practitioners *18*, 52-56.

Savage, P. (2013). Development and economic trends in cancer therapeutic drugs: An updated analysis of modern and historical treatment costs compared to the contemporary GDP per capita. Journal of Clinical Oncology *31*, 259-259.

Savage, P., and Mahmoud, S. (2015). Development and economic trends in cancer therapeutic drugs: a 5-year update 2010–2014. British Journal of Cancer *112*, 1037-1041.

Schlessinger, J. (2002). Ligand-induced, receptor-mediated dimerization and activation of EGF receptor. Cell *110*, 669-672.

Schmidt, C.M., Wang, Y., and Wiesenauer, C. (2003). Novel combination of cyclooxygenase-2 and MEK inhibitors in human hepatocellular carcinoma provides a synergistic increase in apoptosis. Journal of gastrointestinal surgery : official journal of the Society for Surgery of the Alimentary Tract *7*, 1024-1033.

Schulze, W.X., Deng, L., and Mann, M. (2005). Phosphotyrosine interactome of the ErbB-receptor kinase family. Molecular systems biology *1*, 2005.0008.

Scott, W.J., Hentemann, M.F., Rowley, R.B., Bull, C.O., Jenkins, S., Bullion, A.M., Johnson, J., Redman, A., Robbins, A.H., Esler, W., *et al.* (2016). Discovery and SAR of Novel 2,3-Dihydroimidazo[1,2-c]quinazoline PI3K Inhibitors: Identification of Copanlisib (BAY 80-6946). ChemMedChem *11*, 1517-1530.

Sebolt-Leopold, J.S., Dudley, D.T., Herrera, R., Van Becelaere, K., Wiland, A., Gowan, R.C., Tecle, H., Barrett, S.D., Bridges, A., Przybranowski, S., *et al.* (1999). Blockade of the MAP kinase pathway suppresses growth of colon tumors in vivo. Nature medicine *5*, 810-816.

Sergina, N.V., and Moasser, M.M. (2007). The HER family and cancer: emerging molecular mechanisms and therapeutic targets. Trends in molecular medicine *13*, 527-534.

Sergina, N.V., Rausch, M., Wang, D., Blair, J., Hann, B., Shokat, K.M., and Moasser, M.M. (2007). Escape from HER-family tyrosine kinase inhibitor therapy by the kinase-inactive HER3. Nature *445*, 437-441.

Serrano, M., Lin, A.W., McCurrach, M.E., Beach, D., and Lowe, S.W. (1997). Oncogenic ras provokes premature cell senescence associated with accumulation of p53 and p16INK4a. Cell *88*, 593-602.

She, Q.-B., Solit, D.B., Ye, Q., O'Reilly, K.E., Lobo, J., and Rosen, N. (2005). The BAD protein integrates survival signaling by EGFR/MAPK and PI3K/Akt kinase pathways in PTEN-deficient tumor cells. Cancer cell *8*, 287-297.

Shima, F., Yoshikawa, Y., Ye, M., Araki, M., Matsumoto, S., Liao, J., Hu, L., Sugimoto, T., Ijiri, Y., Takeda, A., *et al.* (2013). In silico discovery of small-molecule Ras inhibitors that display antitumor activity by blocking the Ras–effector interaction. Proceedings of the National Academy of Sciences *110*, 8182-8187.

Shimura, T., Noma, N., Oikawa, T., Ochiai, Y., Kakuda, S., Kuwahara, Y., Takai, Y., Takahashi, A., and Fukumoto, M. (2012). Activation of the AKT/cyclin D1/Cdk4 survival signaling pathway in radioresistant cancer stem cells. Oncogenesis *1*, e12-.

Siegel, R.L., Miller, K.D., Fedewa, S.A., Ahnen, D.J., Meester, R.G.S., Barzi, A., and Jemal, A. (2017). Colorectal cancer statistics, 2017. CA: A Cancer Journal for Clinicians *67*, 177-193.

Siegel, R.L., Miller, K.D., and Jemal, A. (2016). Cancer statistics, 2016. CA: A Cancer Journal for Clinicians *66*, 7-30.

Simanshu, D.K., Nissley, D.V., and McCormick, F. (2017). RAS Proteins and Their Regulators in Human Disease. Cell *170*, 17-33.

Skalicky, D.A., Kench, J.G., Segara, D., Coleman, M.J., Sutherland, R.L., Henshall, S.M., Musgrove, E.A., and Biankin, A.V. (2006). Cyclin E expression and outcome in pancreatic ductal adenocarcinoma. Cancer epidemiology, biomarkers & prevention : a publication of the American Association for Cancer Research, cosponsored by the American Society of Preventive Oncology *15*, 1941-1947.

Slamon, D.J., Clark, G.M., Wong, S.G., Levin, W.J., Ullrich, A., and McGuire, W.L. (1987). Human breast cancer: correlation of relapse and survival with amplification of the HER-2/neu oncogene. Science (New York, NY) *235*, 177-182.

Sobrero, A.F., Maurel, J., Fehrenbacher, L., Scheithauer, W., Abubakr, Y.A., Lutz, M.P., Vega-Villegas, M.E., Eng, C., Steinhauer, E.U., Prausova, J., *et al.* (2008). EPIC: Phase III Trial of Cetuximab Plus Irinotecan After Fluoropyrimidine and Oxaliplatin Failure in Patients With Metastatic Colorectal Cancer. Journal of Clinical Oncology *26*, 2311-2319.

Souchek, J.J., Baine, M.J., Lin, C., Rachagani, S., Gupta, S., Kaur, S., Lester, K., Zheng, D., Chen, S., Smith, L., *et al.* (2014). Unbiased analysis of pancreatic cancer radiation resistance reveals cholesterol biosynthesis as a novel target for radiosensitisation. Br J Cancer *111*, 1139-1149.

Spencer, S.L., Cappell, S.D., Tsai, F.C., Overton, K.W., Wang, C.L., and Meyer, T. (2013). The proliferation-quiescence decision is controlled by a bifurcation in CDK2 activity at mitotic exit. Cell *155*, 369-383.

Stamos, J., Sliwkowski, M.X., and Eigenbrot, C. (2002). Structure of the epidermal growth factor receptor kinase domain alone and in complex with a 4-anilinoquinazoline inhibitor. J Biol Chem *277*, 46265-46272.

Sun, C., Hobor, S., Bertotti, A., Zecchin, D., Huang, S., Galimi, F., Cottino, F., Prahallad, A., Grernrum, W., Tzani, A., *et al.* (2014). Intrinsic resistance to MEK inhibition in KRAS mutant lung and colon cancer through transcriptional induction of ERBB3. Cell reports *7*, 86-93.

Tao, Z., Le Blanc, J.M., Wang, C., Zhan, T., Zhuang, H., Wang, P., Yuan, Z., and Lu, B. (2016). Coadministration of Trametinib and Palbociclib Radiosensitizes KRAS-Mutant Non-Small Cell Lung Cancers In Vitro and In Vivo. Clinical cancer research : an official journal of the American Association for Cancer Research *22*, 122-133.

Thomas, R.K., Baker, A.C., Debiasi, R.M., Winckler, W., Laframboise, T., Lin, W.M., Wang, M., Feng, W., Zander, T., MacConaill, L., *et al.* (2007). High-throughput oncogene mutation profiling in human cancer. Nat Genet *39*, 347-351.

Tsuchida, N., Ryder, T., and Ohtsubo, E. (1982). Nucleotide sequence of the oncogene encoding the p21 transforming protein of Kirsten murine sarcoma virus. Science (New York, NY) *217*, 937-939.

Tsuchida, N., and Uesugi, S. (1981). Structure and functions of the Kirsten murine sarcoma virus genome: molecular cloning of biologically active Kirsten murine sarcoma virus DNA. Journal of virology *38*, 720-727.

Tuominen, V.J., Ruotoistenmäki, S., Viitanen, A., Jumppanen, M., and Isola, J. (2010). ImmunoRatio: a publicly available web application for quantitative image analysis of estrogen receptor (ER), progesterone receptor (PR), and Ki-67. Breast Cancer Research *12*, 1-12.

Turke, A.B., Song, Y., Costa, C., Cook, R., Arteaga, C.L., Asara, J.M., and Engelman, J.A. (2012a). MEK inhibition leads to PI3K/AKT activation by relieving a negative feedback on ERBB receptors. Cancer research *72*, 3228-3237.

Turke, A.B., Song, Y., Costa, C., Cook, R., Arteaga, C.L., Asara, J.M., and Engelman, J.A. (2012b). MEK inhibition leads to PI3K/AKT activation by relieving a negative feedback on ERBB receptors. Cancer research *72*, 3228-3237.

Turner, N.C., Liu, Y., Zhu, Z., Loi, S., Colleoni, M., Loibl, S., DeMichele, A., Harbeck, N., André, F., Zhang, Z., *et al.* (2018). Abstract CT039: Cyclin E1 (CCNE1) expression associates with benefit from palbociclib in metastatic breast cancer (MBC) in the PALOMA3 trial. Cancer research *78*, CT039-CT039.

Tzahar, E., Waterman, H., Chen, X., Levkowitz, G., Karunagaran, D., Lavi, S., Ratzkin, B.J., and Yarden, Y. (1996). A hierarchical network of interreceptor interactions determines signal transduction by Neu differentiation factor/neuregulin and epidermal growth factor. Molecular and cellular biology *16*, 5276-5287.

Ueki, K., Matsuda, S., Tobe, K., Gotoh, Y., Tamemoto, H., Yachi, M., Akanuma, Y., Yazaki, Y., Nishida, E., and Kadowaki, T. (1994). Feedback regulation of mitogen-activated protein kinase kinase kinase activity of c-Raf-1 by insulin and phorbol ester stimulation. The Journal of biological chemistry *269*, 15756-15761.

Vakana, E., Pratt, S., Blosser, W., Dowless, M., Simpson, N., Yuan, X.J., Jaken, S., Manro, J., Stephens, J., Zhang, Y., *et al.* (2017). LY3009120, a panRAF inhibitor, has significant anti-tumor activity in BRAF and KRAS mutant preclinical models of colorectal cancer. Oncotarget *8*, 9251-9266.

Vaughn, C.P., Zobell, S.D., Furtado, L.V., Baker, C.L., and Samowitz, W.S. (2011). Frequency of KRAS, BRAF, and NRAS mutations in colorectal cancer. Genes, chromosomes & cancer *50*, 307-312.

Vivanco, I., and Sawyers, C.L. (2002). The phosphatidylinositol 3-Kinase AKT pathway in human cancer. Nat Rev Cancer *2*, 489-501.

Vodermaier, H.C. (2004). APC/C and SCF: controlling each other and the cell cycle. Curr Biol *14*, R787-796.

Wan, P.T., Garnett, M.J., Roe, S.M., Lee, S., Niculescu-Duvaz, D., Good, V.M., Jones, C.M., Marshall, C.J., Springer, C.J., Barford, D., *et al.* (2004). Mechanism of activation of the RAF-ERK signaling pathway by oncogenic mutations of B-RAF. Cell *116*, 855-867.

Wang, I.C., Chen, Y.J., Hughes, D., Petrovic, V., Major, M.L., Park, H.J., Tan, Y., Ackerson, T., and Costa, R.H. (2005). Forkhead box M1 regulates the transcriptional network of genes essential for mitotic progression and genes encoding the SCF (Skp2-Cks1) ubiquitin ligase. Molecular and cellular biology *25*, 10875-10894.

Wang, L., Tsutsumi, S., Kawaguchi, T., Nagasaki, K., Tatsuno, K., Yamamoto, S., Sang, F., Sonoda, K., Sugawara, M., Saiura, A., *et al.* (2012). Whole-exome sequencing of human pancreatic cancers and characterization of genomic instability caused by MLH1 haploinsufficiency and complete deficiency. Genome Research *22*, 208-219.

Wartmann, M., Hofer, P., Turowski, P., Saltiel, A.R., and Hynes, N.E. (1997). Negative Modulation of Membrane Localization of the Raf-1 Protein Kinase by Hyperphosphorylation. Journal of Biological Chemistry *272*, 3915-3923.

Wee, S., Jagani, Z., Xiang, K.X., Loo, A., Dorsch, M., Yao, Y.M., Sellers, W.R., Lengauer, C., and Stegmeier, F. (2009). PI3K pathway activation mediates resistance to MEK inhibitors in KRAS mutant cancers. Cancer research *69*, 4286-4293.

Welsh, J.B., Gill, G.N., Rosenfeld, M.G., and Wells, A. (1991). A negative feedback loop attenuates EGF-induced morphological changes. The Journal of Cell Biology *114*, 533-543.

Wennogle, L.P., Liang, H., Quintavalla, J.C., Bowen, B.R., Wasvary, J., Miller, D.B., Allentoff, A., Boyer, W., Kelly, M., and Marshall, P. (1995). Comparison of recombinant cyclooxygenase-2 to native isoforms: aspirin labeling of the active site. FEBS Lett *371*, 315-320.

Whyte, D.B., Kirschmeier, P., Hockenberry, T.N., Nunez-Oliva, I., James, L., Catino, J.J., Bishop, W.R., and Pai, J.-K. (1997). K- and N-Ras Are Geranylgeranylated in Cells Treated with Farnesyl Protein Transferase Inhibitors. Journal of Biological Chemistry *272*, 14459-14464.

Will, M., Qin, A.C., Toy, W., Yao, Z., Rodrik-Outmezguine, V., Schneider, C., Huang, X., Monian, P., Jiang, X., de Stanchina, E., *et al.* (2014). Rapid induction of apoptosis by PI3K inhibitors is dependent upon their transient inhibition of RAS-ERK signaling. Cancer discovery *4*, 334-347.

Wingate, H., Puskas, A., Duong, M., Bui, T., Richardson, D., Liu, Y., Tucker, S.L., Van Pelt, C., Meijer, L., Hunt, K., *et al.* (2009). Low molecular weight cyclin E is specific in breast cancer and is associated with mechanisms of tumor progression. Cell cycle (Georgetown, Tex) *8*, 1062-1068.

Witkiewicz, A.K., Borja, N.A., Franco, J., Brody, J.R., Yeo, C.J., Mansour, J., Choti, M.A., McCue, P., and Knudsen, E.S. (2015a). Selective impact of CDK4/6 suppression on patient-derived models of pancreatic cancer.

Witkiewicz, A.K., McMillan, E.A., Balaji, U., Baek, G., Lin, W.C., Mansour, J., Mollaee, M., Wagner, K.U., Koduru, P., Yopp, A., *et al.* (2015b). Whole-exome sequencing of pancreatic cancer defines genetic diversity and therapeutic targets. Nature communications *6*, 6744.

Wong, K.K., Engelman, J.A., and Cantley, L.C. (2010). Targeting the PI3K signaling pathway in cancer. Current opinion in genetics & development *20*, 87-90.

Xu, K., and Shu, H.-K.G. (2013a). The FOXM1 transcription factor interacts with Sp1 to mediate EGF-dependent COX-2 expression in human glioma cells. Molecular cancer research : MCR *11*, 875-886.

Xu, K., and Shu, H.K. (2013b). Transcription factor interactions mediate EGF-dependent COX-2 expression. Mol Cancer Res *11*, 875-886.

Yarbrough, W.G., Buckmire, R.A., Bessho, M., and Liu, E.T. (1999). Biologic and biochemical analyses of p16(INK4a) mutations from primary tumors. Journal of the National Cancer Institute *91*, 1569-1574.

Yip-Schneider, M.T., Barnard, D.S., Billings, S.D., Cheng, L., Heilman, D.K., Lin, A., Marshall, S.J., Crowell, P.L., Marshall, M.S., and Sweeney, C.J. (2000). Cyclooxygenase-2 expression in human pancreatic adenocarcinomas. Carcinogenesis *21*, 139-146.

Zacharek, S.J., Xiong, Y., and Shumway, S.D. (2005). Negative regulation of TSC1-TSC2 by mammalian D-type cyclins. Cancer research *65*, 11354-11360.

Zhang, Z., and DuBois, R.N. (2001). Detection of differentially expressed genes in human colon carcinoma cells treated with a selective COX-2 inhibitor. Oncogene *20*, 4450-4456.

Zhang, Z., Kobayashi, S., Borczuk, A.C., Leidner, R.S., Laframboise, T., Levine, A.D., and Halmos, B. (2010). Dual specificity phosphatase 6 (DUSP6) is an ETS-regulated negative feedback mediator of oncogenic ERK signaling in lung cancer cells. Carcinogenesis *31*, 577-586.

Zhao, Y., and Adjei, A.A. (2014). The clinical development of MEK inhibitors. Nature Reviews Clinical Oncology *11*, 385.

Zhen, Y., Li, D., Li, W., Yao, W., Wu, A., Huang, J., Gu, H., Huang, Y., Wang, Y., Wu, J., *et al.* (2016). Reduced PDCD4 Expression Promotes Cell Growth Through PI3K/Akt Signaling in Non-Small Cell Lung Cancer. Oncology research *23*, 61-68.

Zhou, Y., and Hancock, J.F. (2015). Ras nanoclusters: Versatile lipid-based signaling platforms. Biochimica et Biophysica Acta (BBA) - Molecular Cell Research *1853*, 841-849.

Zhou, Y., Prakash, P., Liang, H., Cho, K.J., Gorfe, A.A., and Hancock, J.F. (2017). Lipid-Sorting Specificity Encoded in K-Ras Membrane Anchor Regulates Signal Output. Cell *168*, 239-251.e216.

Ziemke, E.K., Dosch, J.S., Maust, J.D., Shettigar, A., Sen, A., Welling, T.H., Hardiman, K.M., and Sebolt-Leopold, J.S. (2015). Sensitivity of KRAS Mutant Colorectal Cancers to Combination Therapy that Co-Targets MEK and CDK4/6. Clinical cancer research : an official journal of the American Association for Cancer Research.